

PKC- δ , its C2 domain and Breast Cancer Cell Lines

Hannah Elizabeth Scott, BSc. (Hons.)

Thesis submitted to the University of Nottingham

For the degree of Doctor of Philosophy

July 2012

Abstract

Protein kinase C δ (PKC- δ) is a novel member of the PKC family of serine-threonine kinases. PKC- δ structure is widely conserved within the PKC family and has a catalytic region and regulatory region. The regulatory region has two main sub domains C1 and C2. Although several studies have investigated the role of the C1 domain, little is known about the function of the C2 domain, however there is some evidence that it acts as a protein interaction domain.

PKCs are involved in a wide variety of cellular functions within cancer. PKC- δ has been demonstrated to have a particular involvement with the apoptotic processes of a cancer cell. A pro-apoptotic role for PKC- δ has been identified, whereby tyrosine phosphorylation of particular residues induces translocation to the nucleus, alongside a similar translocation event for caspase-3. In the nucleus, caspase-3 cleaves the regulatory and catalytic regions to form a free catalytic domain that is uninhibited by the regulatory portion. This free catalytic region causes the induction of the apoptotic pathway. Conversely an anti-apoptotic role has also been identified for PKC- δ . This was found in MDA-MB-231 cells, which have a *ras* mutation. Due to this mutation in these cells, ERK1/2 phosphorylation is high. Without PKC- δ activity the high phosphorylation levels induce apoptosis. PKC- δ acts on a pathway to reduce ERK1/2 phosphorylation, thus facilitating cell survival.

This study aimed to investigate the role of the PKC- δ C2 domain within breast cancer cells. Through use of these techniques, the role of the C2 domain was examined in order to consider its utility as a drug target to treat breast cancer.

- Constructs were developed of pIRESneo2 vector with myc-tagged C2 domain and myc-tagged PKC- δ sequences
- Breast cancer cell lines, MDA-MB-468, MDA-MB-231 and MCF-7, were stably transfected with a vector control and myc- δ C2 construct. MDA-MB-231 and MCF-7 were also transfected with myc-PKC- δ .
- Cell lines developed were examined for alterations due to the presence of the C2 domain or PKC- δ over-expression

As the C2 domain is proposed to be a protein interaction domain, we hypothesized that over-expression of this domain would interfere with endogenous PKC- δ interactions, through competitive inhibition, and thus we could identify C2 domain roles. The effect on the cells of the endogenous PKC- δ would be opposed by the C2 domain. Thus the role of endogenous PKC- δ could also be clarified for a particular situation - it would be the opposite of the effects induced by the myc- δ C2 on the cells.

In the MDA-MB-468 stable cell lines, immuno-fluorescence examination of the myc- δ C2 cells showed the myc- δ C2 was localised at the ends of actin protrusions from the bulk of the cell. The myc- δ C2 expressing cells had a more extensive cytoskeleton than the Vector control cells, possibly suggesting improved attachment to a surface. An experiment examining this illustrated that the myc- δ C2 cells appeared to attach in a shorter time period. This implies that the role of the endogenous PKC- δ is to discourage cell attachment and promote an invasive phenotype, this is in agreement with the literature.

During sub-culture of the MDA-MB-468 cell lines it became apparent that the myc- δ C2 cells were growing at an increased rate over the Vector cell lines. This was quantified and indeed the myc- δ C2 cells did increase in cell number more than the

Vector cells. This was also the case with the MDA-MB-231 cells but not with the MCF-7 cells. Growth is a balance of proliferation and apoptosis. This effect indicates that PKC- δ is pro-apoptotic, or anti-proliferative. MCF-7 cells lack caspase-3 and thus pro-apoptotic effects of PKC- δ would be affected in this cell line. As the myc- δ C2 did not have an effect in these cells we examined apoptosis to see if these effects could be attributed to differences in apoptosis.

The MDA-MB-468 cells expressing myc- δ C2 had higher viability than the Vector cells. This fits with the cell number data, indicating that a lower level of apoptosis has led to a greater cell number, and advocates a pro-apoptotic role for PKC- δ . This was not the case in MDA-MB-231 cell lines where Vector cells had higher viability. This agrees with the literature describing PKC- δ displaying an anti-apoptotic role in this cell line, but does not fit with the cell number data. Thus, differences in cell number are likely due to effects on proliferation, although this was not investigated. MCF-7 cells showed no differences indicating the apoptotic program of these cells is indeed affected by the lack of caspase-3.

Serum starvation is a commonly used method to induce apoptosis. MDA-MB-468 cell lines were serum starved in order to examine the effects. The apoptosis profile was altered and myc- δ C2 cells showed lower viability than the Vector cells, indicative of an anti-apoptotic effect of PKC- δ . An anti-apoptotic effect is observed in MDA-MB-231 cells, where the effect was proteasome dependent. This was also the case in this situation. The anti-apoptotic effect is related to levels of phosphorylated ERK1/2, where high levels are pro-apoptotic. The phosphorylation status was examined and illustrated a much higher level of phosphorylation in myc- δ C2 cells over Vector cells when starved. This indicates myc- δ C2 is inhibiting the de-phosphorylating role of PKC- δ in these apoptotic cells. Thus it appears that the C2 domain acts as a 'sensor'

to serum status, appropriating PKC- δ effects in apoptotic pathways according to the serum status, the method of which is unknown.

This study has highlighted the importance of the PKC- δ C2 domain in breast cancer apoptosis. The effects appear to require a fully active PKC- δ pro-apoptotic pathway, and are dependent on the serum status of the cells. Further investigation would be required to identify a level of serum for use *in vitro* that is relevant to an *in vivo* tumour situation. If low levels are more relevant to a clinical state then it may be possible to target the C2 domain with drugs to allow induction of apoptosis. The differences between the cell lines clearly show that the phenotypic analysis of tumours would be vital to identifying whether such treatment would be applicable, as effects of any drug would vary greatly across tumour types. MDA-MB-468 and MDA-MB-231 are both triple negative cell lines (i.e. they do not express progesterone, oestrogen or HER2 receptors); however the strong differences seen in this case indicate further phenotypic analysis would be essential.

Acknowledgments

I would like to acknowledge the help of my supervisor Dr Lodewijk Dekker. His extensive knowledge of the area and guidance in pursuit of this research project has been invaluable. I would also like to thank my second supervisor Dr Tracey Bradshaw for her insight, guidance and support. In addition, I would like to express my gratitude to the Breast Cancer Campaign for funding this research.

Thank you to all my colleagues in C57 and C62, particularly to Lyn Warner for her support and patience and acting as my 'critical friend'. Special thanks go to Charlie Matthews and Helene Myrvang-Priestley for generously sharing their considerable expertise whilst coaching me in techniques that were new to me, and offering encouragement in applying the knowledge they provided. Special thanks also to Dr Hilary Collins, for supplying the histone antibody, and to Tim Self for patiently training me in confocal microscopy.

On a more informal level, I extend my thanks to Dr Prudence Mutowo for her support, both in person and via email - also to my colleagues Lee, Ian, Graeme, Charlie, Chris and Lucy for providing much-needed stress-relieving conversations and the occasional distraction over tea breaks! I also wish to thank my friends for their encouragement, particularly Jennifer, Toby, Ashley and Nathaniel.

Many thanks go to my parents for their continuing support and help editing. Finally I wish to acknowledge my amazing husband Daniel for keeping me positive and laughing even through the most stressful times, and being there whenever I needed him.

Contents

Abstract	ii
Acknowledgments	vi
Contents	vii
List of Figures	xii
List of Tables	xvi
Abbreviations	xvii
Chapter 1: Introduction	1
1.1 Cancer	1
1.2 Breast cancer	3
1.2.1 Epidemiology	3
1.2.2 Anatomy of normal breast tissue	4
1.2.3 Breast cancer development, progression and manifestation	5
1.2.4 Breast cancer molecular classification	8
1.2.5 Breast cancer monitoring and treatment	10
1.2.5.1 Markers	10
1.2.5.2 Treatment	12
1.3 PKC-δ	15
1.3.1 The Protein kinase C family	15
1.3.2 PKC- δ primary structure	16
1.3.2.1 The catalytic domain	16
1.3.2.2 The regulatory domain	21
1.3.2.3 PKC- δ C1 domain	22
1.3.2.4 PKC- δ C2 domain	24
1.3.3 PKC- δ regulation	26
1.3.4 PKC- δ functional studies	29
1.3.4.1 Gene knockout and knockdown studies	29
1.3.4.2 The role in apoptosis	31
1.3.4.3 Other important cancer related functions	33
1.3.5 PKC- δ C2 interactions	35
1.4 PKC-δ and breast cancer	38
1.4.1 Clinical correlations	38
1.4.2 Cellular studies	39

1.4.3	Apoptosis	40
1.4.4	Cytoskeleton and metastasis	41
1.5	Studying PKC-δ C2 domain in breast cancer cell lines	43
1.6	Aims	45
Chapter 2:	Materials and Methods	47
2.1	Materials	47
2.2	Methods	52
2.2.1	Cloning pIRES-myc- δ C2	52
2.2.2	Cloning pIRES-myc-PKC- δ	54
2.2.3	Plasmid purification	54
2.2.4	Cell culture	55
2.2.5	Stable transfection	55
2.2.5.1	MDA-MB-468 cells	55
2.2.5.2	MDA-MB-231 and MCF-7 cells	57
2.2.6	Cell lysis	58
2.2.7	Bradford assay	59
2.2.8	SDS-PAGE	60
2.2.9	Western blotting	60
2.2.10	Immuno-precipitation	61
2.2.11	Sub-cellular fractionation	62
2.2.12	Immuno-fluorescence	64
2.2.13	Annexin V/propidium iodide flow cytometry assay	65
2.2.14	Cell attachment	66
2.2.15	Statistical analysis	67
Chapter 3:	Development of stable cell lines expressing myc-δC2 or myc-PKC-δ	84
3.1	Introduction	86
3.1.1	pIRESneo2	86
3.1.2	Using pIRESneo2	89
3.1.3	Approaches to transfection	91
3.2	Results	94
3.2.1	Untransfected cell line endogenous expression	94
3.2.2	Generation of the pIRES-myc- δ C2 and pIRES-myc-PKC- δ constructs	97
3.2.3	Stable transfection and confirming protein expression	101
3.2.3.1	Pre-transfection	101
3.2.3.2	Transfection of MDA-MB-468	103
3.2.3.3	Transfection of MDA-MB-231	107

3.2.3.4 Transfection of MCF-7	112
3.3 Discussion	114
Chapter 4: Localisation of myc-δC2 and associated differences	116
4.1 Introduction	117
4.2 Results	118
4.2.1 The myc- δ C2 domain localises to the periphery of the cell in membrane protrusions	118
4.2.2 The relationship of myc- δ C2 localisation and actin localisation	121
4.2.3 Comparing the actin cytoskeleton structure between Vector control and myc- δ C2 expressing cells	125
4.2.4 Studies of sub-cellular localisation of PKC- δ show similar profiles in Vector and myc- δ C2 cells	129
4.2.5 Degree of attachment differs between the Vector and myc- δ C2 cell lines following a 15-minute incubation period	135
4.3 Discussion	137
Chapter 5: Investigation of cell growth and apoptosis in the stable cell lines	141
5.1 Introduction	143
5.1.1 Analysing proliferation of a population by cell number	144
5.1.2 Flow cytometry	144
5.1.3 Analysing apoptosis	147
5.2 Results	150
5.2.1 MDA-MB-468	150
5.2.1.1 Cell numbers are higher in myc- δ C2 than Vector cells	150
5.2.1.2 Cells expressing myc- δ C2 have higher viability than Vector cells	153
5.2.2 MDA-MB-231	158
5.2.2.1 Cell numbers of myc- δ C2 expressing cells increase greater than Vector cells	158
5.2.2.2 The myc- δ C2 cells have lower viability than Vector cells	159
5.2.2.3 Expression of myc-PKC- δ is associated with increased cell numbers over Vector control	164

	cells	
	5.2.2.4 Apoptosis does not differ between Vector cells and PKC- δ over-expressing cells	166
5.2.3	MCF-7	169
	5.2.3.1 Cell numbers do not differ between Vector and myc- δ C2 expressing cells	169
	5.2.3.2 Apoptotic profiles do not differ between myc- δ C2 and Vector cells	170
	5.2.3.3 PKC- δ over-expressing cells show decreased cell numbers from the Vector control at day 5	173
	5.2.3.4 There are no differences in apoptosis between PKC- δ over-expressing and Vector cells	175
5.3	Discussion	178
Chapter 6:	Investigations of the apoptotic pathway in MDA-MB-468 under starvation conditions	183
6.1	Introduction	185
6.2	Results	187
6.2.1	When Cells are serum-starved the apoptotic profile alters so that cells containing myc- δ C2 show more apoptosis	187
6.2.2	Src does not appear to be involved in PKC- δ tyrosine phosphorylation. Overall tyrosine phosphorylation levels do not differ between the Vector and myc- δ C2 cells	189
	6.2.2.1 Src inhibition using SU 6656	189
	6.2.2.2 Tyrosine phosphorylation	192
6.2.3	Proteasome activity is vital for anti-apoptotic activity under starvation conditions	196
6.2.4	ERK phosphorylation status	200
	6.2.4.1 ERK1/2 phosphorylation in not-starved and starved conditions	200
	6.2.4.2 ERK1/2 phosphorylation following MG132 treatment	205
6.2.5	Sub-cellular fractionation demonstrates that although the cell lines do not demonstrate any significant differences between each other, starvation does induce differences in the profile of PKC- δ localisation	209
6.3	Discussion	211

Chapter 7: Conclusions	216
7.1 Preparing the cell lines	218
7.2 The cytoskeleton	220
7.3 Cell numbers	222
7.4 Apoptosis	225
7.5 The effects of no serum	229
7.6 Key discoveries	232
7.7 Further work	233
Chapter 8: References	236

List of Figures

Figure 1.1	A schematic of the development of cells from the mammary stem cells in the duct and lobular unit in normal breast tissue	5
Figure 1.2	Classical PKC structure compared with novel PKC structure	16
Figure 1.3	Blast analysis of PKC- δ protein sequence showing comparison with PKC- θ .	17
Figure 1.4	Crystal structure of the catalytic domain of PKC- θ	19
Figure 1.5	The structure of the activation loop and α C helix necessary for catalysis.	21
Figure 1.6	PKC- δ C2 domain structure showing the 8 β -strands	25
Figure 1.7	The involvement of MUC-1, β -catenin and PKC- δ in cell adhesion and motility.	35
Figure 1.8	Model for the hypothesis of how the myc- δ C2 over-expression will affect endogenous PKC- δ .	45
Figure 2.1	The pEFLINKtag-myc- δ C2 insert sequence.	53
Figure 2.2	Primer sequences for either side of the myc- δ C2 sequence.	53
Figure 3.1	pIRES vector map showing details of the multiple cloning site (MCS).	89
Figure 3.2	Endogenous expression levels of PKC- δ in MDA-MB-468, MDA-MB-231 and MCF-7 cell lines.	95
Figure 3.3	Ligation scheme for developing the pIRES-myc- δ C2 construct	98
Figure 3.4	Ligation scheme for developing the pIRES-myc-PKC δ construct.	99
Figure 3.5	Maps of the constructs pIRES-myc- δ C2 and pIRES-mycPKC- δ .	100
Figure 3.6	Expression of myc- δ C2 in the 468-myc- δ C2 clonal cell lines and its absence in the vector control clonal cell lines	105
Figure 3.7	Expression of myc- δ C2 in the 468-myc- δ C2 pool cell line and the absence of the band in the vector control pool cell line	106
Figure 3.8	The development of transfected cells.	109
Figure 3.9	Expression of myc-PKC- δ in the 231-myc-PKC- δ cell line, this band is absent in the 231-myc- δ C2 and vector control cell lines	111
Figure 3.10	Expression of myc- δ C2 is seen in the MCF7-myc- δ C2 cell line, but is absent in both the MCF7-myc-PKC- δ and vector control cell lines	113
Figure 4.1	Myc-tag staining of four Vector control and four myc- δ C2 cells	119
Figure 4.2	Actin cytoskeletal staining in combination with myc-tag staining of Vector control and myc- δ C2 cells	122
Figure 4.3	Graphic illustrating myc- δ C2 positioning in relation to actin cytoskeletal protrusions in myc- δ C2 cells	123
Figure 4.4	Actin cytoskeletal staining of 468-myc- δ C2 and Vector control	126

	cells.	
Figure 4.5	Manufacturers evidence for the fractionation protocol providing the particular fractions as stated.	131
Figure 4.6	Check of the chromatin-bound nuclear fraction using histone 3 antibody.	132
Figure 4.7	Example of fractionation data showing distribution of PKC- δ	134
Figure 4.8	A suggested model for myc- δ C2 domain action with respect to cytoskeletal differences	139
Figure 5.1	Configuration of the sensors and filters in the Coulter Epics XL Flow Cytometer	145
Figure 5.2	An example of the AnnexinV – PI apoptosis data showing the four quadrants which enable determination of the apoptotic status of the population	148
Figure 5.3	The effect of myc- δ C2 expression on growth rates of two clonal populations of MDA-MB-468 transfected cells when compared to two clonal populations of the vector control cells	151
Figure 5.4	The effect of myc- δ C2 expression on growth rates of MDA-MB-468 transfected cells when compared to the vector control	152
Figure 5.5	Analysis of apoptosis in the 468-myc- δ C2 and 468 Vector control cell lines using the AnnexinV - propidium iodide assay illustrated the decrease in levels of apoptosis in cells	154
Figure 5.6	Analysis of apoptosis in the 468-myc- δ C2 and 468 Vector control cell lines when apoptosis is induced by camptothecin treatment using the AnnexinV - propidium iodide assay	156
Figure 5.7	The effect of myc- δ C2 expression on growth rates of pool populations of MDA-MB-231 transfected cells when compared to the vector control pool cells	158
Figure 5.8	Analysis of apoptosis in the MDA-MB-231-myc- δ C2 and MDA-MB-231 Vector control cell lines using the AnnexinV - propidium iodide assay	160
Figure 5.9	Analysis of apoptosis in the MDA-MB-231-myc- δ C2 and MDA-MB-231 Vector control cell lines when apoptosis is induced by camptothecin treatment using the AnnexinV - propidium iodide assay	161
Figure 5.10	The effect of over-expression of PKC- δ in MDA-MB-231 cells is to increase the rate of growth compared to the vector control cells	164
Figure 5.11	Analysis of apoptosis in the MDA-MB-231-myc-PKC- δ and MDA-MB-231 Vector control cell lines using the AnnexinV - propidium iodide assay	166
Figure 5.12	Analysis of apoptosis in the MDA-MB-231-myc-PKC- δ and MDA-MB-231 Vector control cell lines when apoptosis is induced by camptothecin treatment using the AnnexinV - propidium iodide	168

	assay.	
Figure 5.13	The effect of myc- δ C2 expression on growth rates of pool populations of MCF-7 transfected cells compared with the vector control pool cells	169
Figure 5.14	Analysis of apoptosis in the MCF-7 myc- δ C2 and MCF-7 Vector control cell lines using the AnnexinV - propidium iodide assay	171
Figure 5.15	Analysis of apoptosis in the MCF-7-myc- δ C2 and MCF-7 Vector control cell lines when apoptosis is induced by camptothecin treatment using the AnnexinV - propidium iodide assay.	172
Figure 5.16	There is no effect on the growth rate where there is over-expression of PKC- δ in MCF-7 cells compared to the vector control cells.	174
Figure 5.17	Analysis of apoptosis in the MCF-7-myc-PKC- δ and MCF-7 Vector control cell lines using the AnnexinV - propidium iodide assay	176
Figure 5.18	Analysis of apoptosis in the MCF-7-myc-PKC- δ and MCF-7 Vector control cell lines when apoptosis is induced by camptothecin treatment using the AnnexinV - propidium iodide assay	177
Figure 5.19	A suggested model for the response to myc- δ C2 expression in MDA-MB-468 cells.	179
Figure 6.1	Apoptosis measured following 72 hours starvation showed mycC2 cells have lower viability and more apoptosis than Vector cells	188
Figure 6.2	The effects of Src inhibitor SU6656 on cells following 24 hour treatment.	190
Figure 6.3	Two IP results where PKC- δ was used to immunoprecipitate and anti-p-tyrosine used to probe.	193
Figure 6.4	IP results of myc- δ C2 tyrosine phosphorylation study.	195
Figure 6.5	The effects of proteasome inhibitor MG132 and starvation on cells following 72 hours of starvation including the final 5 hours MG132 treatment.	197
Figure 6.6	The effects of proteasome inhibitor MG132 and starvation on cells following 24 hours of treatment.	198
Figure 6.7	Phosphorylated and Total ERK1/2 levels in Vector control and myc- δ C2 cells under 10% serum conditions	201
Figure 6.8	Phosphorylated and Total ERK1/2 levels in not-starved cells where Vector is set at 100%	202
Figure 6.9	Phosphorylated and Total ERK1/2 levels in Vector control and myc- δ C2 cells under starvation conditions	203
Figure 6.10	Phosphorylated and Total ERK1/2 levels in starved cells where Vector is set at 100%	204
Figure 6.11	Phosphorylated ERK1/2 and total ERK1/2 showing differences	206

	with Vector control and myc- δ C2 in starved conditions, with and without MG132 proteasome inhibitor present	
Figure 6.12	Phosphorylated ERK1/2 levels in starved cells with MG132 treatment where Vector is set at 100%	206
Figure 6.13	Total ERK1/2 levels in starved and MG132 treated cells where vector is set at 100%; shows starved untreated and treated cells where the Vector cells are set at 100%	208
Figure 6.14	The anti-apoptotic pathway in which PKC- δ is involved	212
Figure 6.15	The C2 appears to be involved in 'sensing' the serum status and appropriately directing PKC- δ activity.	215

List of Tables

Table 1.1	The five sub-types of breast cancer	10
Table 1.2	Differences between MDA-MB-468, MDA-MB-231 and MCF-7 cell lines	44
Table 2.1	Buffers	47
Table 2.2	Antibodies	49
Table 2.3	Cell lines	50
Table 2.4	Volumes of serum-free (SF) RPMI, DNA and FuGENE6 in transfection samples.	56
Table 2.5	Volumes of serum-free (SF) RPMI and DNA in transfection samples.	58
Table 2.6	Volumes of fractionation buffers used.	63
Table 3.1	Kill-time experiment data, for testing the G418 concentration necessary to kill MDA-MB-468 cells in 5-7 days	102
Table 3.2	Kill-time experiment data, for testing the G418 concentration necessary to kill MCF-7 cells in 5-8 days	103
Table 4.1	Number of myc- δ C2 cells positive for 9E10 staining at the ends of protrusions from the actin cytoskeleton.	124
Table 4.2	Number of cells showing protrusions from the actin cytoskeleton.	127
Table 4.3	Distribution of PKC- δ amongst the five localisation extracts when cells are grown in normal growth conditions (10% serum).	133
Table 4.4	Percentage of cells unattached after 15 minutes since introduction to a surface.	136
Table 6.1	Distribution of PKC- δ amongst the five localisation extracts comparing not-starved cells and starved cells.	210

Abbreviations

AH	Atypical hyperplasias
DAPI	4',6-diamidino-2-phenylindole
DCIS	Ductal carcinoma in situ
DNA	Deoxyribonucleic acid
FITC	Fluorescein isothiocyanate
IP ₆	Inositol hexaphosphate
LCIS	Lobular carcinoma in situ
LDS	Lithium dodecyl sulphate
MCF-7	Michigan Cancer Foundation-7
MMP	Matrix metalloproteinase
PBS	Phosphate buffered saline
PBST	Phosphate buffered saline with 0.1% Tween 20
PBSTM	Phosphate buffered saline with 0.1% Tween 20 and 5% milk
PI	Propidium iodide
PKC	Protein kinase C
RPMI	Roswell park memorial institute
SDS	Sodium dodecyl sulphate
TGF	Transforming growth factor
TNF	Tumour necrosis factor
VEGFR	Vascular endothelial cell growth factor receptor

Chapter 1: Introduction

1.1 Cancer

Cancer is the third largest cause of death in the world (following cardiovascular disease and infectious and parasitic disease). As such, treatment of this complicated disease is a major concern across the world (Mathers et al., 2008). Historically, toxic agents have been used as cancer treatments. However this type of treatment frequently demonstrates extensive effects upon non cancerous cells leading to toxicity problems and poor tolerance levels (Hanahan and Weinberg, 2011).

Cancers can develop from a single mutated cell. Expansion of the mutant cell forms a tumour. The mutations acquired by this cell are enabling and hereditary (Hanahan and Weinberg, 2011); they allow the cell to undergo dynamic changes that greatly affect the genotype and phenotype. Tumourigenesis is a multistep process involving the acquisition of numerous genetic alterations that may

produce either dominant gain of function or recessive loss of function effects. Particular mutations will enable the cells to have an advantage over surrounding cells, thus allowing the population to expand.

Hanahan and Weinberg have catalogued several traits of cancer cells; these describe the key issues which cells must overcome in order to develop into a cancer. These hallmarks are: self-sufficiency in growth signals, insensitivity to anti-growth signals, tissue invasion & metastasis, limitless replicative potential, sustained angiogenesis and evading apoptosis, deregulating cellular energetics, avoiding immune destruction, genome instability & mutation and tumour-promoting inflammation (Hanahan and Weinberg, 2000; Hanahan and Weinberg, 2011).

By understanding the hallmarks of cancer and learning more about how cancer works and progresses, we have enabled research to be targeted into producing successful treatments for this intricate disease. Reflection upon these hallmarks can assist us in constructing a successful treatment protocol. The pathways involved must be considered, and possible alterations allowing cell survival predicted. Several components may be targeted at once in order to provide the best outcome by limiting the ability for the cells to further mutate and survive. The targeted approach shows great promise for future therapies.

1.2 Breast cancer

1.2.1 Epidemiology

Breast cancer produces the highest number of cancer cases in women across the world (Bonadonna et al., 2001; Mathers et al., 2008), and also in the UK (Ferlay et al., 2010). In England in 2008, 39,681 women were diagnosed (Office for National Statistics, 2010). Breast cancer is the most common cause of death from cancer in females in the Americas, Eastern Mediterranean, and Europe. It is second most common in Africa and South-East Asia, and fifth in the Western Pacific (Mathers et al., 2008). The development of effective treatments is therefore a major concern for the hundreds of thousands of patients across the world.

The occurrence of breast cancer is affected by the surrounding culture and environment. This is exemplified in a study comparing rates of breast cancer in Osaka, Japan compared with Japanese migrants to Hawaii, USA between 1988 and 1992. The rates of breast cancer in this migrant population were seen to increase to approach the rates in the local population (Weinberg, 2007).

Several risk factors for breast cancer have been identified; these are related to an overall increase in exposure to the hormone oestrogen. Factors that increase breast cancer risk include: early menarche, late menopause, postmenopausal obesity and hormone replacement therapy (Bonadonna et al., 2001). Studies have demonstrated that oestrogen can induce and promote rodent mammary tumours (Forrest, 1974). This data correlates cell-based studies with

epidemiological data indicating that oestrogen plays a very important role in breast cancer. The administration of anti-oestrogens has anti-tumour effects. Anti-oestrogenic therapy is used in the clinic against oestrogen receptor positive cancers to great effect (Early Breast Cancer Trialists' Collaborative Group, 1998).

1.2.2 Anatomy of normal breast tissue

The normal breast tissue is fatty and contains many lobes where milk is produced following child-birth. The lobes are made up of many lobules, where the milk is secreted. The lobules drain into ducts that channel the milk to the nipple. Hormonal changes during the menstrual cycle cause the tissue to proliferate and shrink back again. In pregnancy, the proliferation is more sustained and extensive remodelling occurs, whereby more ducts and lobules form. The ability for breast tissue to grow and shrink suggests the presence of mammary stem cells (Polyak, 2007). These would divide upon hormonal stimulation. The exact mechanisms of breast tissue development and homeostasis remain to be elucidated.

Within the breast tissue, the ductal and lobular structure is retained within a basement membrane (Fig. 1.1). Studies indicate that breast stem cells divide and differentiate into two subtypes, myo-epithelial and luminal. The myoepithelial cells attach to the basement membrane, whilst the luminal cells further differentiate into luminal/alveolar or ductal epithelial cells. Ductal cells may, or may not, have oestrogen receptors.

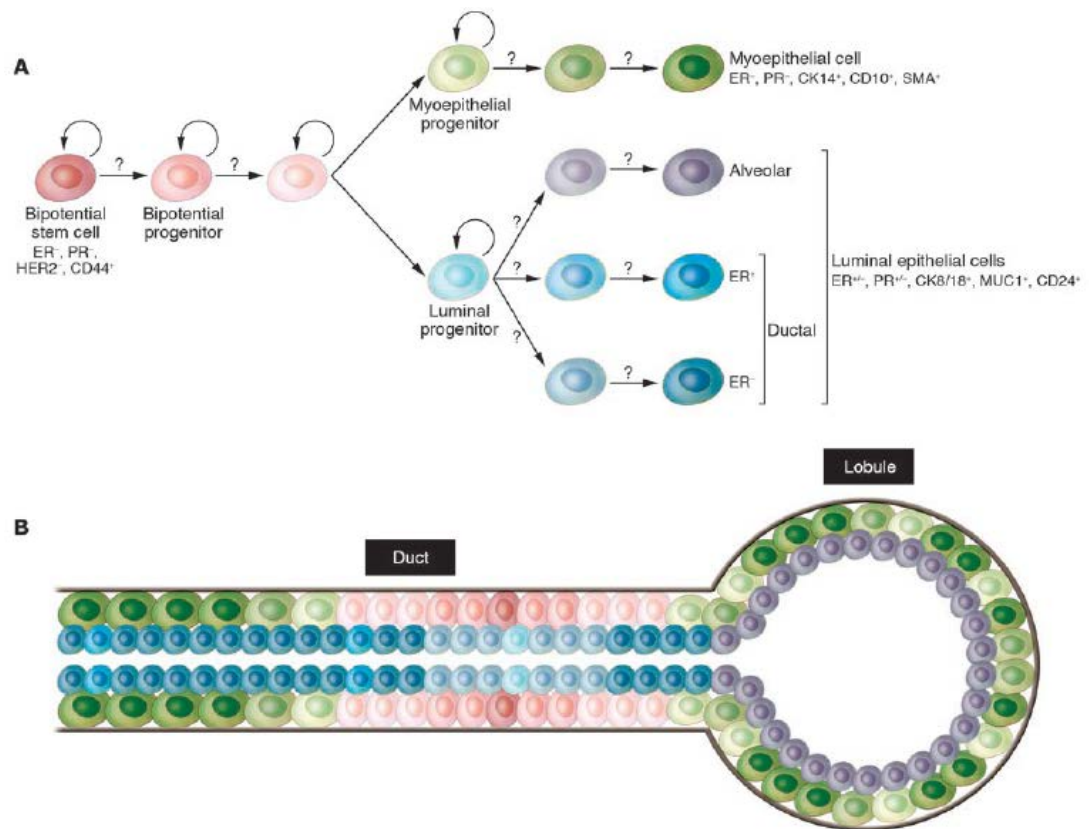


Figure 1.1: A schematic of the development of cells from the mammary stem cells in the duct and lobular unit in normal breast tissue (Polyak, 2007). The grey line surrounding the duct and lobule indicates the basement membrane.

1.2.3 Breast cancer development, progression and manifestation

Breast cancer, like other cancers, begins with an initiation event, where carcinogenic action causes mutation (King and Robins, 2006). This is followed by promotion, where the mutated cell proliferates; in breast cancer this can be caused by oestrogen. The mutated breast cell is promoted to survive and proliferate; more mutations may occur during this process, which results in the

formation of a tumour. Following this, the tumour undergoes progression into a more aggressive phenotype (King and Robins, 2006).

The early events of breast cancer have not been fully identified, however certain histological events have been associated with an increased risk of breast cancer; these are lobular or ductal atypical hyperplasias (AH) (Roses, 1999). The presence of AH does not mark the site/s at which breast cancer will develop, but act as markers for breast cancer development in the ensuing 10-15 years, which may be in either breast. AH include lobular carcinoma in situ (LCIS). LCIS is different to ductal carcinoma in situ (DCIS), which can progress into an invasive cancer (Roses, 1999). Between 12-20% of cases will recur within 10 years despite surgery to conserve the breast and radiotherapy (Thompson et al., 2008).

In breast cancer, lesions are primarily in the form of DCIS. DCIS is the term used to describe a situation where cells originating from the epithelium of the ductal structures proliferate abnormally following an initiation event. The abnormal proliferation is a result of a malignant transformation of cells. In DCIS the cells are retained at their origin by the basement membrane. Approximately 50% of DCIS will progress into invasive disease if untreated (Thompson et al., 2008). Development from DCIS involves breaking through the basement membrane; this occurs as the cells progress into a more aggressive phenotype. The loss of the basement membrane allows the tumour to be invasive and metastatic (Polyak, 2007). Breast cancer most commonly develops from the epithelium of ductal structures. The mechanisms behind progression from DCIS require investigation.

Where breast cancer develops an invasive and metastatic phenotype it will spread beyond the original tumour site. There have been suggestions that tumours can act on distant tissues to 'condition' them in order to provide suitable sites for colonisation (Sleeman and Cremers, 2007). The hypothesis of pre-metastatic niche formation is supported by the observation that particular tumour types have a penchant for metastasising to particular organs (Sleeman and Cremers, 2007). In breast cancer secondary tumours often form in the skin, the subcutis of the chest wall and the lymph nodes (Bonadonna et al., 2001). The mechanism surrounding this predisposition is not elucidated. However, recent studies have indicated that production of growth factors and cytokines from tumour cells can recruit VEGFR1⁺ bone marrow progenitor cells and myeloid cells to a specific region (Sleeman and Cremers, 2007). The bone marrow progenitors add to the vasculature and extracellular matrix of the pre-metastatic niche, while the myeloid cells produce S100A8 and S100A9 proteins which attract disseminating tumour cells (Hiratsuka et al., 2006; Sleeman and Cremers, 2007). Growth factors and cytokines inducing a pre-metastatic niche is demonstrated where conditioned media from tumour cells that are capable of specific metastases is injected into animals. A pre-metastatic niche then forms in relevant organs (Sleeman and Cremers, 2007).

1.2.4 Breast cancer molecular classification

Breast cancer is slightly unusual amongst cancers due to the hormonal involvement in the homeostasis of the tissue; many cancers are not affected by hormones. This hormonal involvement means that the cancer cells may express oestrogen and/or progesterone receptors; if this is the case they are considered to be ER⁺ and/or PR⁺ (Metz and Hampshire, 2007). These tumours respond to the oestrogen and/or progesterone in the blood, which stimulates the growth of the cells. Where the receptor is absent, the hormone has no effect on growth. This dependence provides an opportunity for treatment of the cancer. The anti-oestrogen drug tamoxifen acts by preventing oestrogen binding the receptors on the cell surface. Aromatase inhibitors which decrease the levels of oestrogen in the blood can be used in post-menopausal patients (Metz and Hampshire, 2007). Study of breast cancer is complicated by it being a conglomeration of diseases, where different cells in a tumour have multiple characteristics (Polyak, 2007). These differences create clinical issues whereby the cancer varies greatly between patients. Tumour profiling has revealed five major subtypes of breast cancer cells: luminal A, luminal B, HER2⁺/ER⁻, normal breast-like and basal-like (Polyak, 2007) (Table 1.1). HER2⁺ is also referred to as *Erb-B2*. These subtypes are evident at DCIS. The sub-types of breast cancer relate to differences in the patient's relapse-free period and their overall survival (Hu et al., 2006). In general, tumours consisting of basal-like cells lead to a worse prognosis, with those consisting of luminal A subtype giving the best prognosis (Polyak, 2007).

The normal breast-like tumour sub-set, have a similar gene expression pattern to normal, non-cancerous, tissue. They are negative for all five key markers: ER, PR, HER2, cytokeratins 5/6 and EGFR (Munirah et al., 2011; Nielsen et al., 2004). The luminal sub-types express the ER gene and also express keratins 8/18, as found in luminal epithelia. Expression of ER is also correlated with the transcription factors GATA-binding protein 3, X-box binding protein 1 and hepatocyte nuclear factor 3 α (Perou et al., 2000). The luminal sub-types can be further divided into A and B. Luminal A cancers have a better prognosis and a greater average age of diagnosis (Hu et al., 2006). High expression of ER α , GATA-binding protein 3, X-box binding protein 1, hepatocyte nuclear factor 3 α , trefoil factor 3 and oestrogen-regulated *LIV-1* indicates a luminal A sub-type. Low to medium expression levels indicates a luminal B sub-type (Sørli et al., 2006). The HER2⁺, or *Erb-B2* tumour sub-set express the *Erb-B2* oncogene and the genes co-expressed with this but do not express ER. These tumours are sensitive to the drug herceptin (Menard et al., 2003). Basal-like tumours express the keratins found in breast basal cells, keratins 5/6 and/or 17. They do not express ER or any of the co-expressed genes described above, for example GATA-binding protein 3, or HER2+.

Table 1.1: The five sub-types of breast cancer

Sub-type	Expression
Luminal A	Express keratins 8/18 and high levels of ER α , GATA-binding protein 3, X-box binding protein 1, hepatocyte nuclear factor 3 α , trefoil factor 3 and LIV-1
Luminal B	Express keratins 8/18 and low to medium levels of ER α , GATA-binding protein 3, X-box binding protein 1, hepatocyte nuclear factor 3 α , trefoil factor 3 and LIV-1
HER2⁺/ER⁻	Express the Erb-B2 oncogene. Negative for ER
Normal breast-like	Negative for ER, PR, HER2, cytokeratins 5/6 and EGFR
Basal-like	Express keratins 5/6 and/or 17. Negative for ER

ER: Oestrogen Receptor, PR: Progesterone Receptor, EGFR: Epidermal Growth Factor Receptor

1.2.5 Breast cancer monitoring and treatment

A treatment program tailored to a tumour profile remains elusive. However, recent development and approval of drugs such as Herceptin (for HER2⁺ tumours) is demonstrative of expansion of research in this area.

1.2.5.1 Markers

In breast cancer, markers can be used for staging, determining prognosis, and monitoring throughout treatment. Markers are proteins associated with tumour

cells that are detectable in tissue or body fluids. Markers may be on the cell surface, secreted, or molecules that mark cell turnover in a non-specific manner (Pannall and Kotasek, 1997).

Carcinoembryonic antigen (CEA) is a cell surface glycoprotein with a role in cell-cell adhesion (Pannall and Kotasek, 1997). In individuals with early disease, CEA is elevated in 25% of cases, while with advanced disease elevation occurs in 75% of patients. CEA is particularly notable with bone and liver metastases and can be studied to monitor a response to therapy.

The CA 15-3 assay is most useful for monitoring breast carcinoma, it uses two antibodies and detects Mucin-1 (MUC-1). MUC-1 is a membrane bound highly glycosylated protein. It is frequently less glycosylated in cancer (Agrawal et al., 1998) where expression is elevated (Mukherjee et al., 2005). In normal glandular epithelium, MUC-1 is expressed at the apical membrane (Quin and McGuckin, 2000). In breast carcinoma, MUC-1 protein is found throughout the cytoplasm; where high cytoplasmic expression is identified, the patient prognosis is poorer. The concentration detected in the assay can reflect the tumour burden, while a particularly high level is indicative of metastatic cancer (Pannall and Kotasek, 1997). In early breast cancer assay sensitivity varies from 0-36%; however it is 100% sensitive in advanced disease. Elevation can occur in other benign and malignant diseases. During monitoring of breast cancer, a decrease demonstrates a treatment response. However, lack of a decrease does not exclude the existence of a response (Pannall and Kotasek, 1997). Normal levels

after treatment indicates better prognosis compared with those where it does not.

Monitoring of breast cancer can also use tissue polypeptide antigen (TPA) which is reflective of cell proliferation rather than tumour mass, thus arguably a more sensitive progression indicator (Pannall and Kotasek, 1997). TPA originates from cytokeratins; soluble fragments are released during cell growth and division. TPA levels are related to the breakdown of cytokeratins 8, 18 and 19, which are more abundant in malignant tissues. Increase can also occur with infection.

In addition the HER2 and ER status of tumours can be examined. This aids identification of the tumour subtype (see 1.2.4). This enables a more directed approach to be utilised in cancer treatment. For example, HER2⁺ tumours can be treated using Herceptin, whilst tumour cells negative for HER2 expression will not respond to this treatment.

1.2.5.2 Treatment

Traditionally breast cancer has been treated using chemotherapies commonly utilised throughout a variety of cancers. These are not designed against a specific target, instead they are designed to affect cells that grow at an increased rate to the majority of cells in the body. Such cells include cancer cells, but also bone marrow, where new blood cells are constantly being produced. Thus chemotherapy can also have side-effects on these cells and cause the patient to develop anaemia or even leukemias. These drugs may target DNA to cause

damage, thus initiating the cells' intrinsic detection mechanisms and inducing apoptosis. In breast cancer, typical regimens include doxorubicin and cyclophosphamide for 3 months, or cyclophosphamide, methotrexate and fluorouracil for 6 months (Metz and Hampshire, 2007). Chemotherapy may be given prior to surgery in order to try and shrink the tumour and make excision less difficult.

Hormone therapy is a more recent treatment option. These are designed to inhibit binding of a stimulatory factor with the cell surface receptors in question. This treatment is traditionally against oestrogen receptors and prevents the growth-stimulatory effects of oestrogen binding. ER⁺ tumours can be treated with tamoxifen (Metz and Hampshire, 2007). Tamoxifen is usually taken for 5 years following surgery. This treatment dramatically reduces recurrence risks whilst also prolonging survival and preventing the development of a secondary breast cancer in the other breast. Aromatase inhibitors are a newer therapy that decreases the oestrogen levels in the body (Metz and Hampshire, 2007). Drugs for this treatment include letrozole. These are only given in post-menopausal women.

HER2/neu⁺ tumours can also be targeted using a similar mechanism, but involving the HER2/neu receptor. Herceptin, a monoclonal antibody, is used for this type of treatment. HER2/neu is a growth factor receptor, where growth factors binding the cells are stimulated to divide. Herceptin-receptor binding prevents this stimulatory signalling and prevents cell division. This causes the cell

to enter apoptosis. Herceptin is often given with traditional chemotherapeutic regimens (Metz and Hampshire, 2007).

1.3 Protein kinase C δ

1.3.1 The Protein kinase C family

PKC- δ is a 78kDa member of a large family of kinases, which fall within a subgroup of the AGC kinases (Hanks and Hunter, 1995). PKCs are generally activated by the presence of calcium ions (Ca^{2+}) and diacylglycerol (DAG); however, the diversity amongst the family members is considerable. Consequently, the influence of calcium and DAG is only applicable for the classical PKCs, PKC- α , β 1, β 2 and γ (Mellor and Parker, 1998). Novel PKC isozymes, PKC- δ , ϵ , η and θ , do not respond to Ca^{2+} but remain responsive to DAG (Mellor and Parker, 1998). Finally, the atypical PKCs, PKC- ζ and ι are unresponsive to both. These differences in activation are mirrored by structural differences (Fig. 1.2). The classical isoforms contain 4 conserved domains (C1-C4). The C1 responds to DAG and the C2 to calcium. However in novel isoforms, the classical C2 domain is absent, instead there is a C2-like domain which has an altered structure preventing its ability to respond to calcium (Pappa et al., 1998).

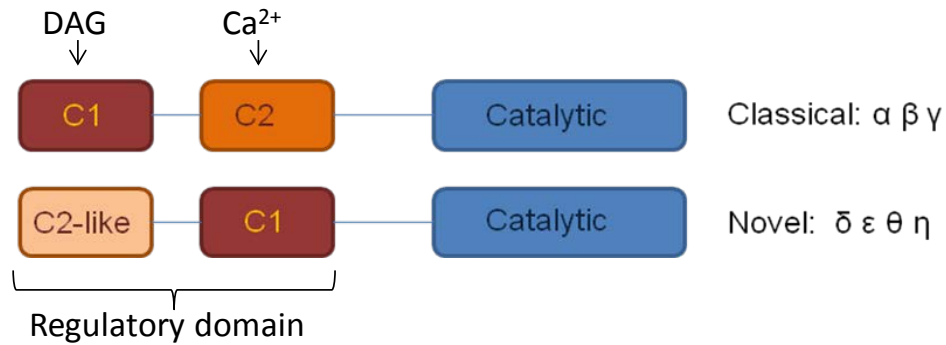


Figure 1.2: Classical PKC structure compared with novel PKC structure

1.3.2 PKC-δ primary structure

1.3.2.1 The catalytic domain

PKC-δ comprises of catalytic and regulatory portions. The catalytic domain has two conserved domains C3 and C4 that are conserved amongst all PKCs. The pseudosubstrate site of the regulatory domain, positioned between the C1 and C2 domains, binds at the C4 domain where it (auto)-inhibits kinase activity (Xu et al., 2004). The crystal structure of the PKC-δ catalytic domain has not been solved but it is available for the most closely related PKC-θ catalytic domain. The PKC-θ structure was solved in complex with staurosporine, a protein kinase inhibitor that acts by preventing ATP binding (Xu et al., 2004). Alignment analysis using CLUSTALW2 shows 64% identical protein sequence between the two isoforms (Fig. 1.3).

CLUSTAL 2.1 multiple sequence alignment

```

sp|Q05655|KPCD_HUMAN      MAPFLRIAFNSYELGSLQ-AEDEANQPFCAVMKKEALSTERGKTLVQKQKPTMYPEWKSTF 59
sp|Q04759|KPCT_HUMAN      MSPFLRIGLSNFDGSCQSCQGEAVNPHYCAVLVKEYEVESENGQMYIQKKPTMYPWDSTF 60
*:*:*:*:*:*:*:*:*:*:*:*:*:*:*:*:*:*:*:*:*:*:*:*:*:*:*:*:*:*:*:*:*:*:*:*

sp|Q05655|KPCD_HUMAN      DAHIYEGRVIQIVLMRAAEPEVSEVTVGVSVLAERCKKNGKAEFWLDLQPAKVLMSVQ 119
sp|Q04759|KPCT_HUMAN      DAHINKGRVMQIIVKGNVDLISSETTVELYSLAERCRKNGKTEIWLELKPQGRMLMNR 120
****:*:*:*:*:*:*:*:*:*:*:*:*:*:*:*:*:*:*:*:*:*:*:*:*:*:*:*:*:*

sp|Q05655|KPCD_HUMAN      YFLEDVDCKQSMRSEDEAKFPPTMNRGAIKQAKIHYIKNHEFIATFFGQPTFCSVCKDFV 179
sp|Q04759|KPCT_HUMAN      YFLEMSDTKDMNEFETEGFFALHQRRGAIKQAKVHHVKCHEFTATFFPQPTFCSVCHFEV 180
****:*:*:*:*:*:*:*:*:*:*:*:*:*:*:*:*:*:*:*:*:*:*:*:*:*:*:*:*

sp|Q05655|KPCD_HUMAN      WGLNKQGYQCRQCNAAIHKKCIDKIIIGRCTGTAANSRDTIFQKERFNIDMPHRFKVHNYM 239
sp|Q04759|KPCT_HUMAN      WGLNKQGYQCRQCNAAIHKKCIDKVIKCTGSAINSRETMPHKERFKIDMPHRFKVNYK 240
*****:*:*:*:*:*:*:*:*:*:*:*:*:*:*:*:*:*:*:*:*:*:*:*:*

sp|Q05655|KPCD_HUMAN      SPTFCDHCGSLWGLVKQGLKCEDCGMNVHHCREKVANLCGINQKLLAEALNQVT---- 295
sp|Q04759|KPCT_HUMAN      SPTFCEHCGTLLWGLARQGLKCDACGMNVHHCQTKVANLCGINQKLLAEALAMIESTQQ 300
*****:*:*:*:*:*:*:*:*:*:*:*:*:*:*:*:*:*:*:*:*:*:*:*:*

sp|Q05655|KPCD_HUMAN      QRASRRSDSASSE-PVGI-----YQGFEEKTVGAGEDMQDNSGTGYGKIW 338
sp|Q04759|KPCT_HUMAN      ARCLRDTEQIFREGPVEIGLPCSIKNEARPPCLPTPGKREPQGISWESPLDEVDMKCHLP 360
*.*:*:*:*:*:*:*:*:*:*:*:*:*:*:*:*:*:*:*:*:*:*:*:*:*

sp|Q05655|KPCD_HUMAN      EG-----SSKCNINNFIFHKVLGKGSFGKVLGELKGRGEYFAIKALKKDVVLIDD 389
sp|Q04759|KPCT_HUMAN      EPELNKERPSLQIKLKIEDFILHKMLGKGSFGKVFLEAFKKTNQFFAIKALKKDVVLMD 420
*.*:*:*:*:*:*:*:*:*:*:*:*:*:*:*:*:*:*:*:*:*:*:*:*

sp|Q05655|KPCD_HUMAN      DVECTMVEKRVLTLLAENPFLTHLICTFQTKDHLFFVMEFLNGGDLMYHIQDKGRFELYR 449
sp|Q04759|KPCT_HUMAN      DVECTMVEKRVLSLAWHPFLTHMFPCTFQTKENLFFVMEYLNNGGDLMYHIQSCHKFDLSR 480
*****:*:*:*:*:*:*:*:*:*:*:*:*:*:*:*:*:*:*:*:*:*:*:*

sp|Q05655|KPCD_HUMAN      ATFYAAEIMCGLQFLHSGKGIYRDLKLDNVLLDRDGHKIIADFGMCKENIFGESRASTFC 509
sp|Q04759|KPCT_HUMAN      ATFYAAEIIILGLQFLHSGKGIYRDLKLDNILLDKDGHKIIADFGMCKENMLGDAKTNTF 540
*****:*:*:*:*:*:*:*:*:*:*:*:*:*:*:*:*:*:*:*:*:*:*:*

sp|Q05655|KPCD_HUMAN      GTPDYIAPEIILQGLKYTFSDVWWSFGVLLYEMLIGQSPFHGDEDELFSIRVDTPHYPR 569
sp|Q04759|KPCT_HUMAN      GTPDYIAPEIILGQKYNHSDVWWSFGVLLYEMLIGQSPFHGQDEEELFHSIRMDNPFYPR 600
*****:*:*:*:*:*:*:*:*:*:*:*:*:*:*:*:*:*:*:*:*:*:*

sp|Q05655|KPCD_HUMAN      WITKESKDILEKLFEREPTKRLGVTGNIKIHPFFKTINWTLLEKRRLEPPFRPKVKSPPD 629
sp|Q04759|KPCT_HUMAN      WLEKEAKDLLVKLFVREPEKRLGVRGDIRQHPLFREINWEELEKERKIDPPFRPKVKSPPD 660
*:*:*:*:*:*:*:*:*:*:*:*:*:*:*:*:*:*:*:*:*:*:*:*

sp|Q05655|KPCD_HUMAN      YSNFDQEFLENEKARLSYSDKNLIDSMDQSAFAGFSFVNPKEHLLLED 676
sp|Q04759|KPCT_HUMAN      CSNFDKEFLNEKPRLSFADRALINSMDQNMFRNFSFMNPGMERLIS 706
*****:*:*:*:*:*:*:*:*:*:*:*:*:*:*:*:*:*:*:*:*:*:*

```

Results for Total Sequence

SeqA	Name	Length	SeqB	Name	Length	Score
1	sp Q05655 KPCD_HUMAN	676	2	sp Q04759 KPCT_HUMAN	706	64.0

Results for Kinase Domain Sequence (highlighted)

SeqA	Name	Length	SeqB	Name	Length	Score
1	sp Q05655 KPCD_HUMAN	334	2	sp Q04759 KPCT_HUMAN	333	72.0

Figure 1.3: Alignment analysis of PKC-δ protein sequence showing comparison with PKC-θ performed using CLUSTALW2. PKC-δ sequence (KPCD_HUMAN) (GENE ID: 5580 PRKCD (Homo sapiens)), PKC-θ sequence (KPCT_HUMAN) (GENE ID: 5588 PRKCQ (Homo sapiens)). Highlighted region shows PKC-θ

kinase domain protein sequence expressed by Xu et al, in comparison with PKC- δ .

The Xu et al paper (2004) determines the kinase domain (of PKC- θ) expressed for structural studies to be residues 362 to 706. Alignment analysis of this region of the PKC- θ sequence identifies a region of the PKC- δ sequence which has 72% identical sequence (Fig. 1.3 highlighted). The domain studied by Xu et al is highly conserved with that of the PKC- δ sequence, thus it is likely to bear strong similarities in structure.

The PKC- θ crystal structure shows the conserved core of the catalytic domain consists of a small N-terminal lobe and a larger C-terminal lobe. The two are linked by a hinge of four amino acid residues. The N-terminal lobe consists of a β -sheet structure, which contains five β -strands (β 1-5 in Fig. 1.4), and two α -helices (α B-C in Fig. 1.4). The C-terminal lobe is primarily helical consisting of eight α -helices. Positioned at the interface between the N-terminal and C-terminal lobes is the active site. This is formed by an adjacent ATP binding site and a peptide-substrate binding site. A glycine-rich loop, between the N-terminal lobe β 1 and 2 strands, indicated in Figure 1.4, binds phosphate. The loop appears very mobile as a multitude of conformations are seen amongst crystals.

There are three catalytically vital residues, one lysine and two aspartic acid, which are conserved among all protein kinases. Surrounding the active site is

helix αC , this aligns and binds the substrate for catalysis. An activation loop, containing one of the essential aspartic acid residues, also contains a essential phospho-threonine residue (position 538) shown in Figure 1.4. Phosphorylation of this threonine residue is required for activity (Liu et al., 2002); it enables the active site to form the correct conformation.

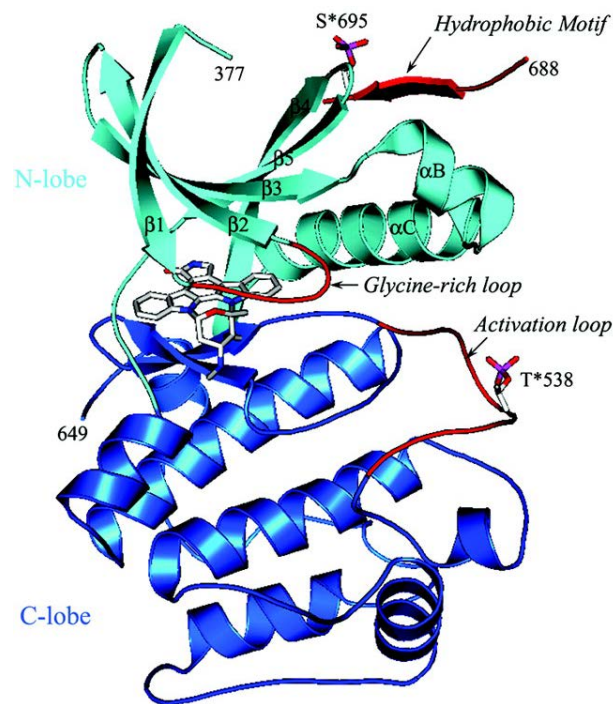


Figure 1.4: Crystal structure of the catalytic domain of PKC- θ . The N-terminal lobe is in light blue and the C-terminal lobe in dark blue. The ring structure in the centre is staurosporine. (Xu et al., 2004)

In the ATP-binding site, staurosporine bonds, via hydrogen-bonds, with three residues. Similar hydrogen bonding between the staurosporine lactam ring and

the glutamic acid and leucine residues has been seen on each occasion the ATP binding site region of a protein kinase structure has been solved.

Structural studies indicate that there are three main conformations of the catalytic domain: 'open', 'closed' and 'intermediate' (Johnson et al., 2001; Xu et al., 2004). In the Xu et al study, the N and C-terminal lobes generally form the 'intermediate' state. The positioning of the glycine-rich loop (which binds phosphate) is more variable. In this PKC- θ structure, the glycine-rich loop is seen to position inside the phosphate-binding site. In an ATP-binding situation this positioning would interfere with the nucleotide phosphate by allowing a closed conformation to be both induced and stabilised. The residues critical for catalysis are significantly inaccessible in this case. These conformational changes exemplify the flexibility of the PKC- θ structure in response to ligand binding.

The activation loop, part of the C-terminal lobe, forms part of the substrate binding surface. In combination with α C helix it can also create a docking surface for co-factors. Amongst the wider group of kinases, these two regions, the activation loop and the α C helix, are highly variable. Phosphorylation of the activation loop can induce structural changes whereby folding allows formation of an active site. For PKC- θ , the phosphorylated residue is threonine 538, positioned between two invariable motifs of Asp-Phe-Gly and Thr-Pro-Asp. All three oxygens of the phosphate group on Thr-538 are involved in hydrogen-bonding (Fig. 1.5). The phosphorylation of this residue is critical for catalysis, and alanine substitution reduces enzyme activity 100-fold (Liu et al., 2002) whereas a

mutant of T538E shows a three-fold decrease in enzymatic activity (Xu et al., 2004).

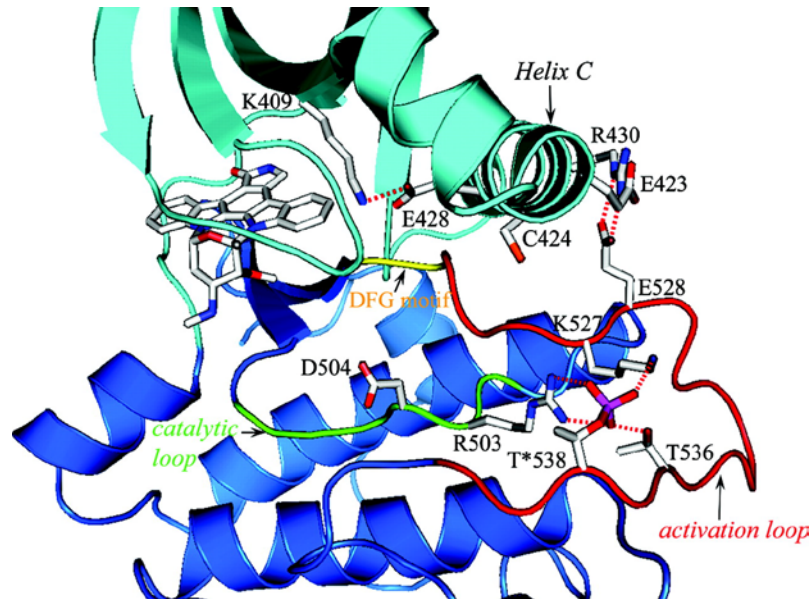


Figure 1.5: The structure of the activation loop and α C helix necessary for catalysis. Light blue indicates the N-terminal lobe and dark blue the C-terminal lobe.

1.3.2.2 The regulatory domain

The regulatory domain of PKCs was first identified in 1986, as a region separate to the catalytic part, able to bind diacylglycerol, calcium ions and phosphatidylserine (Lee and Bell, 1986). The regulatory portion of the protein is further segmented into a C1 domain, an autoinhibitory or pseudosubstrate sequence, and a C2 domain. In novel forms the C2 domain is replaced by a C2-like

domain, which is positioned at the N-terminus (Steinberg, 2008). In the inactive state the PKC regulatory region folds over and interacts with the catalytic region, thus regulating inappropriate catalytic activity. Activation of PKC- δ induces the release of C1 and C2, thus freeing the catalytic domain and allowing it to act.

The pseudosubstrate sequence is N-terminal to the C1 domain and resembles the consensus sequence at which PKC isozymes bind and phosphorylate (Mellor and Parker, 1998). However, the phosphate-receiving serine or threonine is replaced by an alanine residue. In PKC- δ , binding of DAG or phorbol esters induces an activating conformational change. This releases the pseudosubstrate site, and leads to protein activation (Steinberg, 2008).

1.3.2.3 PKC- δ C1 domain

The C1 domain is a region of the regulatory domain of all PKCs. In classical and novel PKCs it is activated by DAG or phorbol ester binding (Ono et al., 1989). It is a 5kDa globular domain comprising of two β -sheets (Zhang et al., 1995) and is rich in cysteine residues (Ono et al., 1989). The C1 domain is a conserved domain that is not only present in the PKC isoforms, but also in several other proteins including DAG kinase and PKD. In classical and novel isozymes there are two cysteine-rich regions; in atypical isozymes there is only one of these regions (Solodukhin et al., 2002). The cysteine-rich regions form zinc finger structures; these are coordinated by two Zn^{2+} ions (Kazanietz et al., 1995). When the two β -

sheets of the C1 domain are moved apart, a DAG and phorbol ester binding pocket is revealed (Giorgione et al., 2006).

The C1 domain has been shown to sub-divide into two regions, a C1A and a C1B region (Hurley et al., 1997). Each of these regions contains a cysteine-rich zinc finger. These regions respond to DAG and phorbol esters (which mimic the action of DAG) (Cho, 2001). In PKC- α , - β II, - δ and - ϵ C1A is seen to bind with a high affinity to DAG and C1B to phorbol esters (Stahelin et al., 2004; Steinberg, 2008). The differences in the C1 domain of the atypical isoforms means that it does not retain its normal function due to an impaired ligand-binding pocket (Giorgione et al., 2006).

Binding of DAG to the PKC- δ C1 domain is phosphatidylserine (PS) dependent (Mellor and Parker, 1998; Stahelin et al., 2004). Interactions with PS allow the positioning of the C1 domain to be such that it can penetrate the membrane bilayer and bind DAG (Steinberg, 2008). Binding to DAG allows membrane targeting; the C1 is critical for this localisation and activation (Stahelin et al., 2004). The PKC- δ C1 domain has a further capability that has not been identified in other isoforms. Tyrosine residues 155 and 187 can be phosphorylated. This can induce signalling differences that may, for example, cause enhanced growth (see 1.3.3).

1.3.2.4 PKC- δ C2 domain

The C2 domain is another domain of the PKC regulatory region. In classical isoforms the domain interacts with calcium ions, but this ability is lost in the C2 domain of the novel isoforms (Ponting and Parker, 1996). The C2 domain is larger than the C1 domain with an approximate size of 16kDa (Giorgione et al., 2006). It is also globular and composed primarily of β -strands, 8 in all, positioned anti-parallel. Strands β 1, β 4, β 7 and β 8 form one β -sheet, whilst strands β 2, β 5 and β 6 form another (Figure 1.6). The C2 domain is conserved in synaptotagmins and phospholipases as well as PKCs (Ponting and Parker, 1996). The conservation of the C2 domain is demonstrated in crystal structures of numerous proteins; these indicate that there are two types of C2, the S-type and P-type (Essen et al., 1997). The two types show different arrangement of folding. The S-type variant is seen in synaptotagmin 1, whilst the P-type variant is seen in phospholipase C- δ and phospholipase A2 (Essen et al., 1997). Sequence analysis of PKC C2 domains indicates that classical PKCs adopt the S-type topology, whilst novel PKCs adopt the P-type.

The PKC- δ C2 crystal structure confirms the P-type topology (Pappa et al., 1998). Superimposition of this structure with the relevant domains of synaptotagmin I and phospholipase C- δ reveal a similar core of four hydrophobic residues of leucine (position 5), proline (position 28), Phenylalanine (position 59) and a further leucine (position 108).

The PKC- δ C2-like domain does not respond to calcium ion levels as, although it has the general C2 domain features, it does not feature the loops that coordinate with calcium ions (Pappa et al., 1998). In fact the part of the C2 structure demonstrating the greatest contrast to other C2 structures is the area important in calcium ion-binding. This area is adjacent to three loops towards one end of the structure. In the PKC- δ C2 these loops show a considerably different conformation. Four out of the five residues which normally co-ordinate with the calcium ions are absent. The residue remaining is Asp79, which plays a structural role in the domain. Although there are many structural differences, the C2 domain does still bind PS (Pappa et al., 1998). Binding of PS in novel PKCs appears to be constitutive.



Figure 1.6: PKC- δ C2 domain structure showing the 8 β -strands (1-8). C indicates the C-terminal end, and N, the N-terminal end of the domain.

It is thought that the C2-like domain functions as a protein interaction domain in PKC- δ (Dekker and Parker, 1997; Mellor and Parker, 1998). For example, Lopez-Lluch et al (2001) showed the C2 domain binding f-actin in neutrophils. This was an important interaction for enabling the redistribution of f-actin.

1.3.3 PKC- δ regulation

The PKC family of proteins are traditionally known to be activated via calcium ion and lipid binding (in the form of diacylglycerol (DAG)). Novel forms of PKCs, such as PKC- δ , are not affected by calcium ions, but can still be activated by DAG. This binding occurs at the C1 domain and allows the PKC- δ to be recruited to a membrane. In classical forms of PKC, the C2 domain shows some affinity for membranes where, following calcium activation, the C2 domain targets the membrane where C1 can bind. In PKC- δ , the C2 domain has no affinity for membranes; instead the C1 domain has an increased affinity (two orders of magnitude higher) (Giorgione et al., 2006). The C1A portion of the C1 domain is the region that interacts with the DAG (Stahelin et al., 2004). PKC- δ preferentially relocates to phosphatidylserine (PS) rich membranes. Interaction with PS allows the C1 to 'unlock' and bind DAG. The residue Glu177 is key in controlling DAG accessibility to the C1 domain (Stahelin et al., 2004).

There are several tyrosine residues in PKC- δ and it has been considered that this may be a method of targeting the protein to the correct cellular region in order

to exert its effects appropriately. For example, the literature describes a situation where tyrosine phosphorylation occurred at two residues Tyr64 and Tyr155 in order to cause translocation of PKC- δ to the nucleus where it is cleaved and has pro-apoptotic effects (Humphries et al., 2008).

Phosphorylation of different tyrosine residues has been identified after treatment of cells with etoposide. In this case, the affected residues are Tyr64 and Tyr187 (Blass et al., 2002). Phosphorylation of these residues appears to be linked to etoposide-induced apoptosis. Following etoposide treatment, the PKC- δ became phosphorylated. This induced nuclear translocation where it was subsequently cleaved by caspases. Both the regulatory and catalytic domains were found necessary for this apoptotic pathway to occur. Mutants of PKC- δ , where 5 tyrosine residues were mutated to phenylalanine, showed decreased apoptosis. Caspase-3 activation and cleavage of the mutant PKC- δ were also lowered (Blass et al., 2002). Subsequent generation of mutants identified Tyr64 and 187 as the key participants.

H₂O₂ stimulation has been found to affect tyrosine phosphorylation. Tyrosine phosphorylation of residues 311, 332 (in the hinge region) and 512 (in the catalytic domain) has been identified (Konishi et al., 2001). Tyr311 appears to be the predominant site of phosphorylation. This tyrosine phosphorylation coincides with an increase in the activity of PKC- δ ; however membrane targeting does not occur. An *in vitro* study identified that Lck could phosphorylate the Tyr311 residue, and that this produced an increase in PKC- δ activity. Mutation analysis

was performed on the three residues, and although all three are phosphorylated following H₂O₂ stimulation, only Tyr311 mutation to phenylalanine produced an effect on activity.

With respect to protein binding in H₂O₂ stimulated conditions, Morita et al (2008) found that EGFR phosphorylates Tyr332, but does not also do this under EGF treatment. They also identified PKC- δ p-tyr binding with an adaptor protein p66Shc (which contains two p-tyr binding domains), which they hypothesize may play a role in stress-signalling.

Tyrosine 311 has been identified to be phosphorylated under further conditions. It is seen in $\alpha_M\beta_2$ (integrin) signalling, where clustering caused translocation of PKC- δ to the plasma membrane and Tyr311 phosphorylation by Hck and Lyn (Xue et al., 2010). Activation of PKC- δ has been found to be required for angiotensin II induced migration of vascular smooth muscle cells. Phosphorylation of Tyr311 was identified as vital for this process (Nakashima et al., 2008).

Additional phosphorylated tyrosine residues have also been identified. A Tyr52 residue was identified to become phosphorylated in response to IgE receptor binding. Mutation studies showed the mutant was not phosphorylated following stimulation (Szallasi et al., 1995).

Thrombin activity was found to cause tyrosine phosphorylation of Tyr311 and Tyr565 in platelets (Hall et al., 2007). Thrombin binding receptors PAR1 and PAR4 induced activity of Src kinase and phospholipase C (PLC). Treatment of PMA also induced this phosphorylation and was dependent on Src activity. Membrane

recruitment of the PKC- δ was essential for phosphorylation, but phosphorylation was not required for membrane localisation. Both thrombin and PMA induce this translocation, however PMA does this independently of PLC. The thrombin activation causes an increase in PKC- δ activity (Hall et al., 2007).

1.3.4 PKC- δ functional studies

1.3.4.1 Gene knockout and knockdown studies

In order to study the function of PKC- δ , several groups have prevented PKC- δ activity through the use of knockouts, or knockdowns using siRNA (Leitges et al., 2001; Miyamoto et al., 2002; Steinberg, 2004). PKC- δ knockouts are able to develop and reproduce normally but have defects in immunity and vascularisation (Steinberg, 2004). With respect to the immune system, the knockouts have hyperproliferative B-cells. This leads to the development of immune-complex glomerulonephritis, which is inflammation of the glomeruli in the kidney; this can result in renal failure. Hyperproliferation can also cause lymphocyte infiltration into organs (Miyamoto et al., 2002). There are also defects in neutrophil function. This was discovered in a stroke model where the absence of PKC- δ led to a reduction in reperfusion injury following thrombolysis. This was found to be associated with reduced migration of neutrophils into the tissue (Chou et al., 2004).

The PKC- δ knockout mice have also been examined with respect to their likelihood to develop arteriosclerotic lesions where veins had been grafted into

carotid arteries. Vessels from the mice were further examined *in vitro* where the vessel from knockout mice showed further differences. Following UV irradiation fewer reactive oxygen species were produced. In addition when H₂O₂ treated, they were resistant to apoptosis (Leitges et al., 2001).

In addition, studies have examined PKC- δ knockout mice for differences in apoptosis. PKC- $\delta^{-/-}$ mice were examined to see if the absence of PKC- δ would protect salivary gland from apoptosis following treatment with γ -irradiation. This was the case, as the induction of apoptosis was suppressed by more than 60%. The knockout mice parotid cells showed defects in cytochrome C release following etoposide treatment. Caspase-3 activation was also reduced. The activation of p53 was examined following etoposide and γ -irradiation; this showed no differences between knockout or wild-type cells. This indicated activity of PKC- δ was after this point in the apoptotic induction mechanism. JNK is differentially activated between the cell types, suppression of activation is noted in knockout mice. PKC- δ must, therefore, act upstream of this point in DNA-damage induced apoptosis (Humphries et al., 2006; Reyland et al., 1999).

PKC- δ siRNA has been used to knockdown endogenous PKC- δ in order to examine cell binding via E-cadherin. In EGFR over-expressing cells, EGF can induce cell scattering. This process was found to be mediated by PKC- δ . EGF signalling caused internalisation of E-cadherin, thus releasing cell binding and allowing motility. By knocking-down PKC- δ , the internalisation of E-cadherin was prevented and therefore cell scattering was also inhibited (Singh et al., 2009).

1.3.4.2 The role in apoptosis

Apoptosis, programmed cell death, is a method of eliminating cells for tissue homeostasis. The activation of this mechanism is complex with numerous activating and inhibiting proteins involved (Koriyama et al., 1999). PKC- δ has been identified to have a role in the apoptotic mechanism, and although this role has not been fully elucidated, numerous stages of this pathway have been revealed (see below).

During induction of apoptosis the full PKC- δ protein is cleaved, thus activating it and allowing it to initiate the apoptotic program in the nucleus, however its precise activity remains unknown (Koriyama et al., 1999). When treated with apoptotic agents, camptothecin or etoposide, cleaved protein fragments at 40kDa can be identified on a western blot. Caspase-3 (or caspase-3-like) was found to be the enzyme responsible for cleavage of PKC- δ . This was discovered when Ac-DEVD-cho (acetyl-Asp-Glu-Val-Asp aldehyde), which specifically prevents caspase-3 family activity, had an inhibitory effect on fragment formation (Koriyama et al., 1999). The caspase-3 cleavage sites are unknown, however the size of fragments indicates that cleavage occurs in the hinge region.

As mentioned above, in order to perform its apoptotic function, PKC- δ was found to translocate to the nucleus; such translocation would require a nuclear localisation signal (NLS). The NLS of PKC- δ was found to be in the C-terminal end

of the protein (Humphries et al., 2008). The reason why this sequence does not localise PKC- δ to the nucleus in non-apoptotic cells, and instead allows it to remain in the cytoplasm is as yet unclear. There is suggestion that tyrosine phosphorylation is involved in this process. Without this phosphorylation the PKC- δ is in a conformation wherein the nuclear localisation signal is shielded, thus preventing translocation. Phosphorylation at tyrosine residues 64 and 155, in the N-terminal regulatory domain, has been found to induce a change that reveals the NLS, thus directing nuclear translocation. Mutation of these residues to phenylalanine prevented apoptotic induction. However the phosphorylation itself is not seen to be vital for nuclear localisation, as a mutant from tyrosine to aspartic acid, which is phosphomimetic, allows nuclear accumulation.

The tyrosine phosphorylation of PKC- δ can be induced through treatment of apoptotic agents such as etoposide (Humphries et al., 2008). Etoposide treatment of parC5 cells shows an increase in PKC- δ phosphorylation at 30 minutes of treatment, peaking at 60 minutes and decreased to normal levels after 90 minutes of treatment (Humphries et al., 2008). The proteins responsible for this phosphorylation are Src-like tyrosine kinase family members and c-Abl; inhibition of these proteins using the Src inhibitor PP2, blocks both basal tyrosine phosphorylation and that induced by etoposide treatment (Kajimoto et al., 2010).

1.3.4.3 Other important cancer-related functions of PKC- δ

In multicellular organisms the processes of proliferation and apoptosis are regulated in order to maintain tissue homeostasis. The two processes are normally regulated in non-cancerous tissues, however where proliferation is increased over the normal levels, neoplasias result, which can be malignant. Uncontrolled cell proliferation is a hallmark of cancer. Proliferation is a highly complex process mediated by cell cycling during which an increase in cell size and volume of intracellular organelles and other material precedes cell division.

PKC- δ has been shown to demonstrate anti-proliferative activity (Vucenik et al., 2005). IP₆ has been seen to have an anti-cancer function in vitro and in vivo, where it has inhibited growth through inducing cell cycle arrest at G₁. IP₆ treatment of MCF-7 cells induced an increase in activity of PKC- δ .

However the role of PKC- δ in proliferation is not clear (Griner and Kazanietz, 2007; Jackson and Foster, 2004). A role of PKC- δ as a positive regulator of growth has also been indicated; this is via activity in the Ras/ERK1/2 pathway (Grossoni et al., 2007; Keshamouni et al., 2002; Lønne et al., 2009). Thus it seems PKC- δ may perform a multitude of downstream functions dependent on the activating signal, differential tyrosine phosphorylation status (Brodie and Blumberg, 2003; Griner and Kazanietz, 2007), and associated proteins.

The structure of the cytoskeleton is important with respect to a cell's ability to become motile and metastasize. Lopez-Lluch et al (2001) described PKC- δ binding the actin cytoskeleton in neutrophils. This interaction was via the C2 domain.

PKC- δ localised with f-actin filaments in the lamellipodia at the leading edge. The binding, and action, of PKC- δ enables the remodelling of the cytoskeleton and motility of the neutrophil (Lopez-Lluch et al., 2001). If this motility was facilitated in cancer, a cell may be able to relocate and form a secondary tumour.

Additional studies have examined the interactions associated with PKC- δ and the cytoskeleton. Chen et al (2007) further demonstrated PKC- δ binding the cytoskeleton and also noted the PKC- δ phosphorylation of adducin. Adducins promote spectrin and actin interactions allowing the formation of a meshwork. Phosphorylation of adducin downgrades these interactions, suggesting that phosphorylation may allow breakdown of the meshwork. Where PKC- δ was over-expressed, membrane protrusions were identified. At the edges of the protrusions, PKC- δ , adducin and phosphoadducin were detected. This indicates that by acting on adducing PKC- δ may enhance cell motility.

A further role for PKC- δ in cytoskeleton structure has been identified; this is related to the MUC-1 protein. The MUC-1 cytoplasmic domain has been found to interact with several proteins including: β -catenin, *erbB* receptors, *src*, GSK-3 β and PKC- δ (Schroeder et al., 2003). PKC- δ phosphorylates a threonine residue in a T41DR sequence, this allows β -catenin to be recruited to the MUC-1 (Ren et al., 2002). β -catenin thus dissociates from E-cadherin, which is important in cell-cell contacts at adherens junctions. When bound to β -catenin, E-cadherin is linked to the cytoskeleton via α -catenin (Ren et al., 2002) (Fig. 1.7). The movement of β -catenin permits loss of contacts, allowing cell motility (Schroeder et al., 2003).

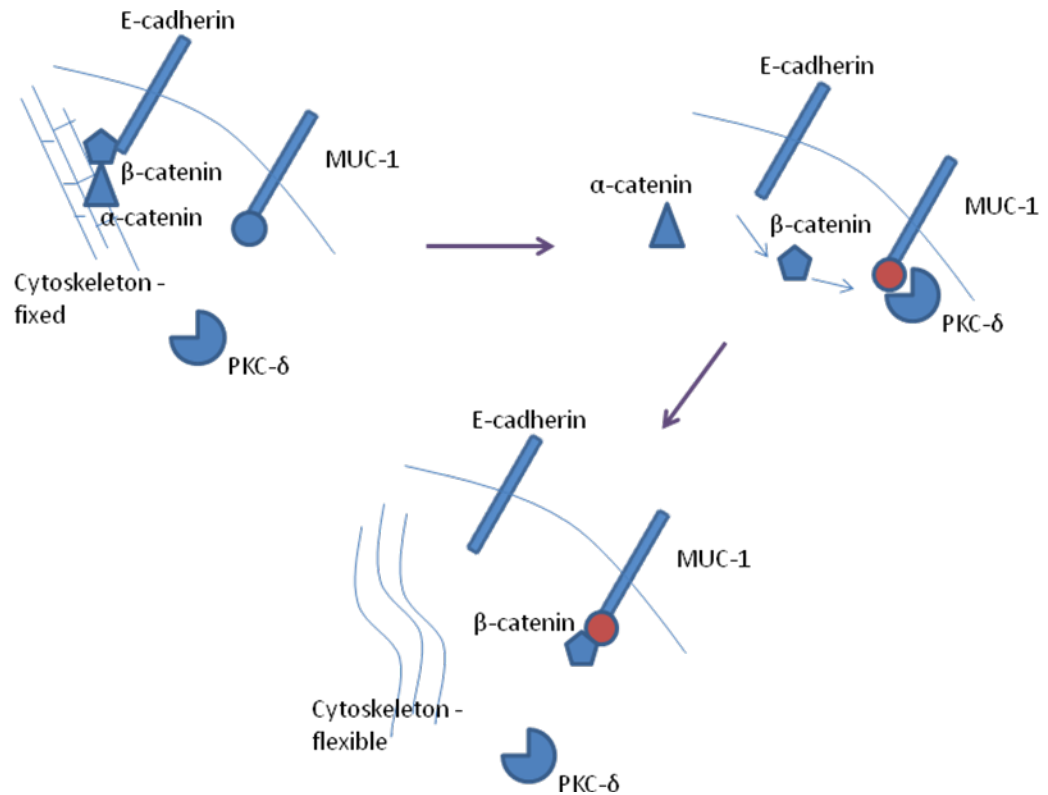


Figure 1.7: The involvement of MUC-1, β -catenin and PKC- δ in cell adhesion and motility. β -catenin binds E-cadherin to the cytoskeleton via α -catenin in order to maintain cell contacts and rigidity. On phosphorylation of MUC-1, by PKC- δ , β -catenin dissociates from E-cadherin, and α -catenin and the cytoskeleton, and bind MUC-1. The loss of β -catenin from the complex enables cell motility (Ren et al., 2002).

1.3.5 PKC- δ C2 interactions

Several studies suggest that the C2 domain of PKC- δ may be a protein interaction domain. Dekker and Parker (1997) were the first to identify a C2-like domain in PKC- δ . They found that this region bound to the PKC- δ substrate GAP-43.

A later study further examined the role of PKC- δ C2 binding in neutrophils (Lopez-Lluch et al., 2001). They discovered that the C2 domain bound f-actin. When the C2 region was injected into areas where there was no localisation of actin, there was major disruption to the actin cytoskeleton.

Benes et al (2005) examined the C2 domain to discover if there was a particular region that could be attributed to the protein binding activity demonstrated in the literature. They found that, in addition to the two families of phosphotyrosine binding (PTB) domains known, there was a third type of which the C2 domain can also be considered a member. PTBs were initially identified in classical PKC's where they allowed calcium and lipid binding. The C2 domain present in PKC- δ is also seen in other PKCs where the calcium binding property is not retained; in PKC- δ the PTB lipid binding property is also lost.

An interaction was identified between PKC- δ and a transmembrane protein CDCP1, which is over-expressed in colon cancer (Benes et al., 2005). A correlation between the CDCP1 tyrosine phosphorylation state and the interaction with the PKC- δ regulatory domain was noted. This suggested that the regulatory domain of PKC- δ contained a PTB region. Screens of a phosphotyrosine peptide library and a subset of peptides containing tyrosine or phenylalanine at a position 3 residues C-terminal to phosphotyrosine showed the regulatory domain did indeed have a PTB with a consensus sequence of Y/F-S/A-V/I-pY-Q/R-X-Y/F-X (Benes et al., 2005). These screens also suggested that MUC-1

may have such a sequence, inferring a possible interaction at the C2 domain in the role described in 1.3.4.3.

1.4 PKC- δ and breast cancer

1.4.1 *Clinical correlations*

A study in 1989 examined clinical samples from normal breast tissue and breast tumours. They identified that the levels of PKC found in the samples from the tumours were higher than in normal breast tissue (O'Brian et al., 1989). A further study (Gordge et al., 1996), showed the increase in PKC activity to be calcium-dependant .

A later study, in 2008, specifically examined PKC- δ expression in clinical samples. PKC- δ expression was greater in ER⁺ tumours compared with ER⁻ tumours. In addition, a higher level of PKC- δ expression correlated with reduced survival of the patient. The grade 3 tumours had higher PKC- δ expression than the grade 1 and 2 tumours, correlating with the findings related to survival (McKiernan et al., 2008).

PKC- α was also found to share a correlation with the ER status of tumours; PKC- α and PKC- δ levels were examined in combination to further investigate this feature. Where PKC- δ and PKC- α levels were examined, high PKC- δ was found in ER⁺ tumours, whilst high PKC- α was found in ER⁻ tumours. Where PKC- δ was expressed and PKC- α was not, these patients had an endocrine response to tamoxifen 6-times longer than those with PKC- δ and PKC- α expression (Assender

et al., 2007). This suggests that examining both PKC- δ and PKC- α levels could enable a treatment regime tailored to the patients requirements.

1.4.2 Cellular studies

In addition to the clinical research, studies in cell lines have also examined PKC levels. These studies showed that PKC levels were higher in tumours that were ER⁻ compared with those that were ER⁺ (O'Brian et al., 1989).

Specific isoform studies examined the correlations between PKC- δ levels and ER status further. Shanmugam et al (1999) found oestrogen treatment of ER⁺ MCF-7 breast cancer cells resulted in decreased PKC- δ protein levels. This indicates a role for PKC- δ in ER signalling. In addition, the expression of the PKC- δ and PKC- α isoforms in ER⁺, either tamoxifen sensitive or resistant, and ER⁻ cell lines were examined. The ER⁺ cells lines expressed PKC- δ but very little PKC- α levels. This was the opposite in ER⁻ cell lines. The tamoxifen resistant ER⁺ cell lines strongly expressed both isoforms (Assender et al., 2007). Treatment resistance is a growing problem in oncology. This data indicates PKC- δ may have a role in tamoxifen resistance. Possible roles of PKC- δ need to be investigated further in order to develop methods for overcoming resistance.

Further investigation into tamoxifen-resistance showed PKC- δ aided cell growth where cells were oestrogen sensitive (Nabha et al., 2005). Over-expression of PKC- δ in tamoxifen sensitive cells led to cells developing resistance. Higher PKC- δ

levels are found in tamoxifen resistant tumours than sensitive tumours. This indicates PKC- δ could be a target for treatment in tamoxifen resistance.

A further study examined radiation sensitivity in relation to PKC- δ activity. PKC- δ was found to protect against ionising radiation. Where cells were treated with an anti-sense oligonucleotide against PKC- δ , cell survival, following 5.6Gy γ -radiation, was inhibited (McCracken et al., 2003).

1.4.3 Apoptosis

In order to better understand how PKC- δ aids or hinders cell survival, the involvement of PKC- δ in apoptosis has been studied in numerous cell types (Brodie and Blumberg, 2003). These studies indicate a pro-apoptotic role for PKC- δ (see 1.3.4.2). Similar studies have been performed in MDA-MB-231 breast cancer cells. These showed that PKC- δ had an anti-apoptotic activity in these cells (Lønne et al., 2009). Investigation of this effect showed that the anti-apoptotic mechanism was active due to a *ras* mutation in the cell line. This mutation causes over-phosphorylation of ERK1/2. The PKC- δ inhibited NEDD4, which would normally ubiquitinylate MKP3 causing its degradation. MKP3 reduced the phosphorylation level of ERK1/2 to a level at which it was not fatal, thus allowing the cells to survive. This activity was proteasome-dependent. Where proteasome activity was inhibited the MKP3 could not be degraded, therefore the de-phosphorylation of ERK1/2 was still possible and the cells survived (Lønne et al., 2009).

1.4.4 Cytoskeleton and metastasis

PKC- δ has been shown to interact with the cytoskeleton in numerous cell types (see 1.3.4.3). The cytoskeleton enables a cell to form a stable structure; the cytoskeleton links to focal adhesions where the cell attaches to a surface. Alterations in the cytoskeletal links to the adhesive structures allow the cell to become flexible and motile. Evidence indicates that PKC- δ interaction with the cytoskeleton may affect the ability of cells to become motile, as described below. Kiley et al (1999b) demonstrated that PKC- δ displayed a positive effect towards metastasis in breast cancer cell lines. Relative levels of PKC- δ were greater in those cell lines which displayed a highly metastatic growth pattern. PKC- δ over-expression in cell lines displaying low or moderate metastatic activity showed significant increase in anchorage-independent cell growth. This anchorage-independent growth was inhibited when the regulatory fragment of PKC- δ was over-expressed. Examination of this effect revealed the sub-cellular localisation of PKC- δ and phosphorylation of adducin was altered. This suggests a link by which PKC- δ may alter a cell's migration and adhesion phenotype.

Further studies by Kiley et al (1999a) have additionally indicated an important role for PKC- δ in metastasis of breast cancer. Cell lines were developed from mammary tumours in the rat fat pad, one of these demonstrated a more rapid growth pattern and greater metastatic potential. Upon examination, a 3-fold greater expression of PKC- δ was discovered. Upon induction of PKC- δ regulatory

fragment expression in mice, the growth of primary tumours was not affected, however the development of metastases were reduced.

PKC- δ interactions demonstrate a clear relationship with metastasis through the literature. However, when contemplating the Kiley papers (1999a; 1999b) it is worth noting that the over-expression of the regulatory domain could create the illustrated effect through 'mopping up' of DAG and thus thwarting PKC- δ activation, rather than binding to the catalytic domain and preventing its action.

1.5 Studying PKC- δ C2 domain in breast cancer cell lines

MDA-MB-468 (Cailleau et al., 1978), MDA-MB-231 (Cailleau et al., 1974) and MCF-7 (Soule et al., 1973) are well characterised cell lines originating from breast adenocarcinomas. All are epithelial type obtained from female patients of 51-69 years of age. Numerous differences have been observed in the literature between these cell lines, some of which are summarised in Table 1.2 (Lønne et al., 2009; Rincon et al., 2004; Shanmugam et al., 2001). Differences in signalling have been noted, whereby inhibition of the ERK1/2 pathway supports survival in MDA-MB-231 cells but does not in MDA-MB-468 and MCF-7 (Lønne et al., 2009). Thus as breast cancer tumours display wide heterogeneity, it is hoped that a more complete picture of PKC- δ involvement, in differing breast cancers, can be obtained by studying these three cell lines which, although all originating from breast epithelial adenocarcinomas, demonstrate significant differences.

Table 1.2: Differences between MDA-MB-468, MDA-MB-231 and MCF-7 cell lines

	MDA-MB-468	MDA-MB-231	MCF-7
Karyotype¹	hypodiploid	hypotriploid	hypotriploid to hypotetraploid
Oestrogen receptor¹	-	-	+
Progesterone receptor¹	-	-	-
Her2 receptor²	-	-	-
Ras mutation³	-	+	-
PKC-δ levels⁴	As MCF-7	Lower than MCF-7	Higher than MDA-MB-231
Retinoic acid activates	-	-	+
PKC-δ to lower IRS-1⁵			
Genistein response⁶	Apoptosis	Growth arrest	Stimulates growth

¹(Cell lines service) ²(Tseng et al., 2006; Yamaguchi et al., 2005) ³(Lønne et al., 2009) ⁴(Shanmugam et al., 2001) and thesis data ⁵(Rincon et al., 2004) ⁶(Dampier et al., 2001)

Literature demonstrates the extensive involvement of PKC- δ in signalling events within the cells (Chen et al., 2009; Kharait et al., 2006; Khwaja and Tatton, 1999; Vucenik et al., 2005). PKC- δ been identified as a key component of the apoptotic pathway, whereby its nuclear translocation and cleavage between the regulatory and catalytic domains allow its action in the nucleus (DeVries-Seimon et al., 2007; Humphries et al., 2008). Due to the wide action of PKC- δ , creating cell lines which over-express the protein, and which over-express the C2 domain of the protein, allows analysis of the effects on cell signalling pathways.

1.6 Aims

The C2 domain is a regulatory domain that has been identified as a protein binding region in particular circumstances. Expression of the C2 domain was hypothesised to interfere with endogenous PKC- δ activity through competitive inhibition of interactions with binding partners; Figure 1.8 is an illustration of this hypothesis. The reactions of the cells to myc- δ C2 expression will indicate the role of the endogenous PKC- δ in the cells. There may be differing roles with the differing cell lines and roles of PKC- δ .

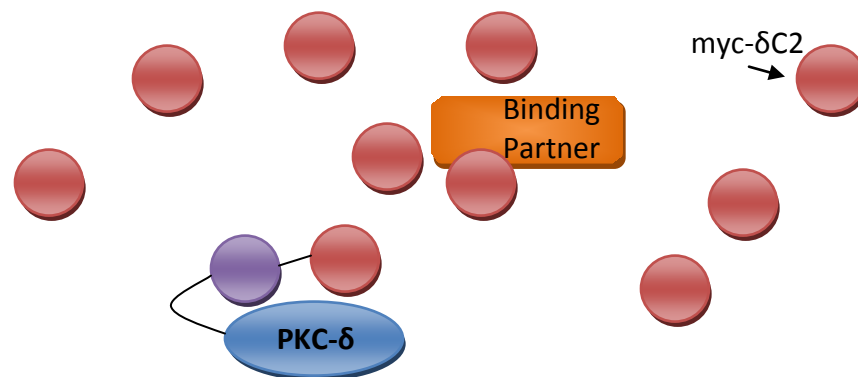


Figure 1.8: Model for the hypothesis of how the myc- δ C2 over-expression will affect endogenous PKC- δ . The endogenous PKC- δ C2 domain is out-competed for the binding partner, thus the normally occurring pathway is affected.

This thesis investigates this premise, and the effects of myc- δ C2, or myc-PKC- δ , expression upon the cell lines. The interruption of endogenous PKC- δ signalling by myc- δ C2 aims to reveal alterations in the cell profile, thus allowing analysis of

endogenous PKC- δ activity. Identification of myc- δ C2 localisation aims to reveal information regarding the role for the C2 domain in PKC- δ function. Subsequent analysis of the cell lines and their differences will allow further, in-depth, clarification of the importance of the C2 domain to PKC- δ activity. Literature evidence indicates PKC- δ plays a role in key factors such as cell death and motility (Humphries et al., 2008; Kiley et al., 1999b). Thus, this investigation aims to reveal a clearer picture as to whether the C2 domain may be a suitable target for interfering with these key processes to provide a cancer treatment.

Chapter 2: Materials and Methods

2.1 Materials

Table 2.1: Buffers

Buffer	Recipe	Storage
10x TAE	0.8M Trizma base(Sigma, Gillingham, UK), 1.1% glacial acetic acid, 0.1M EDTA	Room Temperature (RT)
1x PBS	1 tablet (Oxoid, Basingstoke, UK) dissolved in 100ml water, tablets contain: sodium chloride 8g/l, potassium chloride 0.2g/l, di- sodium hydrogen phosphate 1.15g/l, potassium dihydrogen phosphate 0.2g/l	RT
Cell lysis		
MUC-1 lysis buffer	50mM tris-HCl pH7.6, 150mM NaCl, 0.1% Nonidet P-40 substitute, 1mM dithiothreitol (DTT), 1 (cOmplete mini EDTA-free) Protease inhibitor cocktail tablet (Roche, Basel, Switzerland)	-20°C
IP lysis buffer stock	150mM NaCl, 1% Nonidet P-40 substitute, 50mM Tris-HCl pH8	RT

10x Phosphatase inhibitor mix	250mM β -glycerophosphate, 100mM sodium tartrate, 50mM sodium molybdate, 100mM sodium vanadate	-20°C
IP lysis buffer	90% IP lysis buffer stock, 10% 10x Phosphatase inhibitor mix, 1 Protease inhibitor cocktail tablet	-20°C

SDS-PAGE and Western blotting

20x Running buffer	0.8M Tricine, 1.2M Trizma base, 70mM sodium dodecyl sulphate (SDS), 50mM sodium bisulphite	RT
Towbin transfer buffer	25mM Trizma base, 200mM glycine, 1mM SDS, methanol was added just prior to use in the ratio 8ml buffer to 2ml methanol	RT
PBST	PBS with 0.1% Tween 20	RT
PBSTM	PBST with 0.5% Marvel milk powder	RT

Flow cytometry

10x FITC-AnnexinV binding buffer	0.1M HEPES pH7.4, 1.4M NaCl, 25mM CaCl ₂ , made in water	4°C
Hypotonic fluorochrome solution	40 μ M sodium citrate, 1% Triton X-100, 50 μ g/ml propidium iodide, 0.1mg/ml RNase A (Sigma, Gillingham, UK)	4°C

Immunofluorescence

Fixation buffer	4% formaldehyde, 0.1% glutaraldehyde, in PBS	-20°C
Permeabilization buffer	0.5% triton X-100, in PBS	-20°C
Quenching buffer	1mg/ml sodium borohydride, in PBS	Fresh
Blocking buffer	5% goat serum, in PBS	-20°C
FITC-Phalloidin	0.1% FITC-Phalloidin, in PBS	Fresh

solution

Table 2.2: Antibodies

Antibody	Usage	Storage
PKC-δ (western) antibody	1:500 PKC- δ antibody (C-20 and C-17) diluted in PBST (sc-937 and sc-213, Santa Cruz Biotechnology, Santa Cruz, CA,USA)	Fresh
c-myc (western) antibody	1:500 c-myc antibody (9E10) diluted in PBST (GTX75953, GeneTex, Irvine, CA,USA)	Fresh
ERK1/2 (western) antibody	1:1000 ERK1/2 antibody diluted in PBST (4696S, Cell Signalling Technology, Danvers, MA, USA)	Fresh
Phosphorylated-ERK1/2 (western) antibody	1:1000 phosphorylated ERK1/2 antibody diluted in PBST (9101S, Cell Signalling Technology, Danvers, MA, USA)	Fresh
Phosphorylated-tyrosine (western) antibody	1:500 p-tyrosine antibody diluted in PBST (ab9319, Abcam, Cambridge, UK)	Fresh
Histone (western) antibody	1:2000 histone H3 antibody diluted in PBS and 5% milk (ab1791, Abcam, Cambridge, UK)	-20°C
Anti-rabbit (western) antibody	1:2000 anti-rabbit antibody diluted in PBST (NA934V, GE Healthcare, Little Chalfont, UK)	Fresh
Anti-mouse (western) antibody	1:2000 anti-mouse antibody diluted in PBST (NA931V, GE Healthcare, Little Chalfont, UK)	Fresh
c-myc (immunofluorescence) antibody	1:50 dilution of c-myc antibody (9E10) in blocking buffer (GTX75953, GeneTex, Irvine, CA,USA)	Fresh
Goat anti-mouse antibody (immunofluorescence)	1:500 Goat anti-mouse DyLight 549 conjugated antibody in blocking buffer (35508, Thermo Scientific Pierce Protein Research Products, Rockford, IL,USA)	Fresh

Table 2.3: Cell lines

Cell line	Growth requirements
MDA-MB-468 (Cailleau et al., 1978)	RPMI 1640 (Sigma, Gillingham, UK) and 10% (heat inactivated) Fetal Bovine Serum (Sigma, Gillingham, UK), 37°C and 5% CO ₂
Sourced from ATCC*	Transfectants: 350µg/ml G418 (Source Biosciences Lifescience, Nottingham, UK)
MDA-MB-231 (Cailleau et al., 1974)	RPMI 1640 and 10% (heat inactivated) Fetal Bovine Serum, 37°C and 5% CO ₂
Sourced from ATCC	Transfectants: 350µg/ml G418
MCF-7 (Soule et al., 1973)	RPMI 1640 and 10% (heat inactivated) Fetal Bovine Serum, 37°C and 5% CO ₂
Sourced from ATCC	Transfectants: 500µg/ml G418

*ATCC is the American Type Culture Collection (Teddington, UK)

Restriction enzymes

NotI, BamHI, XbaI, NheI, T4 DNA polymerase and Shrimp Alkaline Phosphatase (Promega, Madison, WI, USA)

Quick ligase and Smal (New England Biolabs, Hitchin, UK)

Other Cloning reagents

Oligonucleotides (Sigma-Genosys, Haverhill, UK)

Strataprep DNA extraction kit (Stratagene, La Jolla, CA, USA)

Loading dye 6x (New England Biolabs, Hitchin, UK)

1Kb DNA Marker (New England Biolabs, Hitchin, UK)

16.7% marker to 66.6% water and 16.7% loading dye

2.2 Methods

2.2.1 Cloning pIRES-myc- δ C2

Primers were designed which would bind either side of the myc- δ C2 sequence in the pEFLINKtag-myc- δ C2 construct (Fig. 2.1 and 2.2, also see Fig. 3.3), and which would enable incorporation of *NotI* and *NheI* restriction sites on either end of the amplified sequence. The sequence was PCR amplified, using *Pfu* polymerase. Following PCR, 3' A-overhangs were added using *Taq* polymerase in order for the insert to be compatible with the pCR2.1 TOPO shuttle vector (Invitrogen, Paisley, UK). Once reacted together, as in the TOPO TA Cloning kit (Invitrogen, Paisley, UK) instructions, the construct was transformed into OneShot Top10 chemically competent *Escherichia coli* (Invitrogen, Paisley, UK) and grown up before collection of the construct using Wizard Plus Minipreps (Promega, Madison, WI, USA) kit. *NotI* and *NheI* enzymes were used for splicing myc- δ C2 sequence from the pCR2.1TOPO vector into pre-digested pIRESneo2 empty vector (Clontech, Saint-Germain-en-Laye, France).

2.2.2 Cloning pIRES-mycPKC- δ

In order to create the pIRES-myc-PKC- δ construct, first the PKC- δ sequence was spliced out of the pEFLINKtag-myc-PKC- δ using XbaI and NotI, but the myc-tag was left in the vector. The δ C2 sequence was then spliced out of the pIRES-myc- δ C2 vector construct using BamHI and NotI, but the myc-tag was left intact within the vector. After running the samples on an agarose gel, the fragments for the PKC- δ sequence and the pIRES-myc were isolated. The two fragments were then ligated together to form the pIRES-myc-PKC- δ construct.

2.2.3 Plasmid purification

When generating more plasmid for cloning reactions, or when growing up transformed colonies to check for the presence of the correct construct, plasmid was purified from the culture using a Wizard Plus Minipreps kit. In this kit, the culture was spun down in order to concentrate the cells into a pellet. Then the pellet was re-suspended and lysed following the kit protocol. The plasmid DNA was eluted from the purification column in 100 μ l nuclease-free water.

When constructs were required for transfection, larger preparations of the constructs were made. First by transforming OneShot *E.coli* with the construct, and then growing up single colonies in 200ml LB broth with 100 μ g/ml ampicillin before extracting the plasmid using Wizard Plus Maxipreps kit (Promega, Madison, WI, USA).

2.2.4 Cell culture

MDA-MB-468 cells were grown in RPMI-1640 medium with 10% FBS in Corning 75cm² vented flasks. To sub-culture, media was aspirated and cells washed in 10ml of sterile PBS solution. 1ml of trypsin (Sigma, Gillingham, UK) was added and the cells incubated at 37°C to allow trypsinisation. Flasks were tapped to dislodge cells and observed under the microscope until detached. 6ml of media was added to neutralise the trypsin. Two new flasks containing 10ml media were prepared and 2ml of the detached cells added to each. Remaining cells were disposed of. Cultures were incubated at 37°C in 5% CO₂ in a humidified incubator.

2.2.5 Stable transfection

2.2.5.1 MDA-MB-468 cells

The MDA-MB-468 cell line was transfected using FuGENE6 (Roche, Basel, Schweiz) transfection reagent. Reactions were set up for transfecting with pIRES-myc- δ C2, pIRES-myc-PKC- δ and pIRES vector alone, along with a cell control.

Cells were seeded at 8.7×10^5 density in a circular plate with a 10cm diameter with 11.6ml media. These were incubated for approximately 2-3 days to ensure attachment had occurred and growth had begun.

The volumes in the reaction mixes are shown in Table 2.4. Volumes of DNA were calculated in order to add 5.6µg DNA. Firstly FuGENE6 was added to a microfuge tube containing the serum-free (SF)-RPMI. The microfuge tubes were vortexed and then incubated at room temperature for 5 minutes. Secondly the DNA was added to these mixtures and the tubes vortexed before incubating at room temperature for 15-30 minutes. The solutions were added dropwise to the plated cells whilst swirling the plate to mix.

Table 2.4: Volumes of serum-free (SF) RPMI, DNA and FuGENE6 in transfection samples.

	<i>SF-RPMI</i>	<i>FuGENE6</i>	<i>DNA</i>
<i>pIRES-myc-δC2</i>	<i>562.6µl</i>	<i>17.4µl</i>	<i>11.8µl</i>
<i>pIRES-myc-PKC-δ</i>	<i>562.6µl</i>	<i>17.4µl</i>	<i>6.7µl</i>
<i>pIRES Vector</i>	<i>562.6µl</i>	<i>17.4µl</i>	<i>10.4µl</i>
<i>control</i>			
<i>Cell Control</i>	<i>580µl</i>	-	-

Cells were incubated for approximately 2-3 days to allow transfection and production of the protein coded for by the transfected plasmid. Then G418 antibiotic was added to the plates so that a concentration of 350µg/ml (identified in a kill-time experiment, see Table 3.1) was reached.

2.2.5.2 MDA-MB-231 and MCF-7 cells

The MDA-MB-231 and MCF-7 cell lines were transfected using FuGENEHD (Promega, Madison, WI, USA) transfection reagent. As with MDA-MB-468 cells, reactions were set up for transfecting with pIRES-myc- δ C2, pIRES-myc-PKC- δ and pIRES vector alone, along with a cell control.

MDA-MB-231 cells were seeded at 2.5×10^6 density in a 10cm plate with 12ml media. MCF-7 cells were seeded at 1.87×10^6 density in a 10cm plate with 12ml media. Plates were incubated for approximately 1-2 days to ensure attachment had occurred and growth begun.

The volumes in the reaction mixes are shown in Table 2.5. Volumes of DNA were calculated in order to add 20 μ g DNA. The SF-RPMI and DNA were mixed in a microfuge tube and vortexed. To these reactions, 60 μ l FuGENEHD was added. The microfuge tubes were vortexed and then incubated at room temperature for 10 minutes. The solutions were added to the plated cells whilst tilting the plate to mix.

Table 2.5: Volumes of serum-free (SF) RPMI and DNA in transfection samples.

	<i>SF-RPMI</i>	<i>DNA</i>
<i>pIRES-mycC2</i>	959 μ l	41 μ l
<i>pIRES-mycPKC-δ</i>	977 μ l	23 μ l
<i>pIRES Vector control</i>	964 μ l	36 μ l
<i>Cell Control</i>	1000 μ l	-

Cells were incubated for approximately 60 hours before G418 was added to the plates. MDA-MB-231 cells were treated for a concentration of 350 μ g/ml. For MCF-7 cells G418 was added to the plates for a concentration of 500 μ g/ml.

2.2.6 Cell lysis

Lysis buffer was added to the cells and incubated on ice for 30 minutes. For a T75, 750 μ l was used, for a 10cm plate, 500 μ l was used. The cells were scraped from the flask/plate and the lysate put into a microfuge tube. The lysate was homogenised using 10 compressions of a syringe with a 25G needle. Cell lysate was cooled briefly on ice and centrifuged at 17000xg for 20 minutes at 4°C.

On occasions where a particular number of cells needed to be lysed, cells were trypsinised and counted, the relevant number of cells was pipetted into a

microfuge tube which was then centrifuged for 3 minutes at 500xg. The supernatant was removed and lysis buffer added (approximately 500µl) to the cell pellet. Cells were resuspended before incubating on ice for 30 minutes to allow lysis. As above the lysate was then homogenized with a needle and centrifuged.

2.2.7 Bradford assay

When the amount of protein loaded onto a gel was required to be equivalent across all samples, a Bradford assay was performed. Bio-Rad protein assay reagent (Bio-Rad Laboratories, Hemel Hempstead, UK) was diluted 1 in 4 with reverse osmosis (RO) filtered water. 1ml of diluted reagent was added to each cuvette required. 2µl sample was added to the cuvette (performed in triplicate) and left to react for a few minutes. Cuvettes were mixed and colour measured, compared to a blank control, on a UV-VIS spectrometer at 595nm. Averages of the triplicates were calculated, and this value used to find the amount of protein in the sample, using a standard curve. The volume of sample required for a particular amount of protein was then calculated, and this was added to a gel.

2.2.8 SDS-PAGE

The 4-20% gradient gel (Expedeon, Harston, UK) was removed from the storage packet and the wells rinsed twice with deionised water. 20x RunBlue running buffer (Expedeon, Harston, UK) was diluted to 1x with deionised water prior to use. This was poured between the cassettes and half way up the reservoir. 4x loading buffer (Expedeon, Harston, UK) was mixed with the samples in the ratio 1 part buffer to 3 parts sample (as manufacturer recommends). The gel was loaded with 7µl RunBlue Prestain Markers (Expedeon, Harston, UK) and approximately 20µl samples and run at 180V for approximately 35-45 minutes.

2.2.9 Western blotting

The SDS-PAGE gel was removed from the cassette and trimmed. Using the Hoefer TE70X semi-dry transfer kit (Hoefer Inc., Holliston, MA, USA), layers were compiled of a Mylar mask (optional), 3x 3MM paper, nitrocellulose membrane, gel and 3x 3MM paper. Bubbles were omitted and the lid closed. The transfer was run for 1½ hours at 38mA per gel.

The blot was blocked in PBST with 0.5% milk powder for 1 hour before incubation overnight at 4°C with primary antibody. One 15 minute wash followed by three 5 minute washes were done in PBST, followed by 1 hour incubation with secondary antibody. A further 15 minute wash followed by three 5 minute washes were

done in PBST, ECL reagent (GE Healthcare, Little Chalfont, UK) was added to the blot and incubated for 1 minute. Films were exposed for variable lengths of time (approximately 15-30 seconds) and developed with Kodak GBX processing chemicals for autoradiography films (Sigma-Aldrich, Dorset, UK).

2.2.10 Immuno-precipitation

The supernatant was removed from the centrifuged lysate and put into a fresh pre-cooled microfuge tube. 10µl of the primary antibody (e.g. PKC-δ antibody) and 50µl of protein A/G agarose beads (Alpha Diagnostics International, San Antonio, TX, USA) were added to the lysate. The samples were incubated in the cold room overnight whilst rotating. Tubes were centrifuged and the pellet washed 3 times in PBS before resuspending in approximately 50µl PBS. Control immunoprecipitation reactions could be run using no primary antibody or no beads. Loading buffer was added to the resuspended reactions, which were heated for 10 minutes at 70°C. The reactions were centrifuged for 10 minutes at 17,000xg and the supernatant removed. The supernatant was added to a SDS-PAGE gel for analysis.

Prior to lysis of samples for immunoprecipitation, some samples were treated with phorbol 12-myristate 13-acetate (PMA) (Sigma, Gillingham UK) for 30 minutes at 100nM.

2.2.11 Sub-cellular fractionation

Cells were harvested and then centrifuged at 500xg for 5 minutes. Cells were washed by resuspending in 1ml PBS at 4°C. Cells were counted on a haemocytometer and between 1 and 6 x10⁶ cells transferred to a 1.5ml microfuge tube. Microfuge tubes were centrifuged for 3 minutes at 500xg before the supernatant was removed. Five buffers (from the Subcellular Protein Fractionation kit, Pierce Biotechnology, Rockford, IL, USA) were used for the various fractions, depending on the number of cells to be lysed, varying volumes of buffer were prepared (Table 2.6). Appropriate volumes of buffers were measured out for the number of samples and Halt inhibitor cocktail was added at 1:100. NEB+ (Bound-nuclear extraction buffer) buffer was supplemented with 5µl of 100mM CaCl₂ per 100µl and 3µl of micrococcal nuclease per 100µl, in addition to the inhibitor cocktail. CEB (cytosolic extraction buffer), MEB (Membrane extraction buffer) and NEB (Nuclear (soluble) extraction buffer) were stored on ice, whilst NEB+ and PEB (Cytoskeletal (pellet) extraction buffer) were left at room temperature.

Table 2.6: Volumes of fractionation buffers used.

Number of cells (x10⁶)	CEB (μl)	MEB (μl)	NEB (μl)	NEB+ (μl)	PEB (μl)
1	100	100	50	50	50
2	200	200	100	100	100
3	300	300	150	150	150
4	400	400	200	200	200
5	500	500	250	250	250
6	600	600	300	300	300

Following addition of CEB to the pellet, the samples were incubated at 4°C mixing for 10 minutes. They were centrifuged at 500xg for 5 minutes and supernatant removed and stored as the cytoplasmic extract. MEB was added to the pellet and samples vortexed for 5 seconds before incubating at 4°C with mixing for 10 minutes. Samples were centrifuged at 3000xg for 5 minutes and the supernatant removed and stored as the membrane extract. NEB was added to the pellet and samples vortexed for 15 seconds before incubating at 4°C with mixing for 30 minutes. Samples were centrifuged at 5000xg for 5 minutes and the supernatant removed and stored as the soluble nuclear extract. NEB+ was added to the pellet and samples vortexed for 15 seconds before incubating at 37°C for 5 minutes. Samples were vortexed for 15 seconds before being centrifuged at 17000xg for 5 minutes and the supernatant removed and stored as the chromatin-bound

nuclear extract. PEB was added to the pellet and samples vortexed for 15 seconds before incubating at room temperature for 10 minutes. Samples were centrifuged 17000xg for 5 minutes and the supernatant removed and stored as the cytoskeletal extract. Sample fractions were stored at -80°C until use for downstream analysis.

2.2.12 Immuno-fluorescence

Coverslips were sterilised by soaking in ethanol and then air-dried in a Category II cabinet. A Type I collagen (Sigma, Gillingham, UK) coating was added by pipetting a 1mg/ml solution onto the surface and allowing to air-dry. Prepared coverslips were then placed in a well of a 6-well plate with 2ml media and cells seeded at approximately 25,000/ml. The plates were incubated for a couple of days.

Coverslips were retrieved from the wells and washed by immersing in PBS. Fixation buffer was added for 20 minutes, followed by 3 PBS washes. Permeabilisation solution was added to the coverslips and incubated for 15 minutes, followed by 4 PBS washes. Quenching buffer was added for 15 minutes, followed by 3 PBS washes. Blocking buffer was added and left for 2 hours before the addition of 1:50 9E10 primary antibody to relevant coverslips. The coverslips were incubated at 4°C overnight. The following day coverslips were washed 4 times in PBS before secondary antibody (at 1:500 dilution) was added and incubated for 30 minutes, whilst covered in foil, followed by a further 3 PBS

washes. FITC-phalloidin solution was added to the cells for 40 minutes, with foil covering, and succeeded by 4 PBS washes. Finally, cells were mounted onto slides, using a drop of Vectashield (with DAPI) (Vector Laboratories Inc., Burlingame, CA, USA), left to dry for approximately 1 hour, and sealed with clear nail varnish. Slides were stored in the dark at 4°C until use.

2.2.13 Annexin V/Propidium iodide flow cytometry assay

Cells were seeded in wells of a 6-well plate at 2×10^5 . They were incubated overnight to attach and grow. Relevant wells were then treated with camptothecin (Sigma, Gillingham, UK) at final concentration of 500nM for MDA-MB-468 cells and 2 μ M for MDA-MB-231 cells. Where SU 6656 (Sigma, Gillingham, UK) was used to treat cells, cells were left to attach for approximately 2hours, and SU 6656 added at 100nM concentration. Cells were then incubated for a further 24 hours.

When starvation was used to challenge the cells, the cells were left to settle, then media with FBS was removed, the wells washed and media without FBS added back in. With MG-132 (Calbiochem, Nottingham, UK) treatment, cells were treated for 24 hours or 5 hours following 65 hours starvation. With the 24hour treatment, 100nM MG-132 was added when the cells were starved. For the 5 hour treatment, 100nM MG-132 was added following the appropriate starvation period, and the plate swirled to mix.

After this incubation the medium (and any floating cells) were removed from the wells and put into labelled FACS tubes. The cells remaining in the wells were then trypsinised in 200µl trypsin. 800µl of media was added to inactivate the trypsin and the cell suspension added to the medium in the relevant FACS tube. The tubes were centrifuged for 5 minutes at 1200rpm. The supernatant was poured off, the pellets flicked to break them up, 2ml media added to the tubes and then they were vortexed gently. The samples were kept on ice whilst the cells were counted on a haemocytometer.

Following counting, 1×10^5 cells were aliquoted into a fresh FACS tube, 1ml PBS added and vortexed gently. Tubes were centrifuged at 12000rpm for 5 minutes. Supernatant was poured off and the tubes flicked to break up the pellet. 100µl 1x binding buffer was added to the pellet and tubes vortexed. 5µl FITC-AnnexinV (BD Pharmingen, Oxford, UK) was added and the tubes vortexed before incubating for 15 minutes at room temperature in the dark. Following this incubation, 400µl 1x binding buffer and 10µl propidium iodide (50µg/ml in PBS) were added and the tubes vortexed. The tubes were incubated for 10 minutes on ice in the dark before analysis.

2.2.14 Cell attachment

Cells were counted and 100,000 added to 1 ml of media in a 6-well plate. For each cell line, three wells were prepared. The plates were incubated for 15

minutes. The plate was swirled to resuspend unattached cells that had settled, and the media removed and placed in a 7ml plastic vial. The cell suspension in each was counted and these counts recorded. The average of the three counts was converted to a percentage; this was the percentage of cells remaining unattached after 15 minutes incubation.

2.2.15 Statistical analysis

Firstly consider the following definitions:

Population: ‘All members of a group about which you want to draw a conclusion’ (Levine and Stephan, 2011). For example, all voters in the UK or the daily output of cream cakes from a factory production line.

Sample: ‘A part of the population selected for analysis’ (Levine and Stephan, 2011). For example, UK voters selected to take part in a survey or 100 cream cakes selected from a production line.

Variable: ‘A characteristic of an item or an individual that will be analysed using statistics’ (Levine and Stephan, 2011). For example, the income of a household or the weight of a cake.

Following collection of a sample from a population, descriptive statistics are used to describe a variable of the sample. Data shows a tendency to group around a particular value, rather than evenly spreading out across a range (Rowntree, 2000). Measures of central tendency are used to identify the properties of a data set. One descriptive statistic that is a measure of central tendency is the 'mean'. The mean aims to find the middle point of the data set, however the calculation of the mean includes all data selected and as such, data points that are extreme can distort the impression of where the central tendency lies.

The mean is calculated as follows:

$$\bar{x} = \frac{\sum x_i}{n}$$

Where \bar{x} is the mean, x_i are the data points and n is the number of data points in the data set (Rumsey, 2010).

For example, in the following sample of student pulse rates:

67, 69, 69, 70, 74, 75, 75, 76, 78, 79 beats per minute

The mean would be:

$$\bar{x} = \frac{67 + 69 + 69 + 70 + 74 + 75 + 75 + 76 + 78 + 79}{10}$$

$$\bar{x} = 73.2 \text{ beats per minute}$$

Data points collected in a sample will vary from each other. Thus it is useful to describe the dispersion of the data points in a sample in order to properly compare two samples. A method of achieving this is to calculate the standard deviation. The standard deviation takes all data points into account (Rowntree, 2000). The standard deviation is a description of the typical distance from any data point to the centre, or the mean (Rumsey, 2010). As with the mean it can also be affected by outliers. If all data points in a sample were exactly the same then the mean would also be the same, as there would be no deviation from this mean amongst the data point, then the standard deviation would be 0 (Rowntree, 2000). The greater the dispersion of the data points in the sample, the larger the standard deviation would be. The equation to calculate the standard deviation is given by:

$$s = \sqrt{\frac{\sum(x_i - \bar{x})^2}{n - 1}}$$

Where s is the standard deviation, x_i is a sample value, \bar{x} is the sample mean and n is the number of values in the sample (Rumsey, 2010).

Consider the following examples:

Example A: 69, 71, 73, 74, 81, 82

Example B: 119, 128, 133, 134, 135, 143

With Example A, the mean is 75, and in Example B, the mean is 132. Let us first consider how far each data point is from the mean:

Example A: 69 71 73 74 81 82

-6 -4 -2 -1 +6 +7

Example B: 119 128 133 134 135 143

-13 -4 -1 +2 +3 +11

If we added up all these deviations, they would equal each other out, with the negative values equalling the positive ones, so to remove the negative signs, we square the values:

Example A: -6 -4 -2 -1 +6 +7

36 16 4 1 36 49

Example B: -13 -4 -1 +2 +3 +11

169 16 1 4 9 121

Next we find the mean of these deviations by adding them together and dividing by the number of values minus 1, or $n-1$, in this case we divide by 5:

Example A:

$$\frac{36 + 16 + 4 + 1 + 36 + 49}{5}$$

Example B:

$$\frac{169 + 16 + 1 + 4 + 9 + 121}{5}$$

This gives the variance, which is the squared standard deviation. In Example A this is 28.4, and in Example B this is 64. By taking the square root of the variance, we can find the standard deviation:

$$\text{Example A: } \sqrt{28.4} = 5.33$$

$$\text{Example B: } \sqrt{64} = 8$$

The standard deviation shows that in Example A there is less deviation from the mean than in Example B. This is indicated by a lower standard deviation value.

Whereas descriptive statistics are used to summarize the observations made, inferential statistics can be used to generalize from that sample to the wider population (Rowntree, 2000). Samples are taken from a population and there will typically be variation amongst the samples. The standard error of the mean is a

measure of how the sample mean varies from a population of sample means. It allows us to understand how accurately we can generalise from the sample statistic to the population parameter. Thus to find the standard error of the population we imagine a population of sample means and examine the sampling distribution of the sample means by finding the standard deviation. However we only have one sample, with a mean and a standard deviation, and must estimate the standard error of the mean from this. Standard error of the mean is dependent on the standard deviation of the sample and the size of the sample. It is calculated as follows (Rumsey, 2010):

$$\sigma_{\bar{x}} = \frac{\sigma_x}{\sqrt{n}}$$

Where $\sigma_{\bar{x}}$ is the standard error of the mean, σ_x is the population standard deviation and \sqrt{n} is the square root of the sample size (Rumsey, 2010). A small standard error of the mean, indicates that the mean of this sample would be close to the mean of the population. For example, if a sample of 100 exam results had a standard deviation of 30 marks:

$$\sigma_{\bar{x}} = \frac{30}{\sqrt{100}} = 3$$

The standard error of the mean is 3 marks. If the standard deviation of the sample is smaller, say 15 marks, there is an impact on the standard error of the mean, as shown below:

$$\sigma_{\bar{x}} = \frac{15}{\sqrt{100}} = 1.5$$

In addition, if the size of the sample is increased, say to 400 exam results, there is also an impact on the size of the standard error of the mean:

$$\sigma_{\bar{x}} = \frac{30}{\sqrt{400}} = 1.5$$

The size of the standard deviation has a greater impact on the size of the standard error of the mean than the sample size. This is observed in the above examples, where a decrease by half in the standard deviation, allows for a decrease of half in the standard error of the mean. However an increase of four times the sample size, only has an impact of halving the standard error of the mean. A change in the numerator has a greater impact on the result than the change in the denominator. This issue is examined below:

Calculation of the standard error of the mean is summarised by the equation: $\frac{s}{\sqrt{n}}$

If both s and n are increased by a factor of 2 we have the following: $\frac{2s}{\sqrt{2n}}$

This can also be written as: $\frac{s}{\sqrt{n}} \times \frac{2}{\sqrt{2}}$

The value 2 is greater than the square root of 2, thus there would be an increase due to the greater impact of a change in the numerator on the result.

A further consideration of inferential statistics is to examine two or more different samples and question whether or not they indicate an actual difference in populations (Rowntree, 2000). This can be done using statistical significance tests; a common test is the Student's t-test.

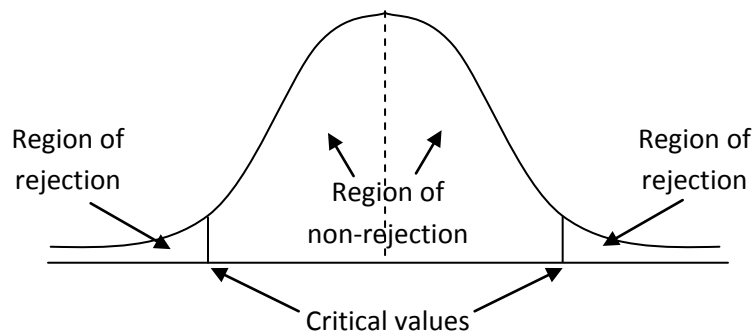
If pulse rates are measured in two random samples of 50 males and 50 females, testing can examine whether they are so similar that they should be considered as one population or if they are so different that two populations are indicated. Tests can examine whether this difference is significant, in terms of either standard deviation (Example A) or mean (Example B) (Rowntree, 2000).



Prior to testing we must consider the cautious convention of the null hypothesis. This is to begin by assuming, or hypothesizing, that there is no real, statistically-significant, difference between the samples (Rowntree, 2000). This hypothesis says that the population parameters of the groups are equal (Levine and

Stephan, 2011). Testing examines this hypothesis to assess the difference and identify whether the null hypothesis is correct or whether a mutually exclusive alternative hypothesis should replace it. A simple alternative hypothesis is that there is a difference between the samples. The null hypothesis remains accepted unless we find the difference between the samples is too great to believe that they could originate from one population, and thus the alternative hypothesis is correct. However, failure to reject the null hypothesis is not proof that it is correct (Levine and Stephan, 2011).

Consider this sampling distribution for the test statistic, say the difference between the mean of the two samples:



We are testing if the mean of sample A is equal to the mean of sample B. There are regions of the sampling distribution where a value would be considered non-rejected and regions where it would be considered to be rejected. Critical values mark the points at which a null hypothesis would be rejected instead of not being rejected. The regions of rejection indicate the areas where the value of the test statistic, in this case the difference between the sample means, would be unlikely to fall if the null hypothesis was correct. If the test statistic value falls within

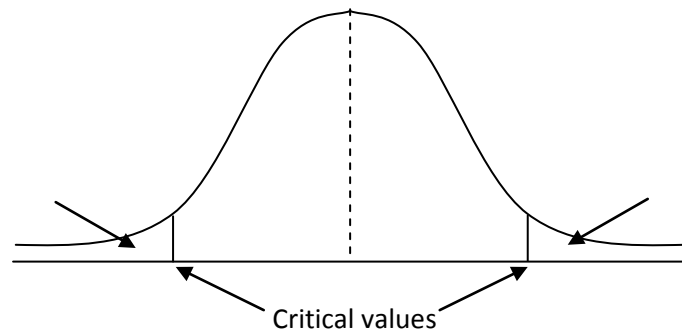
these regions, the null hypothesis is rejected (Levine and Stephan, 2011). The critical values are set by a decision upon the risk considered acceptable of making either a type I or type II error. A type I error is where the null hypothesis is rejected when it is true. For example, if it is stated that there is a difference between two sample means, when in fact there is not. Prior to testing a risk level α is set, traditionally this is 0.05, or smaller (Rowntree, 2000). This would mean that there is a probability that in 5 out of 100 times, a type I error could occur by chance. A type II error occurs if the null hypothesis is not rejected when it is false (Levine and Stephan, 2011). This would mean that the samples are from two distinct populations, but the difference was not determined by the test. A method of limiting type II errors is to use a larger sample size so that differences are more easily detected.

The p -value can be found with statistical testing, this gives an indication of whether the null hypothesis should be rejected (Rumsey, 2010). This is considered in parallel with the risk level α set previously. If the p -value obtained is smaller or equal to α , the null hypothesis should be rejected.

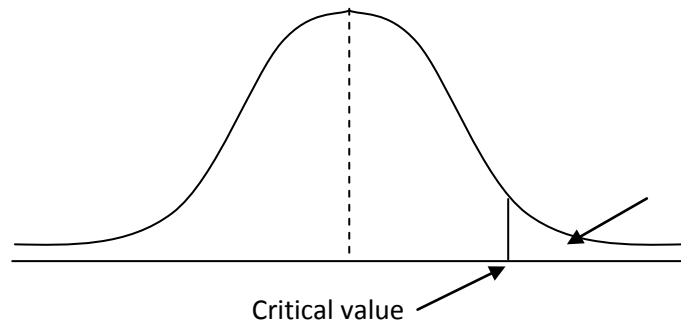
The alternative hypothesis may not be as simple as to say that there is a difference in the samples, it may say, for example, that there is an increase from sample A to B. This is where we consider tailed testing. A two-tailed test is used where the alternative hypothesis states that there is a significant difference between the two sample means (Rowntree, 2000). A one-tailed test would be used where the alternative hypothesis says that there is a significant difference in

a particular direction. As an example, consider a drug treatment that aims to lower blood pressure. The alternative hypothesis may say that there is a difference between a drug-treatment group and a placebo-treatment group, where we should use a two-tailed test. Or the alternative hypothesis may say that the drug-treatment group will have a lower blood pressure than the placebo-treatment group; in this case a one-tailed test should be implemented.

If we were testing using a two-tailed test and using a α of 0.05 (5%), the test would look to see if the value was in the regions of rejection either side of the region of non-rejection. The critical values are set so that there is no more than a 2.5% chance that the drug-treatment mean differs from the placebo-treatment mean, in either direction, for the null hypothesis to be rejected. (Rowntree, 2000).



However if we were using a one-tailed test, the test would focus on one arm of the diagram. Thus the critical value would be lowered. Thus a one-tailed test can make it more likely for a type I error to occur (Rowntree, 2000).



Student's t-tests can be performed as unpaired or paired tests. An unpaired test can be performed on two groups of data to examine if there is a difference in the sample means of the two groups. In this test the sample variance is pooled to form one estimate of the variance covering the two samples (Levine and Stephan, 2011). A paired test is also performed on two samples to test if there is a difference in sample means. However, here the individuals in a sample are paired together, for example with a sample of 6 sets of identical twins. Each set of twins is paired. This has the effect of minimizing the chance of the two sample groups being too different, thus introducing bias (Rumsey, 2010). As an example, we can return to the situation where a drug treatment was used that aimed to reduce blood pressure. At the beginning of the study the blood pressure reading of the patients would be taken, and patients could be paired according to these values, one of the pair would be drug-treated and the other placebo-treated. This pairing would allow a more thorough reflection of the drug effects, rather than being complicated by differences in the beginning blood pressure values present in the two treatment groups (Levine and Stephan, 2011).

Finally let us consider how a Student's t-test works. We will first study a two-tailed, unpaired test. The equation to calculate the t-value is (Levine and Stephan, 2011):

$$t = \frac{(\bar{x}_1 - \bar{x}_2) - (\mu_1 - \mu_2)}{\sqrt{s_p^2 \left(\frac{1}{n_1} + \frac{1}{n_2} \right)}}$$

Where \bar{x} are the sample means, μ are the population means, s_p^2 is the pooled estimate of the variance, and n are the sample sizes. Before using this calculation, the pooled estimate of the variance must be calculated by the following equation:

$$s_p^2 = \frac{(n_1 - 1)s_1^2 + (n_2 - 1)s_2^2}{(n_1 - 1) + (n_2 - 1)}$$

We are going to determine whether the cost of a restaurant meal in a major city differs from the cost of a similar meal in the suburbs (Levine and Stephan, 2011). This will be done using an $\alpha=0.05$ level of significance. Data is collected from 50 city and 50 suburban restaurants. The mean cost in the city restaurants was \$41.46, with a variance of 192.91 squared dollars, whilst the mean cost in the

suburban restaurants was \$39.96, with a variance of 123.99 squared dollars. Thus we first calculate the estimate of the pooled variance:

$$s_p^2 = \frac{(49 \times 192.91) + (49 \times 123.99)}{49 + 49} = 158.45$$

Next we can calculate the t -value (where the population means are unknown and thus are substituted by 0):

$$t = \frac{(41.46 - 39.96) - 0}{\sqrt{158.45 \left(\frac{1}{50} + \frac{1}{50}\right)}} = \frac{41.46 - 39.96}{\sqrt{158.45 \times 0.04}} = \frac{1.5}{\sqrt{6.338}} = 0.596$$

The next step is to look up the critical value of t in the t -tables using $50+50-2=98$ degrees of freedom, under 0.025 ($0.05/2$). The critical value is 1.9845. The t -value we calculated was 0.596, as this is less than the critical value 1.9845, the null hypothesis is not rejected.

Next a two-tailed, paired test; the equation to calculate t is (Levine and Stephan, 2011):

$$t = \frac{\bar{D} - \mu_D}{\frac{s_D}{\sqrt{n}}}$$

Where \bar{D} is the mean difference, μ_D is the difference between the population means, s_D is the sample standard deviation, and n is the sample size. Before using this equation, values for \bar{D} and s_D must be calculated. This is done using the following equations:

$$\bar{D} = \frac{\sum_{i=1}^n D_i}{n}$$

$$s_D = \sqrt{\frac{\sum_{i=1}^n (D_i - \bar{D})^2}{n - 1}}$$

As an example, we want to find whether, to $\alpha=0.05$, a difference exists between the Doppler echocardiography results that two observers made on 23 patients (Levine and Stephan, 2011). Consider the following data:

Patient	Observer A	Observer B	Difference (A-B)
1	4.8	5.8	-1.0
2	5.6	6.1	-0.5
3	6.0	7.7	-1.7
4	6.4	7.8	-1.4
5	6.5	7.6	-1.1
6	6.6	8.1	-1.5
7	6.8	8.0	-1.2
8	7.0	8.1	-1.1
9	7.0	6.6	0.4
10	7.2	8.1	-0.9
11	7.4	9.5	-2.1
12	7.6	9.6	-2.0
13	7.7	8.5	-0.8
14	7.7	9.5	-1.8
15	8.2	9.1	-0.9
16	8.2	10.0	-1.8
17	8.3	9.1	-0.8
28	8.5	10.8	-2.3
29	9.3	11.5	-2.2
20	10.2	11.5	-1.3
21	10.4	11.2	-0.8
22	10.6	11.5	-0.9
23	11.4	12.0	-0.6

The sum of all these differences, $\sum_{i=1}^n D_i$, is -28.3. Thus the \bar{D} is calculated as:

$$\bar{D} = \frac{-28.3}{23} = -1.23$$

From this, the s_D can be calculated:

$$s_D = \sqrt{\frac{8.9687}{22}} = 0.638$$

These figures can be input into the t-test equation (where the μ_D is unknown and thus substituted with 0):

$$t = \frac{\bar{D} - \mu_D}{\frac{s_D}{\sqrt{n}}} = \frac{-1.23 - 0}{\frac{0.638}{\sqrt{23}}} = -9.24$$

This t -value can be looked up in the t -tables to find the critical value of t using 23-1=22 degrees of freedom, under 0.025 (0.05/2). The critical value is -2.0739. As the t -value was -9.24, and this is less than the critical value -2.0739, the null hypothesis can be rejected.

Statistical analysis packages, such as excel, do these calculations and deliver a p -value; when the data shown in the paired t-test example is analysed in excel we obtain a p -value of 4.96×10^{-9} . This means that the probability of obtaining a t -value greater than 2.0739 or less than -2.0739 by chance is less than 0.0000005%, or 5 in 1 thousand million. This is considerably well within our stated α of 5%, and can definitely be considered a significant difference.

Chapter 3: Development of stable cell lines expressing myc- δ C2 or myc-PKC- δ

It is known that PKC- δ is involved in many cellular processes, including apoptosis (Steinberg, 2004); however, little is known about how its C2 domain is involved. In order to study PKC- δ , and its C2 domain in apoptosis of breast cancer cells, cell lines were developed that over-expressed the δ C2 domain or full length PKC- δ . Breast cancer cells (MDA-MB-468, MDA-MB-231 and MCF-7) were transfected with constructs of pIRES-myc- δ C2 pIRES-myc-PKC- δ or pIRES Vector, and stable transfectants selected. For MDA-MB-468 cells, colonies were picked from the plate and grown up as clonal populations. All remaining colonies were pooled together as a collection of clones. For MDA-MB-231 and MCF-7 cell lines, only a pool collection was developed. Expression studies showed that the δ C2 and myc-PKC- δ were expressed in the appropriate cell lines. The transfected populations

will enable examination of how important the C2 domain is in interactions that facilitate the apoptotic role of PKC- δ .

3.1 Introduction

The PKC- δ C2 domain is specific to the protein, it is part of the regulatory domain and has been shown to have protein binding capabilities (Benes et al., 2005; Dekker and Parker, 1997; Mellor and Parker, 1998). We hypothesize that over-expression of the C2 domain will block these protein binding events, through competitive inhibition, thus blocking endogenous PKC- δ activity.

In the literature, groups have utilised several methods to examine the action of PKC- δ (Blass et al., 2002; Chen et al., 2010; Hall et al., 2007; Humphries et al., 2006; Kajimoto et al., 2010). This has included use of PKC inhibitors; however, these are not specific to the PKC- δ isoform (Soltoff, 2007). Studies have also used siRNA; however, use of this is dependent on protein turnover and can have off-target effects (Jackson et al., 2003). Knockout animals could also be used for such studies, however due to the nature of the PKC family having overlapping roles, the development of such animals may lead to compensatory mechanisms developing whereby other family members take over the roles of PKC- δ . In addition, these methods would not enable the specific study of the C2 domain and its roles in PKC- δ activity.

3.1.1 *pIRESneo2*

The pIRESneo2 vector was used because it contains several useful elements for our purpose (Fig. 3.1). The vector contains a human cytomegalovirus (CMV)

major immediate early promoter/enhancer which allows transcription machinery to bind, and for enhancer-binding proteins to also bind allowing an increased rate of transcription (Foeking and Hofstetter, 1986; Pasleau et al., 1985; Thomsen et al., 1984). Following this region is a multiple cloning site (MCS), followed by three stop codons covering all reading frames (Fig. 3.1). The stop codons following the MCS would prevent translation of the protein sequence past this point. A synthetic intron is next in the sequence, this is present as it was found to enhance mRNA stability (Huang and Gorman, 1990). This is followed by an internal ribosome entry site (IRES) (Fig. 3.1) (from encephalomyocarditis virus), which allows translation of a further open reading frame from the same mRNA (Dorner et al., 1984; Jang et al., 1988). The first ribosome site is at the 5' end of the mRNA. This is positioned prior to a neomycin phosphotransferase coding sequence, from which, the protein confers resistance to G418 antibiotic. Lastly is a polyadenylation signal, originating from bovine growth hormone sequence (Goodwin and Rottman, 1992).

The pIRESneo2 vector was designed in such a manner that through positioning the neomycin phosphotransferase gene to a translation position following the gene of interest and the IRES, the inserted gene of interest should always be expressed (Martinez-Salas, 1999; Wagstaff et al., 1998). The selective pressure for antibiotic resistance means that the neomycin phosphotransferase is required for survival, thus the positioning of this gene following the gene of interest means both genes are transcribed, rather than just the neomycin

phosphotransferase. In addition, experimental evidence indicates that expression from an IRES is slightly lower than from a more traditional cap-dependant type (Wagstaff et al., 1998), thus in order to achieve resistance to the G418 antibiotic treatment by neomycin phosphotransferase expression, it is likely that the expression levels of the protein of interest would be slightly higher.

Also contained within the vector is a collection of features designed for replication of the vector within a bacterial system. An ampicillin resistance gene region containing a bacterial promoter, transcription start point, ribosome binding site and β -lactamase coding sequence are positioned for reading and transcription in the opposite direction to the eukaryotic-suitable features. This region allows selection of bacteria that contain the plasmid from a wider population, from which the plasmid can be prepared and used in mammalian cell transfection experiments.

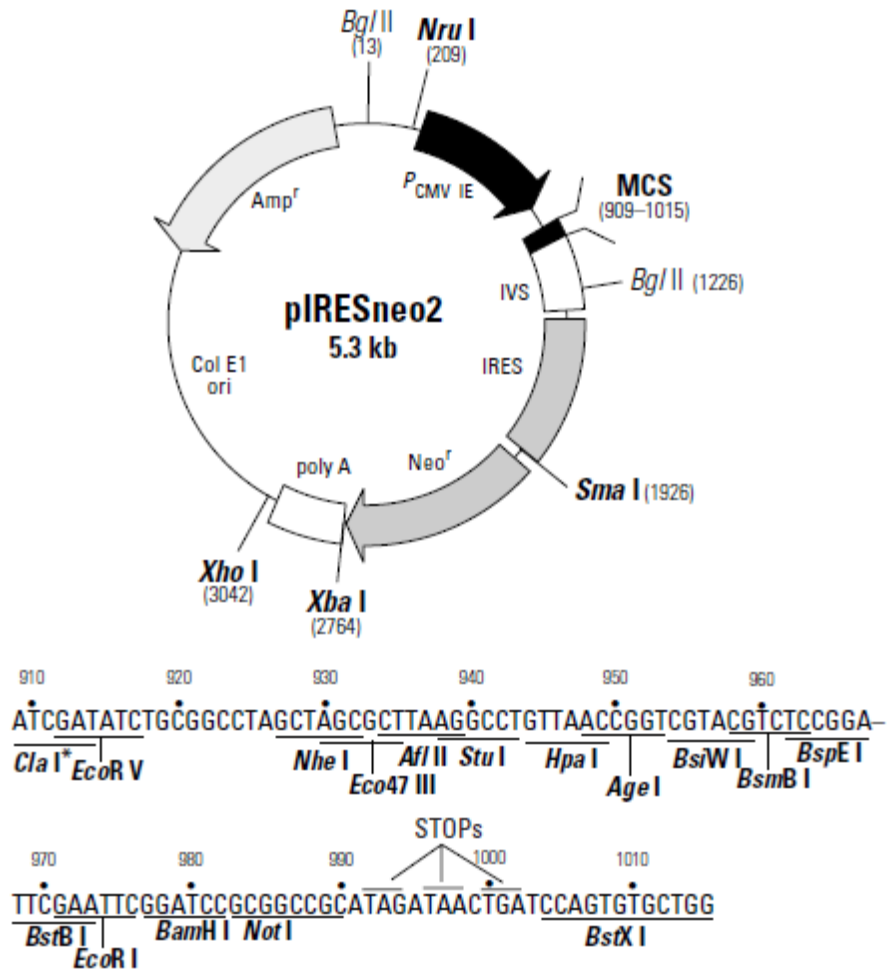


Figure 3.1: pIRES vector map showing details of the multiple cloning site (MCS).

3.1.2 Using pIRESneo2

PKC- δ was available in pEFLINKtag constructs that had previously been made and used within the group. The pEFLINKtag constructs are suitable for expression of protein, however they would have to be co-transfected into cells with an additional construct containing a selectable marker to allow cell line selection. A

potential problem with this method is that the neomycin resistance vector can be incorporated, as it is beneficial to the cells survival, however the construct containing the sequence for the protein required to be expressed may not. The cells were required to express the protein in a stable fashion in order to allow the effects to be seen within the intracellular environment. The pIRESneo2 constructs would contain both a neomycin resistance gene for selection, and the gene of interest.

Once transfected, cells can express the protein whose sequence is contained within the construct, however cells may not necessarily maintain this expression. Constant, stable expression was required for lengthy experiments. The expression of the neomycin resistance gene enables cells to grow in the presence of G418, which is an antibiotic that can stop polypeptide synthesis in both prokarya and eukarya. Thus through G418 treatment of transfected cells, cells can be selected that stably express the construct.

The stable cell line method was chosen so that studies could be done on a relatively homogeneous population. In a transient system, where cells have not been selected for expression, there may be a proportion of the population that are not expressing the construct. Thus small effects of the transfected DNA may be picked up in a selected transfection system, which would not be in a transient system.

3.1.3 Approaches to transfection

There are many methods to achieve transfection of cells. Chemical transfection is a commonly used system (Reese, 2004). The efficiency of transfection is greatly improved when the DNA is precipitated in the presence of cells. This can be simply done by mixing with calcium chloride solution and adding to cells (Graham et al., 1973). The precipitate settles on the cells and is internalised through a process of endocytosis (Reese, 2004). Once inside, a proportion of the DNA will be released into the nucleus where it can be expressed or integrated into the genome.

Electroporation is frequently used in bacterial transformation, but can also be used for mammalian transfection (Reese, 2004). An electric field pulse is used to induce pores to open within the membrane; DNA can enter through these pores (Neumann et al., 1982). Whereas pores can form in 1 μ s, healing can take minutes (Reese, 2004). The pulse amplitude and duration are critical to forming pores to successfully transfect, while also not damaging the cell to the point it cannot repair (Reese, 2004).

For liposome-mediated transfection (Fraleley et al., 1980; Schaefer-Ridder et al., 1982), DNA is contained within a liposome cluster which fuses with the membrane, thus facilitating transport of the DNA into the cell (Reese, 2004). Liposomes used for this process are spheres of cationic lipids which form a unilamellar vesicle; these vesicles bind along the negatively charged DNA. Due to

their cationic nature they are also more readily able to interact with a negatively charged cell membrane than uncharged liposomes, thus promoting fusion and transportation of the DNA across the membrane (Reese, 2004). Liposomal transfection enables the DNA to enter without endocytosis, thus escaping endosome mediated degradation (Reese, 2004).

Several peptide sequences, for example, the tetra-peptide serine-proline-lysine-lysine, have been demonstrated to enable transfection (Legendre and Szoka, 1993; Reese, 2004; Wu et al., 1989; Wu and Wu, 1988). The positive lysine residues interact with the negative DNA backbone and enable close packing. The peptides bind to the DNA, condense it, and increase its amenability for cell entry.

DNA can also be injected directly into cell nuclei (Diacumakos, 1973; Reese, 2004). This is technically difficult and must be done individually to each cell. The integration efficiency of DNA introduced in this manner varies widely, dependant on the organism from which the cells originate. The method has been used on a wider scale for gene therapy for cancer, whereby DNA is injected into tumour or muscle cells in order to encourage expression of an antigen which produces an immune response (Reese, 2004).

Viral vector systems may also be used to introduce DNA into cells, it is referred to as transduction. Desired DNA can be inserted into the viral genome, when the virus is added to cells the DNA is inserted into the cells with the viral genome, as would normally happen with a viral infection (Hamer and Leder, 1979; Mulligan

et al., 1979). Some viruses normally integrate their genome into the host genome (e.g. Adeno-associated Virus), this can be utilised to enable the foreign DNA to enter the genome as well (Reese, 2004). Adeno-associated Viruses display a reliable feature whereby the integration of the DNA is in a predictable location, however other viruses, such as Retroviruses, insert at a random location, thus possibly having detrimental effects on the cell (Reese, 2004).

The cell lines were made following transfection of the cells using a proprietary form of lipid-based delivery of a pIRESneo2 construct. The G418 encouraged integration of the DNA into the genome, as without doing this, the cells would be killed.

3.2 Results

3.2.1 Untransfected cell line endogenous expression

The literature has compared the endogenous PKC- δ levels of MCF-7 and MDA-MB-231 cells (Shanmugam et al., 2001), but not MDA-MB-468 cells. Here, endogenous expression of PKC- δ in all these cell lines was measured. For each cell line the same number of cells were lysed and either the same number of cell equivalents, or the same amount of total protein was analysed (Fig. 3.2).

Examining expression in the lysate of 1.25 million cells, the MDA-MB-231 cells were found to have the lowest level of endogenous PKC- δ (Fig. 3.2A) The MDA-MB-468 and MCF-7 cells have considerably higher expression. Through band intensity analysis it was found that MDA-MB-468 expression is 29 times higher than that of MDA-MB-231 cells. MCF-7 expression has a relative intensity of 25. There is also a lower intensity band in the MDA-MB-468 and MCF-7 cell lines, present around 55kDa, attributed to a breakdown product. When considering both of these bands, it indicates that the levels of PKC- δ in the MDA-MB-468 and MCF-7 cell lines are much higher than the MDA-MB-231 cell line. The difference between the MCF-7 and MDA-MB-231 cell lines has also been identified in the literature (Shanmugam et al., 2001).

When 10 μ g of total protein for each cell line was loaded onto the gel (Fig. 3.2B), an overall similar pattern of expression was observed. The MCF-7 cell line shows

a relative intensity of 3, compared to MDA-MB-231 at 1, and the MDA-MB-468 cell line is higher still at a relative intensity of 6.

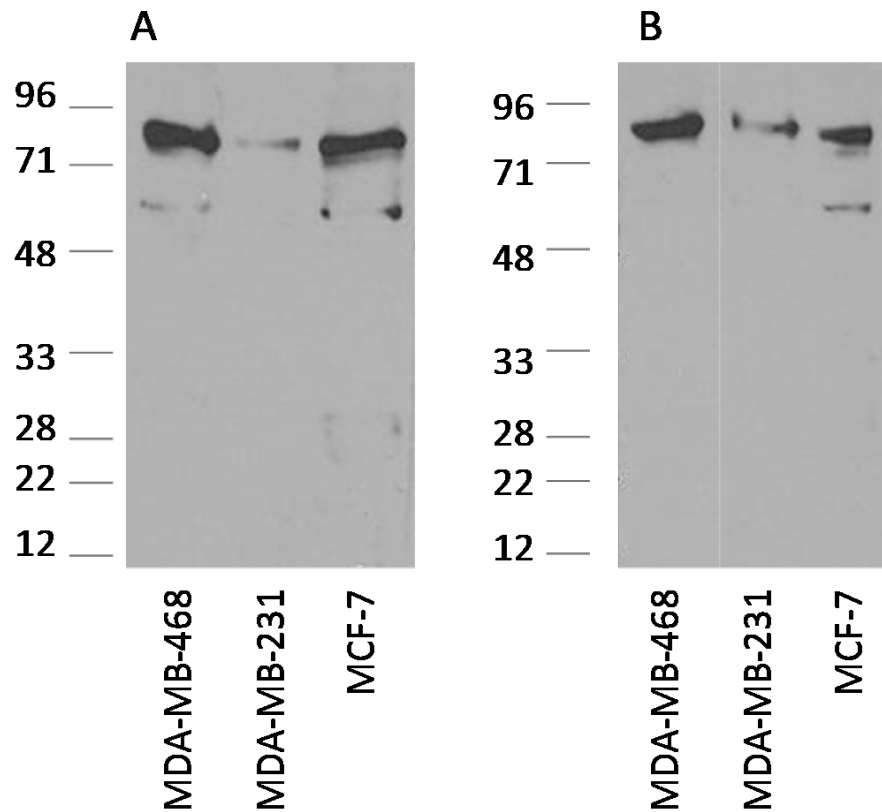


Figure 3.2: Endogenous expression levels of PKC- δ in MDA-MB468, MDA-MB-231 and MCF-7 cell lines. A: equal volume of lysate from 1.25 million cells, B: 10 μ g protein loaded. Equivalent experiments demonstrated comparable patterns across four experiments.

The difference in expression levels of PKC- δ between the cell lines is broad. It may thus be predicted that introducing the PKC- δ C2 domain in different cell

background would lead to different responses due to the different levels of endogenous PKC- δ . Perhaps higher levels of PKC- δ will mean that a greater number of PKC- δ pathways are active, thus affecting the cellular phenotype.

3.2.2 Generation of the pIRES-myc- δ C2 and pIRES-myc-PKC- δ constructs

The pIRES-myc- δ C2 construct was made by amplifying the myc- δ C2 sequence from the pEFLINKtag-myc- δ C2 construct using PCR, and ligating the product into the shuttle vector pCR2.1-TOPO. The sequence was then excised from the shuttle vector and ligated into the digested pIRESneo2 vector (Fig. 3.3).

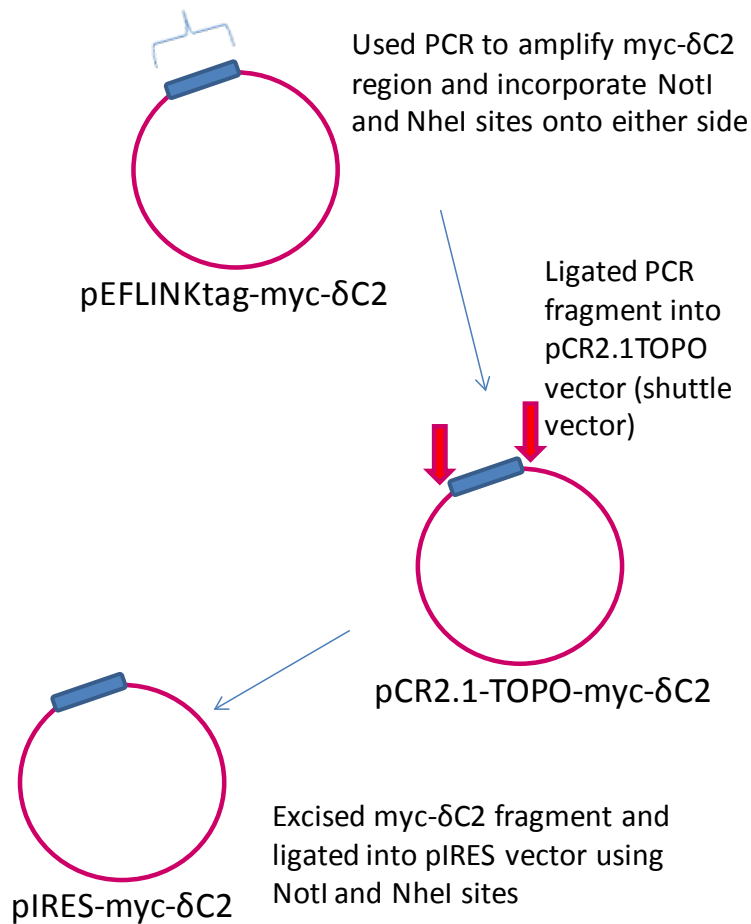


Figure 3.3: Ligation scheme for developing the pIRES-myc- δ C2 construct. The myc-tagged C2 domain was amplified using PCR, and restriction sites added at either end. These were then utilised to incorporate the insert into the cut pIRES vector.

For the pIRES-myc-PKC- δ construct, the pIRES-myc- δ C2 construct was digested in order to remove the C2 sequence, but retain the myc-tag within the vector. Then the 'PKC- δ ' sequence was excised from the pEFLINKtag-myc-PKC- δ construct and

ligated into the pre-digested pIRES construct containing the myc-tag, but not the C2 sequence (Fig. 3.4).

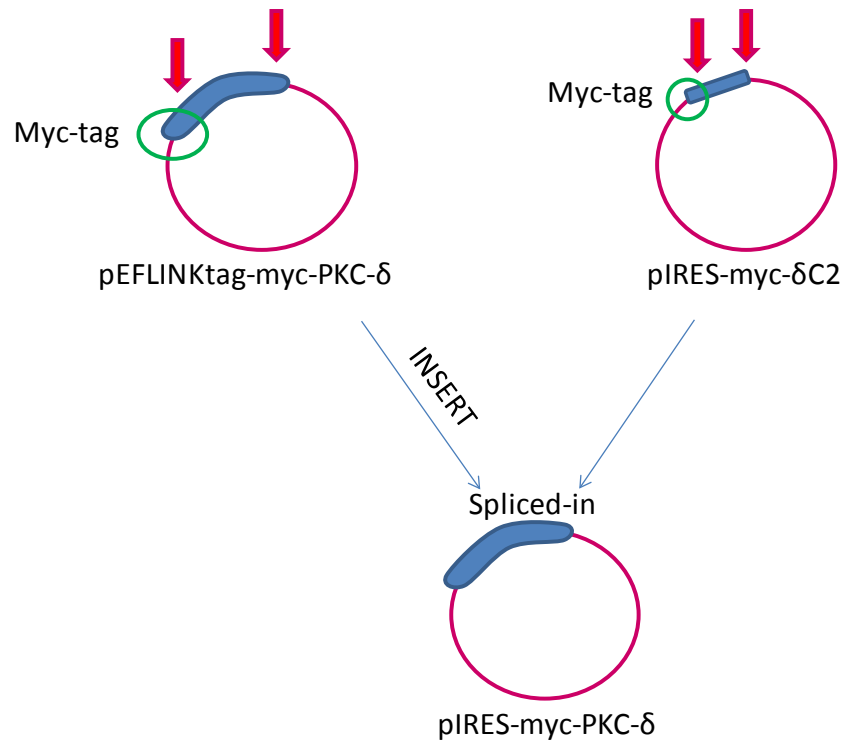


Figure 3.4: Ligation scheme for developing the pIRES-myc-PKC δ construct. The protein inserts were excised, exclusive of the myc-tag, then the PKC- δ insert spliced into the pIRES vector containing the myc-tag.

The maps of the final constructs are shown in Figure 3.5. Both contain the ampicillin resistance and neomycin resistance markers necessary for replication in bacteria, and development of stable cell lines, respectively. The pIRES-myc- δ C2

construct has retained its NotI restriction site, however it has been destroyed in the pIRES-myc-PKC δ construct.

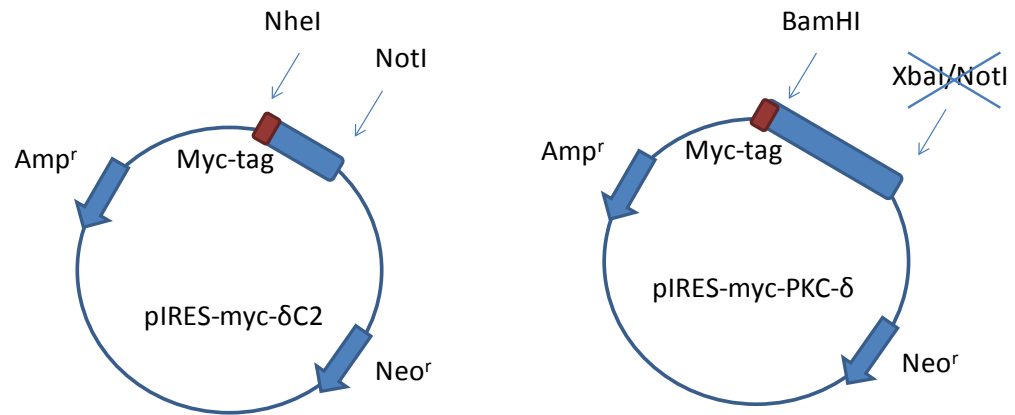


Figure 3.5: Maps of the constructs pIRES-myc- δ C2 and pIRES-myc-PKC- δ . The Blue rectangle signifies the insert, with the red region symbolising the myc-tag sequence. Positions of restriction sites are identified with arrows. Amp^r and Neo^r are the ampicillin and neomycin resistance genes respectively.

3.2.3 Stable transfection and confirming protein expression

3.2.3.1 Pre-transfection

Prior to transfection, a 'kill-time' experiment was performed studying the length of time needed for different G418 concentrations to kill the parent cells. The aim was to find a concentration that killed cells in approximately 5-7 days, as this would enable the cells to be expressing enough protein to be resistant to the G418, if the plasmid was present. If the cells were killed too quickly, there may not be enough time to transcribe and translate the protein, thus even those cells transfected successfully would die. This experiment was run on MDA-MB-468 cells; Table 3.1 shows that 350µg/ml G418 was a suitable concentration for selection of transfectants for this cell line. This concentration was also used for selection in MDA-MB-231 cells.

Table 3.1: Kill-time experiment data, for testing the G418 concentration necessary to kill MDA-MB-468 cells in 5-7 days. +: no killing, ~: some killing (30-70% cells remaining), -: all cells killed.

		Neomycin Concentration ($\mu\text{g/ml}$)					
		0	50	100	200	350	500
Days after treatment	1	+	+	+	+	+	+
	2	+	+	+	+	+	+
	3	+	+	+	+	+	+
	4	+	+	+	+	+	~
	5	+	+	+	+	~	-
	6	+	+	+	~	-	-
	7	+	+	+	-	-	-

Following transfection and selection of MCF-7 cells using 350 $\mu\text{g/ml}$ G418, it became clear that the concentration was not high enough to kill the MCF-7 cells. Thus a further 'kill-time' experiment was run prior to the next transfection to test concentrations from 500 $\mu\text{g/ml}$ and higher (Table 3.2). 500 $\mu\text{g/ml}$ was found to be sufficient.

Table 3.2: Kill-time experiment data, for testing the G418 concentration necessary to kill MCF-7 cells in 5-8 days. +: no killing, ~: some killing (30-70% cells remaining), -: all cells killed.

		Neomycin Concentration ($\mu\text{g/ml}$)					
		500	1000	2000	3000	4000	5000
Days after treatment	3	+	+	-	-	-	-
	6	~	-	-	-	-	-
	7	~/-	-	-	-	-	-
	8	-	-	-	-	-	-

3.2.3.2 Transfection of MDA-MB-468

The MDA-MB-468 cell line was transfected using FuGENE6 transfection reagent, with pIRES-myc- $\delta\text{C}2$, pIRES-myc-PKC- δ or with the pIRES vector alone. A non-transfected control was used to study the progression of cell death following G418 treatment and to observe that no colonies arose following the selection step, as this would indicate plasmid contamination. The MDA-MB-468 cells were seeded at 8.7×10^5 density in a 10cm dish, based upon the manufacturer's recommended seeding of 1.5×10^5 cells in a well of a 6-well plate.

Following transfection and selection procedures, colonies appeared first in the plate for pIRES-myc- $\delta\text{C}2$ transfected cells. Several colonies were picked using trypsin-soaked discs and expanded into clonal populations. The remaining

transfectants were pooled together and grown as a pIRES-myc- δ C2 transfected pool. The next colonies to arise were on the plate for pIRES vector control-transfected cells. Several individual colonies were expanded and a pool population prepared. No colonies developed in the plate for pIRES-myc-PKC- δ transfected cells. Transfection was repeated multiple times but no colonies developed. This may be due to a biological effect of PKC- δ over-expression on these cells. Microscope study of the plates occasionally identified a few cells which appeared apoptotic and did not form colonies.

In order to confirm the expression of the myc- δ C2 fragment in the MDA-MB-468-myc- δ C2 cells (and the absence of this in the Vector control cells) cell lysates were prepared, run on SDS-PAGE, western blotted and probed with the c-myc antibody 9E10. This detects the myc-tag on the myc-C2 expressed protein. In Figures 3.6 and 3.7, the myc- δ C2 band is clearly seen at approximately 15kDa in the MDA-MB-468-myc- δ C2 clone and pool cell lysates; it is absent from the vector control clone and pool cell lines.

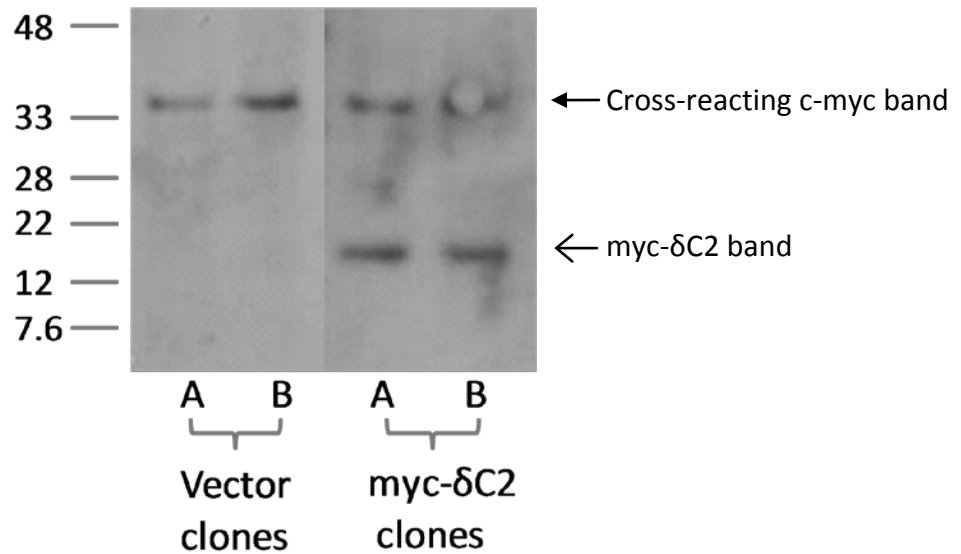


Figure 3.6: Expression of myc- δ C2 in the MDA-MB-468-myc- δ C2 clonal cell lines and its absence in the vector control clonal cell lines (open arrow). The bands seen at approximately 35kDa are endogenous c-myc bands (closed arrow). A and B are two clonal populations of transfectants.

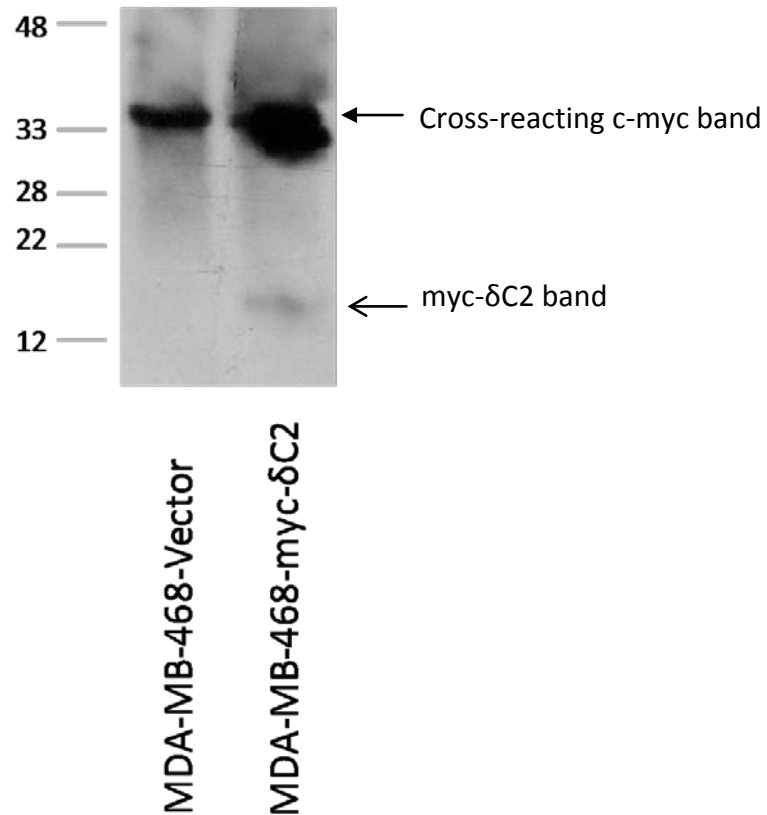


Figure 3.7: Expression of myc- δ C2 in the MDA-MB-468-myc- δ C2 pool cell line and the absence of the band in the Vector control pool cell line (open arrow). The bands seen at approximately 35kDa are endogenous c-myc bands (closed arrow).

During sub-culture of these cells differences in cell growth became apparent, with the myc- δ C2 cells apparently growing faster than the Vector cells. This effect is further investigated in Chapter 5.

3.2.3.3 *Transfection of MDA-MB-231*

The MDA-MB-231 cell line was transfected using FuGENEHD transfection reagent. As with MDA-MB-468 cells, cells were transfected with pIRES-myc- δ C2, pIRES-myc-PKC- δ or with the pIRES vector alone. An untransfected cell control was also prepared. The manufacturer suggested seeding $1-2 \times 10^4$ cells per well of a 96-well plate. Thus by using a 10cm dish, with a relative surface area 170 times greater, $1.7-3.4 \times 10^6$ cells would be required and as such, cells were seeded at 2.5×10^6 density. G418 was added at 350 μ g/ml to enable selection of stable transfectants.

After the selection process, colonies first began to develop in the plate of cells that had been transfected with the pIRES-myc- δ C2 construct, similar to MDA-MB-468. As with the MDA-MB-468 transfection, the next colonies formed were from the plate transfected with the pIRES vector alone, and used as a control cell line. Contrary to the MDA-MB-468 transfections, colonies ultimately did arise on the plate transfected with pIRES-myc-PKC- δ construct.

The differences between the development of transfected cells is exemplified in Figure 3.8. This figure demonstrates the differences between the development of colonies following transfection, where the only difference was the construct transfected into the cells. Panels 1A and 1B were taken 22 days following transfection of the MDA-MB-231 cells. Panel 1A shows pIRES-myc- δ C2 transfected cells and 1B shows pIRES-Vector control transfected cells; there is

approximately 75% confluence in 1A while the first cells have only just arisen in 1B where confluence is approximately 5%. On day 35 after transfection (13 days later) the pIRES-Vector control cells (2A) have significantly increased in number so that they are approximately 60% confluent. At this time point, the pIRES-myc-PKC- δ transfected cells have only just started to grow and are at approximately 5% confluence (2B).

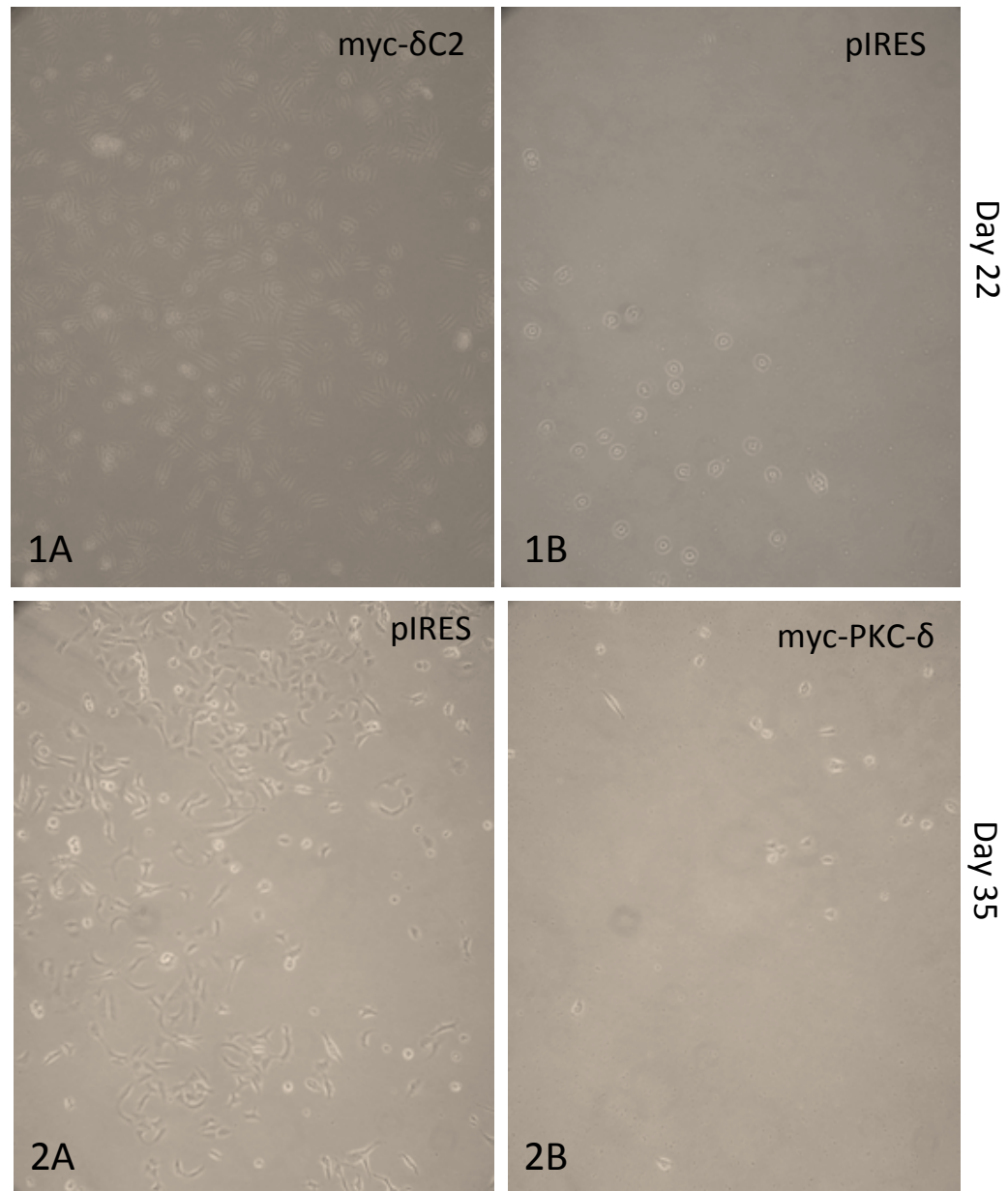


Figure 3.8: The development of transfected cells. Pictures 1A and 1B were taken 22 days following transfection. 1A: pIRES-myc- δ C2 transfected cells, 1B: pIRES-Vector control transfected cells; there is approximately 75% confluence in 1A while in 1B confluence is approximately 5%. At day 35 following transfection, pictures 2A and 2B were taken. 2A: pIRES-Vector control transfected cells, 2B: pIRES-myc-

PKC- δ transfected cells; cells in 2A are approximately 60% confluent, while cells in 2B are approximately 5% confluent.

As with the MDA-MB-468 cell lines, the presence and absence of relevant myc-tagged protein needed to be confirmed. As shown in Figure 3.9, the Vector control cell lysate showed a band at approximately 35kDa. The myc-PKC- δ lysate lane has an additional strong band at approximately 85kDa, which is the correct size for myc-tagged PKC- δ , thus confirming its expression. The myc- δ C2 cell lysate does not show this band but does have a band at approximately 15kDa, the predicted size for the myc- δ C2 fragment. Thus expression of myc-PKC- δ and myc- δ C2 in the selected pools of MDA-MB-231 transfected cells is confirmed.

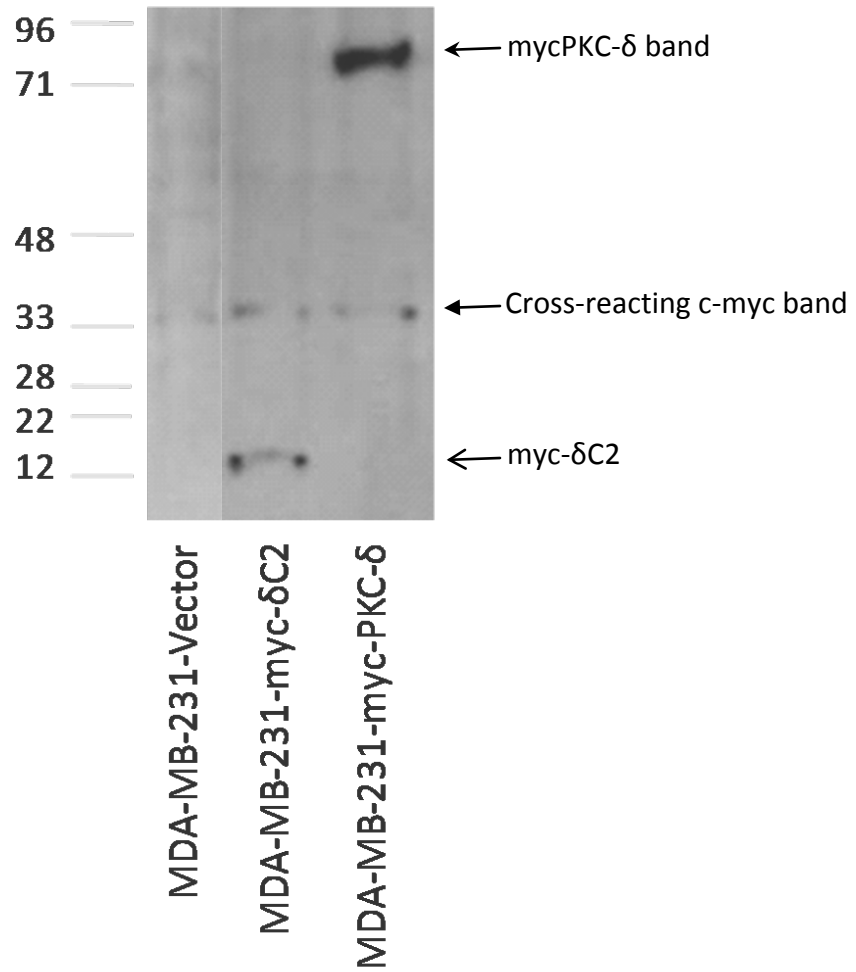


Figure 3.9: Expression of myc-PKC- δ in the 231-myc-PKC- δ cell line, this band is absent in the 231-myc- δ C2 and vector control cell lines (open arrow). Expression of myc- δ C2 is seen in the 231-myc- δ C2 cell line, but is absent in both the 231-myc-PKC- δ and vector control cell lines (curved arrow). The bands seen at approximately 35kDa are endogenous c-myc bands (closed arrow).

As with the MDA-MB-468 cells, the sub-culturing process revealed that there may be differences in the growth of the cell lines. The myc- δ C2 cells also appear to grow faster than the Vector cells. In addition, the myc-PKC- δ cells appeared to be growing at an increased rate. These observations are investigated further in Chapter 5.

3.2.3.4 Transfection of MCF-7

Transfection of the MCF-7 cells followed the same method as with the MDA-MB-231 cell line except that cells were seeded at the slightly lower density of 1.87×10^6 cells per 10 cm dish. Utilising a G418 concentration of 500 μ g/ml (Table 3.2), colonies arose first in the pIRES-myc- δ C2 transfected plate, then the Vector control plate, and finally in the pIRES-myc-PKC- δ transfected plate (as with MDA-MB-231 cells). Pool populations of the three cell lines were established.

The expression of myc-PKC- δ and myc- δ C2 was confirmed by western blotting (Fig. 3.10). A band at approximately 35kDa was observed in the Vector control lane. The myc- δ C2 cell lysate showed an additional band at approximately 15kDa, the expected size for the myc- δ C2 fragment. No 15kDa size band was observed in the myc-PKC- δ cell lysate, but a strong band is observed at the predicted size of myc-PKC- δ (approximately 85kDa).

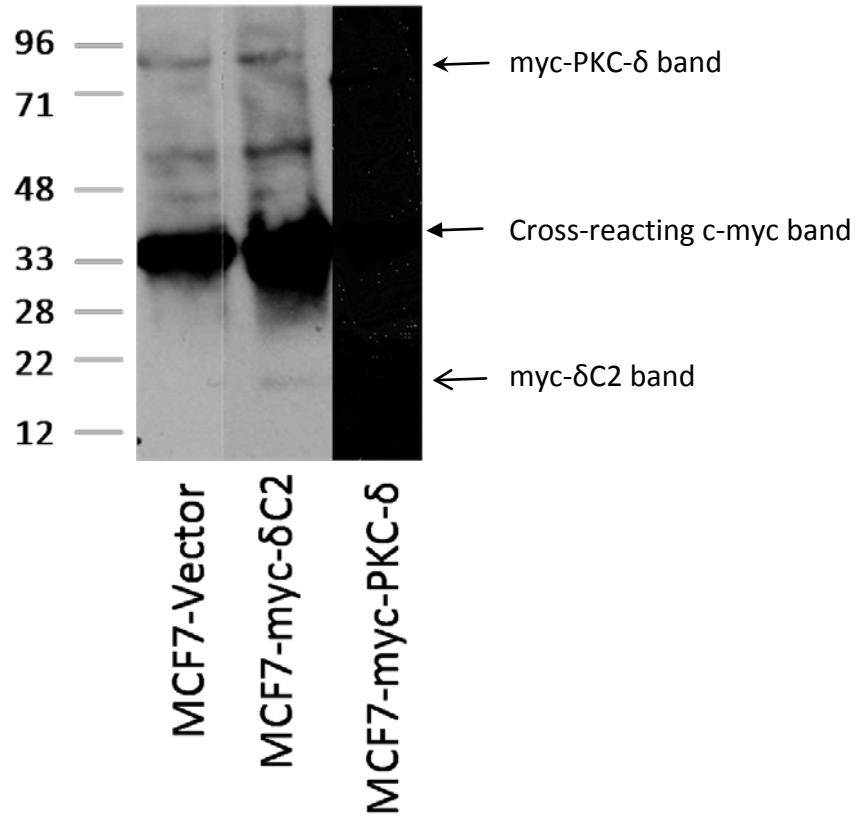


Figure 3.10: Expression of myc- δ C2 is seen in the MCF7-myc- δ C2 cell line, but is absent in both the MCF7-myc-PKC- δ and vector control cell lines (open arrow). Expression of myc-PKC- δ is seen in the MCF7-myc-PKC- δ cell line, this band is absent in the MCF7-myc- δ C2 and vector control cell lines (curved arrow). The bands seen at approximately 35kDa are endogenous c-myc bands (closed arrow).

3.3 Discussion

pIRES constructs were transfected into MDA-468, MDA-231 and MCF-7 cells. Stable cell lines were developed expressing myc- δ C2 or containing pIRESneo2 as a Vector control. Only MDA-MB-231 and MCF-7 cells developed myc-PKC- δ expressing cell lines. This was confirmed by western blotting. This is the first time cell lines have been developed over-expressing the C2 domain of PKC- δ . This will allow the effect of endogenous PKC- δ C2 domain to be examined through competitive inhibition of its activity.

MDA-MB-468 did not develop a myc-PKC- δ cell line, but the other parent cell lines did. However, the myc-PKC- δ expressing cell lines in MDA-MB-231 and MCF-7 took longer to develop than the Vector controls. This suggests that the over-expression of PKC- δ may be detrimental, or even fatal, to the cells and indicates that the MDA-MB-468 cells are more sensitive to PKC- δ over-expression. This effect could be related to the presence of already high PKC- δ levels within these cells, as shown in Figure 3.2. There is evidence that PKC- δ acts in a pro-apoptotic manner (Reyland, 2007), perhaps increasing PKC- δ levels any further floods this pathway and the cells enter apoptosis. The lower endogenous PKC- δ levels in the MCF-7 and MDA-MB-231 cells may prevent this critical level being attained, thus allowing cell survival. The pro-apoptotic pathway of PKC- δ involves caspase-3 (Reyland, 2007). MCF-7 cells also showed high PKC- δ levels, although not as high

as in MDA-MB-468 cells. MCF-7 cells do not express caspase-3, thus perhaps this is a reason why they do not act similarly to MDA-MB-468 cells.

All parental cell lines developed myc- δ C2 expressing cells more quickly than the Vector control (and myc-PKC- δ cells). This is an indication of a positive effect of myc- δ C2 activity on the cells in allowing them to demonstrate improved ability to survive. It seems likely that this may be mirrored in future experiments.

The cell lines developed will allow further investigation into the effects of PKC- δ over-expression and also into the role of the C2 domain in PKC- δ . The literature has illustrated a protein binding role for the C2 domain; we hypothesized that it would be likely that this protein binding role was more extensive than the literature has shown thus far. The specificity of the C2 domain for PKC- δ is a new method which can help identify PKC- δ specific activities that cannot be shown so comprehensively with the inhibitors available at present. The cell lines we have developed here will be examined in further detail, aiming to discover new roles and actions for PKC- δ and the C2 domain.

Chapter 4: Localisation of myc- δ C2 and associated differences

The MDA-MB-468 cell lines are the primary focus of this chapter. We used immuno-fluorescence to look at the positioning of myc- δ C2 and studied the localisation of PKC- δ using sub-cellular fractionation. Myc- δ C2 was localised to the extreme periphery of the cells. Differences in actin cytoskeleton were observed between myc- δ C2 and vector cells, such that the myc- δ C2 cells had a more extended cytoskeleton with protrusions extending from the main bulk. Despite myc- δ C2 having a clear impact on the cells, the localisation of endogenous PKC- δ did not show any difference between the myc- δ C2 and vector cells, as determined by cell fractionation. As the impact of myc- δ C2 on the cytoskeleton increased the cell surface area, it was possible that the attachment of cells may have been affected. This was examined in a brief study looking at the percentage of cells remaining unattached from a surface following 15 minutes incubation. The differences seen with the cells' cytoskeletal structures appear to correlate with attachment.

4.1 Introduction

After the introduction of the myc- δ C2 domain it was important to see where the protein domain was localised. The localisation may indicate possible roles for the domain itself and for PKC- δ and the actions it may be competitively inhibiting.

PKC- δ has been found to bind to the cytoskeletal factors f-actin and adducin (Chen et al., 2007; Lopez-Lluch et al., 2001). Literature evidence suggested PKC- δ may bind to the cytoskeleton via the C2 domain (Lopez-Lluch et al., 2001). Thus we used actin staining to examine the cell lines to see whether the cells expressing myc- δ C2 show any differences in cytoskeletal structure.

Our hypothesis is that the myc- δ C2 domain will interfere with the endogenous action of PKC- δ . Using cell fractionation, we have examined PKC- δ localisation in order to see if by interfering with this action the localisation of PKC- δ is also interfered with. As the positioning of PKC- δ appears important in the actions it performs, it is likely that due to differing actions the localisation is also different.

Following the examination of the cytoskeleton, and observing the differences correlating with the presence of the myc- δ C2 domain, a short study of attachment was performed.

4.2 Results

4.2.1 The myc- δ C2 domain localises to the periphery of the cell in membrane protrusions

In order to examine the localization of myc- δ C2, cells were stained with DAPI (blue), which stains the nucleus, and an antibody to the myc-tag which was visualized using a fluorescently labelled secondary antibody (red). Several fields, taken from several slides, were selected in such a way that single cells could be observed.

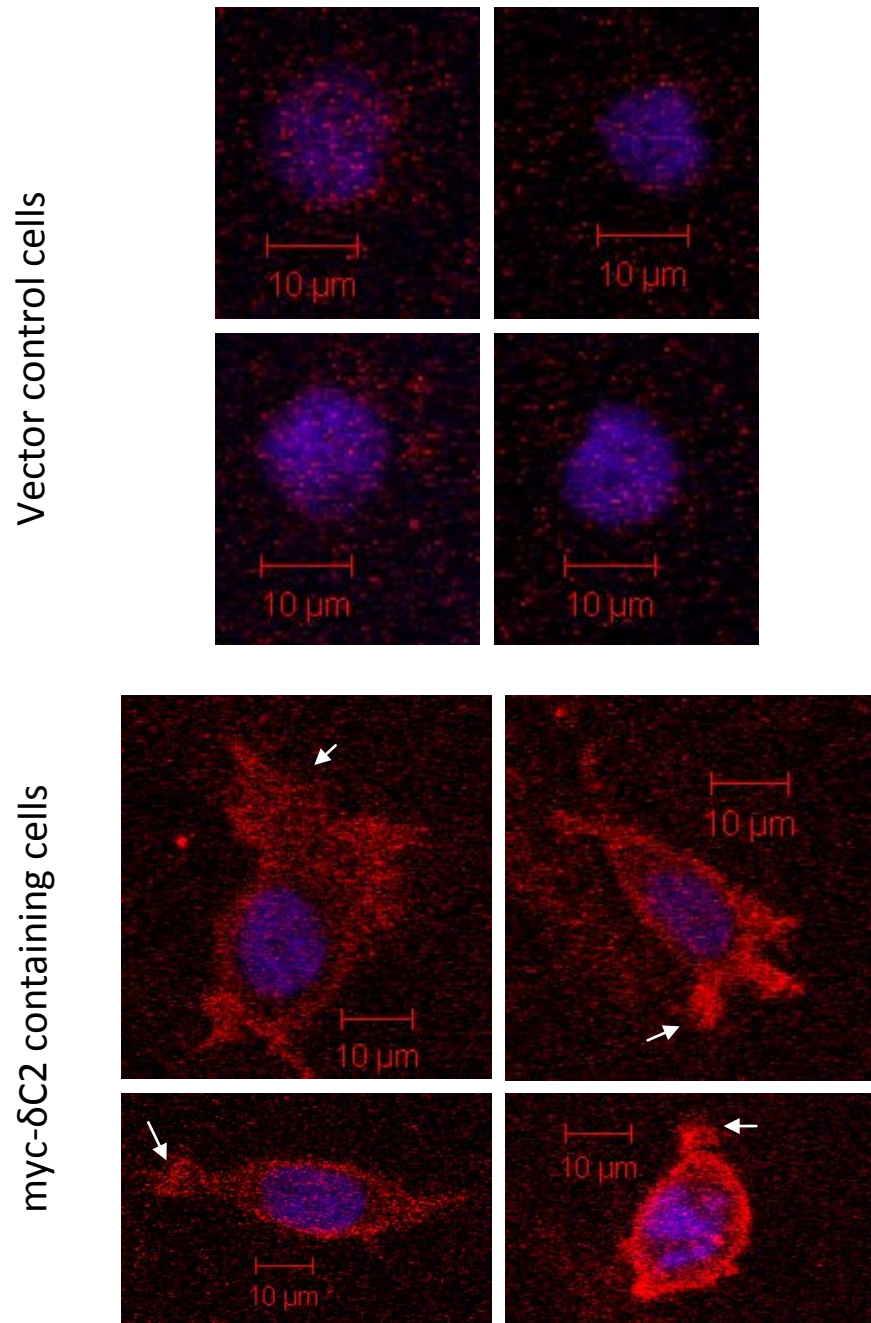


Figure 4.1: Myc-tag staining (red) of four vector control and four myc- δ C2 cells (blue indicates DAPI staining of the nucleus). Little or no myc-tag staining is seen in vector cells due to the lack of myc- δ C2. Any staining present is due to non-specific binding to endogenous c-myc protein, as seen with the western blots. Myc-tag staining shows the

position of myc- δ C2 at the cell periphery, primarily in protrusions from the bulk of the cell (see arrows).

The myc-tag antibody bound the myc- δ C2 where it was present in the cells. A low signal is seen in the vector control cells, possibly due to recognition of endogenous c-myc protein (Figure 4.1). The binding identified in the vector control cells was in the bulk of the cell surrounding the nucleus. In the myc- δ C2-expressing cells, more extensive staining was observed. There was a similar level of staining surrounding the nucleus in the bulk of the cell, but the majority of the staining appeared at the periphery of the cells. The cells expressing myc- δ C2 possessed protrusions from the bulk of the cell. Here the majority of the staining occurred. There is a degree of granularity in these images associated with problems with the myc-tag antibody binding. Low antibody binding required the microscope to be set up to allow detection of a larger degree of red fluorescence, subsequently some background fluorescence is also observed.

The presence of protrusions may indicate an effect of myc- δ C2 on the integrity of the normal cytoskeletal structure of the cell. Through staining of the cytoskeleton we examined firstly, if this is the case, and secondly, how the myc- δ C2 staining relates to this.

4.2.2 The relationship of myc- δ C2 localisation and actin localisation.

Cells were stained, as before, with DAPI (blue) and an antibody to the myc-tag together with a fluorescently labeled secondary antibody (red). In order to study the F-actin cytoskeleton in combination with myc- δ C2 positioning, a FITC-phalloidin stain, was used (green). This enables visualization of the actin structures present in the cell at time of treatment. Several fields, taken from several slides, were selected so that isolated cells could be studied.

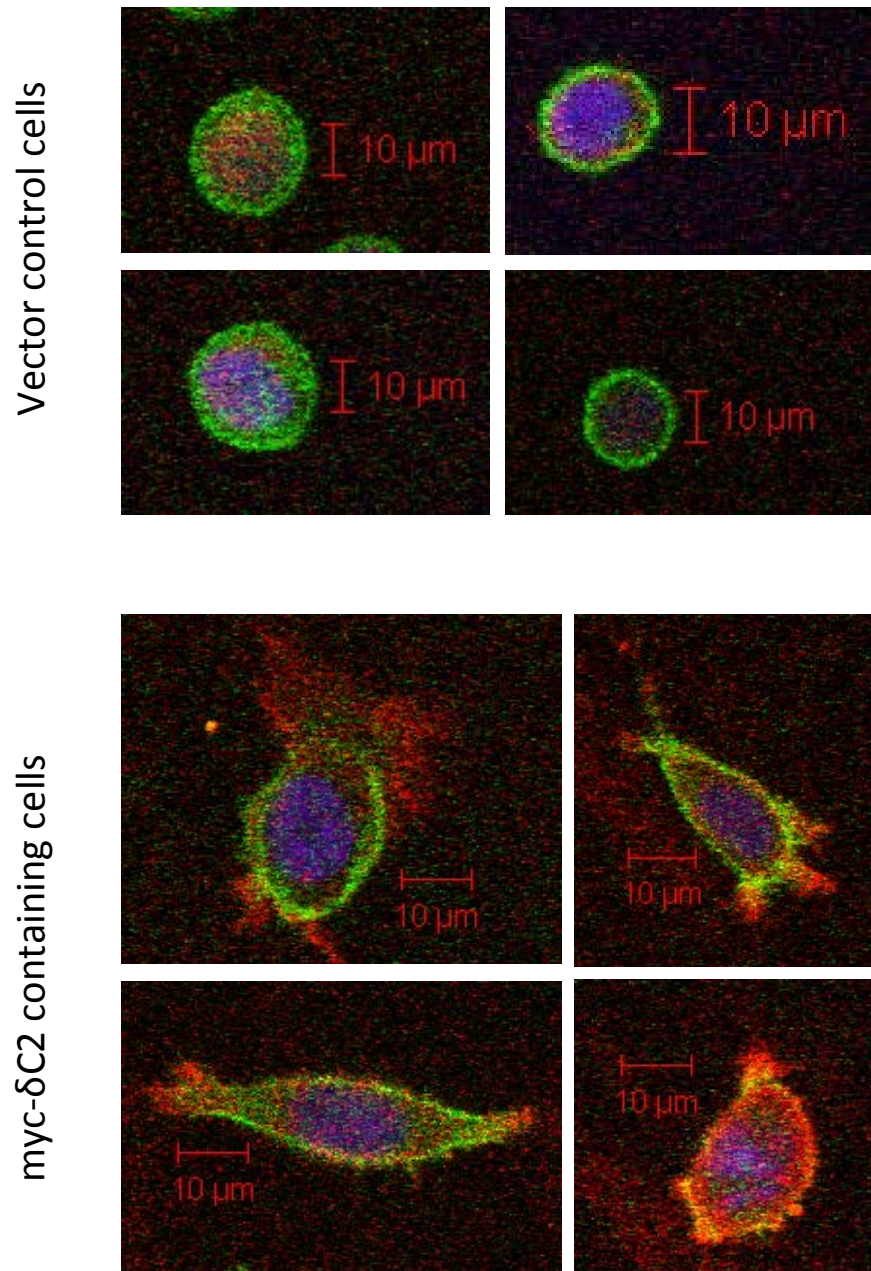


Figure 4.2: Actin cytoskeletal staining (green) in combination with myc-tag staining (red) of vector control and myc- δ C2 cells (blue is nuclear DAPI staining). Little or no myc-tag staining is seen in vector cells due to the lack of myc- δ C2. Any staining present is due to non-specific binding to endogenous c-myc protein, as seen with the western blots. In the myc-

δ C2 cells, myc-tag staining shows the position of myc- δ C2 at the ends of the actin protrusions.

The actin cytoskeleton appears to show extensions from the cell bulk in myc- δ C2 expressing cells. In Figure 4.1 we observed peripheral myc- δ C2 staining, Figure 4.2 shows that this is localised to the edges of the actin cytoskeleton. The actin cytoskeleton does not appear to show these extensions in the vector cells.

In the myc- δ C2 expressing cells, there does not appear to be any particular co-localisation of the myc- δ C2 and the f-actin. In fact the myc- δ C2 appears primarily at the extremities of the actin cytoskeletal staining (Fig. 4.3).

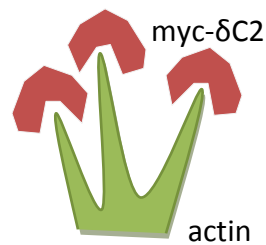


Figure 4.3: Graphic illustrating myc- δ C2 positioning in relation to actin cytoskeletal protrusions in myc- δ C2 cells. Red symbolizes myc- δ C2 positioning and green indicates actin.

In order to examine how frequently the myc- δ C2 was found at the periphery of the actin cytoskeleton, a total of 54 myc- δ C2 cells were examined by three people. They were asked to identify whether there was any indication of 9E10 staining at the ends of any protrusions from the actin cytoskeleton. From Table 4.1 it can be seen that the three people identified this staining pattern to occur in 81.5 to 88.9% (mean 86%) of cases.

Table 4.1: Number of myc- δ C2 cells positive for 9E10 staining at the ends of protrusions from the actin cytoskeleton.

	Person 1	Person 2	Person 3
myc- δ C2 cells	47/54	44/54	48/54
Percentage positive	87.0%	81.5%	88.9%

4.2.3 Comparing the actin cytoskeleton structure between vector control and myc- δ C2 expressing cells.

Following the finding that myc- δ C2 is found at the extremities of expressing cells at the end of actin protrusions, the actin cytoskeleton was examined in further detail using FITC-phalloidin staining. Differences were observed between the two cell types, where myc- δ C2 containing cells demonstrated an increased level of cytoskeletal protrusions than the vector control cells. As with the cell stained for actin and myc- δ C2, several fields were taken from several slides also selected where individual cells were present. From these fields, any cells which were in doublets or clumps were omitted from study.

Examples of the images studied are shown in Figure 4.4, which compares the MDA-MB-468 vector control cells with the MDA-MB-468 myc- δ C2 cells. Two images are shown for each cell type. The vector control cell green-stained actin cytoskeletons have a distinctly round profile and there are no protrusions from this circular state. The myc- δ C2 cells however have a less rounded profile and several green-stained protrusions from the bulk of the cytoskeleton.

MDA-MB-468 vector control cells

MDA-MB-468 myc- δ C2 cells

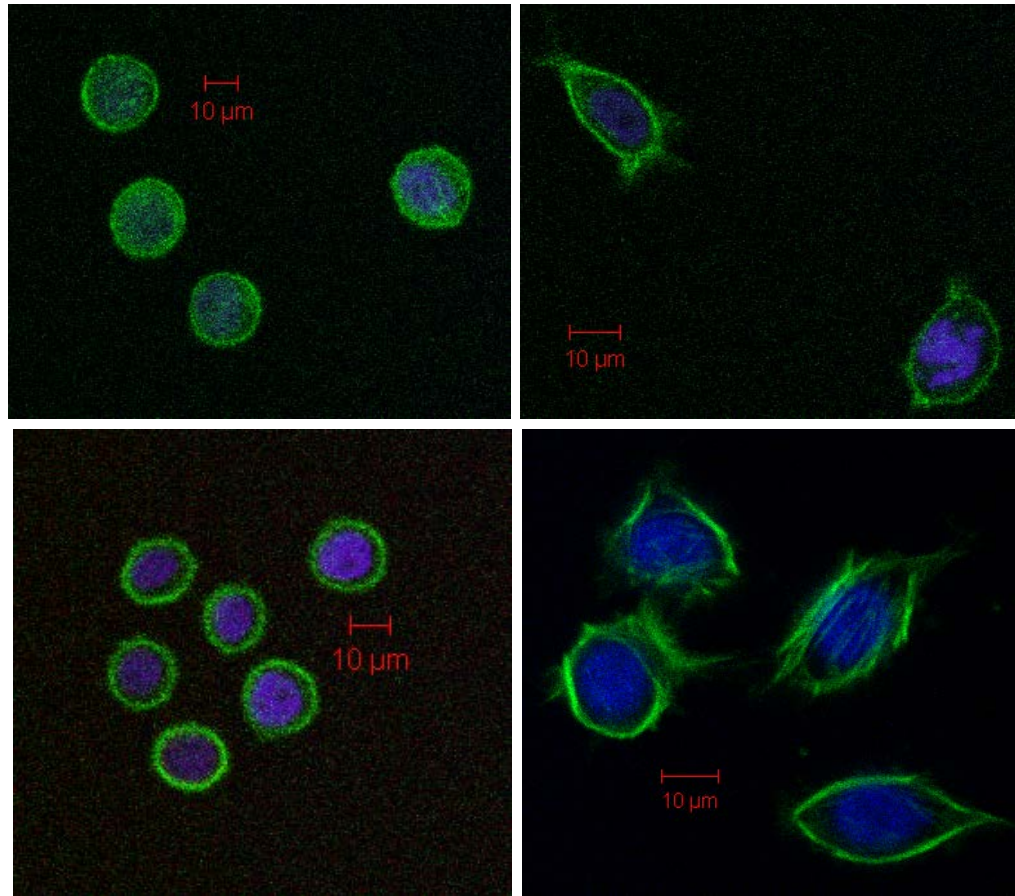


Figure 4.4: Actin cytoskeletal staining (green) of MDA-MB-468 myc- δ C2 and vector control cells (blue indicates nuclear DAPI staining).

A total of 51 vector control cells and 50 myc- δ C2 cells were examined by three people. They were asked to identify whether there was any indication of protrusions from the actin cytoskeleton in these cells. From Table 4.2 it can be

seen that they identified a higher degree of cells positive for protrusions in the cells over-expressing myc- δ C2 (mean 80%) compared to vector only-transfected cells (mean 35.9%).

Table 4.2: Number of cells showing protrusions from the actin cytoskeleton.

	Person 1	Person 2	Person 3
Vector control cells	22/51	13/51	20/51
Percentage	43.1%	25.5%	39.2%
myc-δC2 cells	41/50	39/50	40/50
Percentage	82%	78%	80%

The lack of actin protrusions in vector control cells and the presence in myc- δ C2 expressing cells may point to a role for PKC- δ in this phenomenon. The PKC- δ C2 domain may block an action of endogenous PKC- δ on the F-actin cytoskeleton. Since more protrusions are seen in the myc- δ C2 over-expressing cells, this action would be to suppress the formation of protrusions.

Actin can form several identifiable features, including: lamellopodia, filopodia, microvilli, ruffles and stress fibres (Allen et al., 1997). These protrusions may have a more fixed or a more transient nature. Lamellopodia, filopodia and membrane ruffles are more transient as they are associated with movement of cells (Nobes and Hall, 1995). Stress fibres are F-actin bundles, which can be

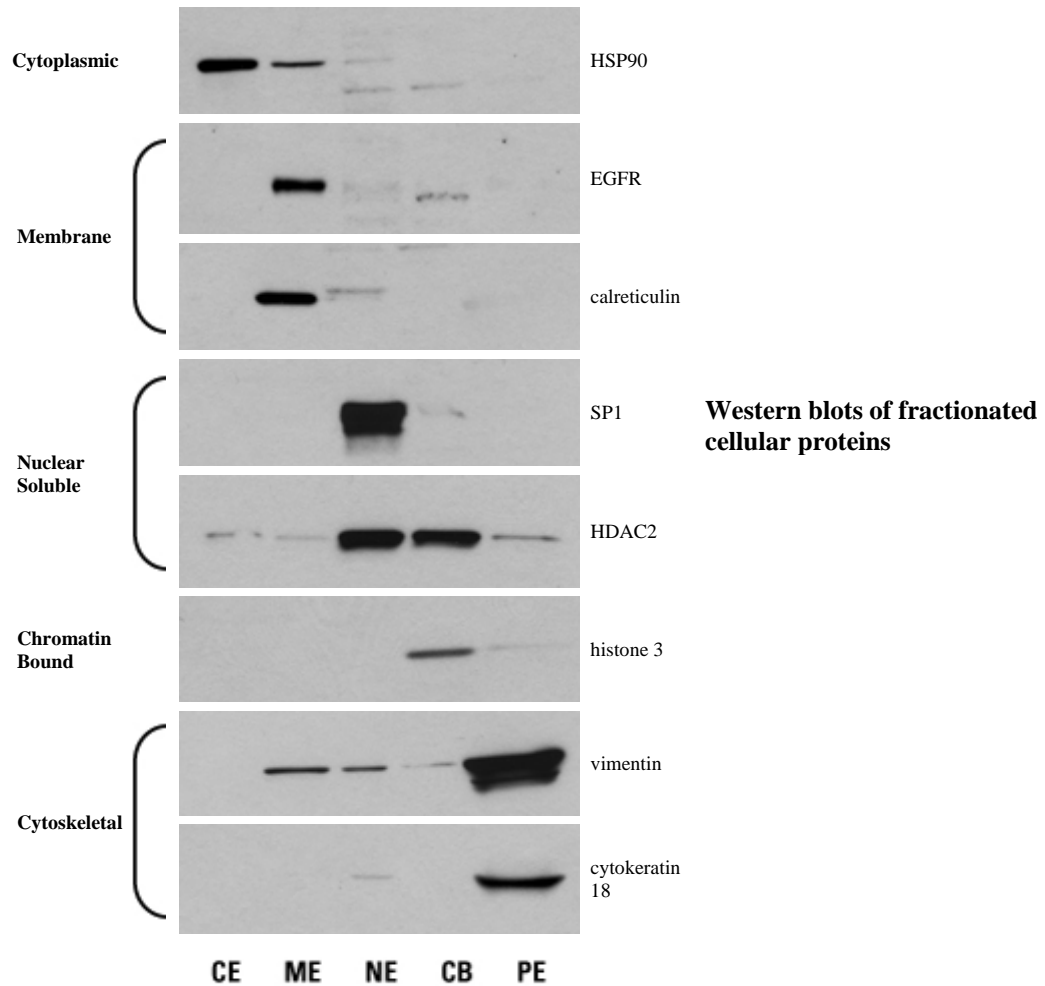
associated with connecting to a surface (Allen et al., 1997; Hall, 1994). Membrane ruffles and lamellopodia are broad structures seen across the leading edge of a cell. Lamellopodia extend from filopodia (Nobes and Hall, 1995). These formations are directional structures that would be associated with cell movement (Nobes and Hall, 1995); such directionality does not appear to be present in this study. In the data presented, extensions frequently project in numerous directions from the bulk of the cell. The extensions also vary in size. If the extensions do not show the directionality involved with cell movement, then attachment is a likely explanation, although the exact nature of the protrusions would require further investigation.

4.2.4 Studies of sub-cellular localisation of PKC- δ show similar profiles in vector and myc- δ C2 cells

As the cytoskeleton of myc- δ C2 cells displayed differences from the myc- δ C2 cells, it was considered that there may be differences induced in the sub-cellular localisation of the endogenous PKC- δ . This was initially examined by immunofluorescence, with confocal microscopy, but it was not possible to derive reliable detection of the endogenous PKC- δ . This may have been due to low levels of endogenous PKC- δ , weak antibody or a combination of the two. Thus the localisation was examined using sub-cellular fractionation.

The sub-cellular fractionation protocol employed a kit system, which created five extracts. Figure 4.5 shows the manufacturer's evidence for the protocol producing the correct fractions. The cytosolic fraction is obtained first. The buffer used induces selective membrane permeabilisation, releasing the soluble cytosolic components. Next the membrane fraction is collected using a buffer that solubilises all membranes except the nuclear membrane. This fraction contains all membrane constituents of the cell lysate: the plasma membrane, the Golgi, the endoplasmic reticulum and the mitochondria. The soluble nuclear fraction is the third fraction. A buffer that solubilises the nuclear membrane is used, releasing soluble components from the intact nuclei obtained previously. The chromatin-bound nuclear fraction is obtained utilising a micrococcal nuclease to release bound nuclear proteins. Finally the remaining pellet is extracted for

cytoskeletal proteins. This pellet can be quite crude and can contain a small amount of protein left over from the chromatin-bound nuclear fraction.



CE: cytoplasmic extract, ME: membrane extract, NE: nuclear extract, CB: chromatin-bound extract, PE: pellet extract.

HeLa cells (2×10^6) were fractionated using the Sub-cellular Protein Fractionation Kit. 10 μ g of each extract were analysed using Western blotting with antibodies against proteins from each fraction, including: cytoplasmic (HSP90), plasma membrane (EGFR), endoplasmic reticulum (calreticulin), nuclear soluble (SP1 and HDAC2), chromatin-bound (histone 3) and cytoskeleton (cytokeratin 18 and vimentin). The blots were probed with goat anti-rabbit HRP or goat anti-mouse HRP and detected with Thermo Scientific SuperSignal West Dura Chemiluminescent Substrate.

Figure 4.5: Manufacturers evidence for the fractionation protocol providing the particular fractions as stated. (Image obtained from www.piercenet.com sub-cellular protein fractionation kit page)

Histone H3 is a chromatin associated protein, and a Histone 3 antibody (Fig. 4.6) was used to confirm the fractionation pattern as claimed by the manufacturer. Fig. 4.6 shows that after fractionation of MDA-MB-468 cells, Histone H3 is located to fraction 4, the chromatin bound nuclear fraction, and not to other fractions, providing evidence for the reliability of the fractionation protocol.

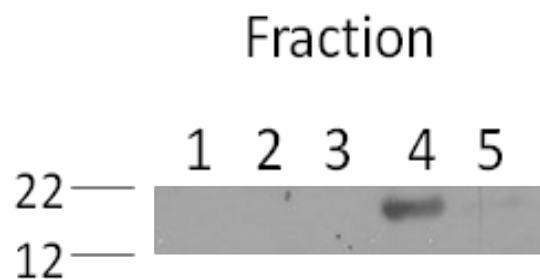


Figure 4.6: Check of the chromatin-bound nuclear fraction using histone 3 antibody. Histone 3 is found in the fraction 4 (chromatin-bound nuclear) and a small amount in fraction 5 (cytoskeletal). This correlates with the manufacturers results.

Fractionation of the vector control cells show the most PKC- δ is present in the membrane, the second largest fraction is the cytosolic fraction and the third the soluble nuclear fraction (Table 4.3). The myc- δ C2 expressing cells show the largest amount of PKC- δ in the soluble nuclear and membrane fractions, followed by the cytosolic fraction. There are no significant differences between the cell

lines due to the wide variation of the extracts across the 5 occasions this was studied. However there are some commonalities in that the bound nuclear and cytoskeletal fractions are both low (Table 4.3 and Figure 4.7).

Table 4.3: Distribution of PKC- δ amongst the five localisation extracts when cells are grown in normal growth conditions (10% serum). Percentage distribution shown \pm standard deviation (n=3).

	Cytosol	Membrane	Soluble nuclear	Chromatin-bound Nuclear	Cytoskeletal
Vector	32.78 \pm 18.1	41.68 \pm 14.0	22.70 \pm 13.4	2.00 \pm 2.1	3.90 \pm 6.2
myc-δC2	27.46 \pm 9.7	37.62 \pm 9.3	35.12 \pm 9.4	1.18 \pm 0.8	1.58 \pm 1.3

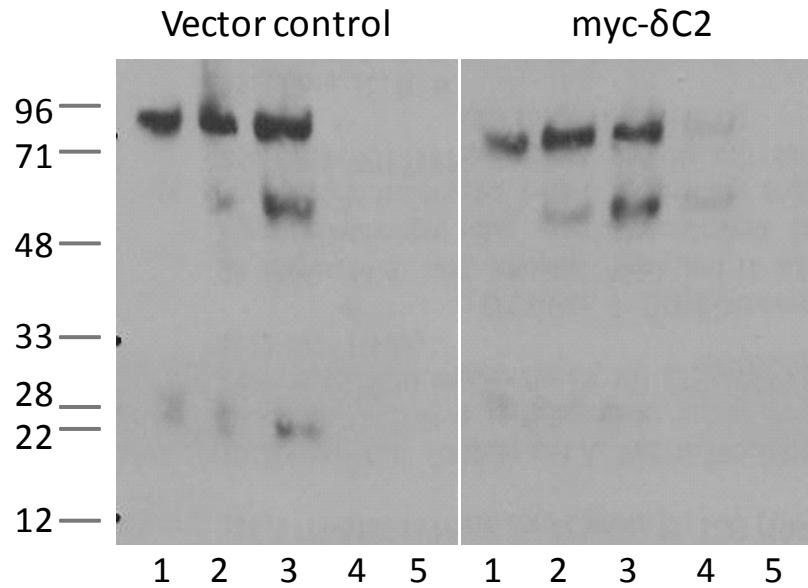


Figure 4.7: Example of fractionation data showing distribution of PKC- δ .

This indicates that the expression of myc- δ C2 is not affecting gross PKC- δ localisation within the major cellular fractions, as hypothesized. It may be that further analysis would be required in order to identify any smaller differences, for example, a shift to or from the mitochondria or Golgi apparatus.

4.2.5 Degree of attachment differs between the vector and myc- δ C2 cell lines following a 15-minute incubation period.

The data examining actin cytoskeletal structures in myc- δ C2 and vector control cells showed actin extensions from myc- δ C2 cells. This created a greater surface area. The literature indicates that PKC- δ plays a role in attachment of a cell (Kiley et al., 1999a). Whilst it is difficult to predict the effect of the cellular actin protrusions for cell behaviour, one possible consequence could be a change in the way the cells attach/adhere to a surface (Hall, 1994). In order to briefly examine this concept, cells were introduced to a surface for 15 minutes and then removed. The cells remaining suspended, and thus unattached, were counted (Table 4.4). The myc- δ C2 cells show a higher degree of attachment than vector control cells following incubation for 15 minutes. Perhaps the myc- δ C2 is interfering with endogenous PKC- δ activity that would allow the cytoskeletal components to become disassociated, thus enabling detachment and motility.

Table 4.4: Percentage of cells unattached 15 minutes after introduction to a surface. The mean is shown \pm the standard error of the mean. The differences between vector control and myc- δ C2 are significant in a paired Student t-test ($p \leq 0.05$).

	Expt 1	Expt 2	Expt 3	Mean
Vector control	96.7%	83.3%	43.3%	74.4% ($\pm 10.7\%$)
myc-δC2	66.7%	53.3%	30%	50% ($\pm 16.0\%$)

4.3 Discussion

This chapter began by examining the localisation of myc- δ C2 in the cell. This data was gathered using immuno-fluorescence where the nucleus was stained along with the myc- δ C2 domain, through utilisation of the myc-tag. This showed that the myc- δ C2 was present at the edges of the cells, extending from the bulk of the cytoplasm. Where actin staining was used, in addition to myc- δ C2 staining, the myc- δ C2 was found at the periphery of actin extensions. A more extensive cytoskeleton was also identified in the myc- δ C2 cells over the vector cells. The protrusions were absent from the vector cells, indicating that they were induced due to the presence of the myc- δ C2. Assuming myc- δ C2 acts as a dominant negative against the function of endogenous PKC- δ , this suggests that the normal function of PKC- δ is to 'round-up' the cells and prevent the formation of these protrusions.

Studies have examined the pathways associated with the development of particular actin formations. Activity of the proteins RhoA, Cdc42 and Rac have been shown to impact on the development of actin stress fibres, filopodia, and lamellopodia and membrane ruffling, respectively (Allen et al., 1997). Stress fibre formation is reliant on RhoA activity. Tyrosine phosphorylation of associated proteins pp125FAK and paxillin was detected upon RhoA activation (Barry and Critchley, 1994). PKC- δ was also found to localise to these stress fibres and focal

adhesions (Barry and Critchley, 1994). The importance of tyrosine phosphorylation in the configuration of these structures and the involvement of tyrosine phosphorylation in PKC- δ localisation, may suggest that tyrosine phosphorylation could also be involved in the targeting of PKC- δ to the area.

However, the fractionation experiments showed that the localisation of PKC- δ did not alter; it remained in the membrane, cytosolic and soluble nuclear fractions. This could be due the level of myc- δ C2 present in the cells not being sufficiently high to alter the localisation. The binding of myc- δ C2 may induce observable differences as it may still have an effect on the binding partners. Perhaps this is by induced auto-effects, despite the fact that the kinase domain is missing and thus serine/threonine phosphorylation events cannot occur.

The spreading effect of the myc- δ C2 on the cytoskeleton increased the surface area that could bind to a surface. This was an indication that there may be an effect on cell surface attachment. This did appear to be the case, as shown by the experiment that showed increased level of attachment after incubation for 15 minutes in myc- δ C2 cells. This experiment is only a brief examination of this feature Further examination of this would be necessary to draw any definitive conclusions. Ability to attach to a surface is a consideration of invasive and metastatic properties of a cell. Cells which have increased attachment would be less likely to move and colonise a distant location. Cells which have this invasive ability are able to grow independent of anchorage. Further examination of these

characteristics is desirable to identify the extent to which differences exist. The literature has shown higher levels of PKC- δ are observed in more metastatic cells (Kiley et al., 1999a; Kiley et al., 1999b). In addition, the expression of PKC- δ in less metastatic cells can enhance this ability. Knockdown of PKC- δ inhibits E-cadherin internalisation, and thus cell scattering (Singh et al., 2009). This evidence illustrates PKC- δ has important roles in cell motility as increasing PKC- δ activity also increases movement, whilst reducing its activity prevents motility.

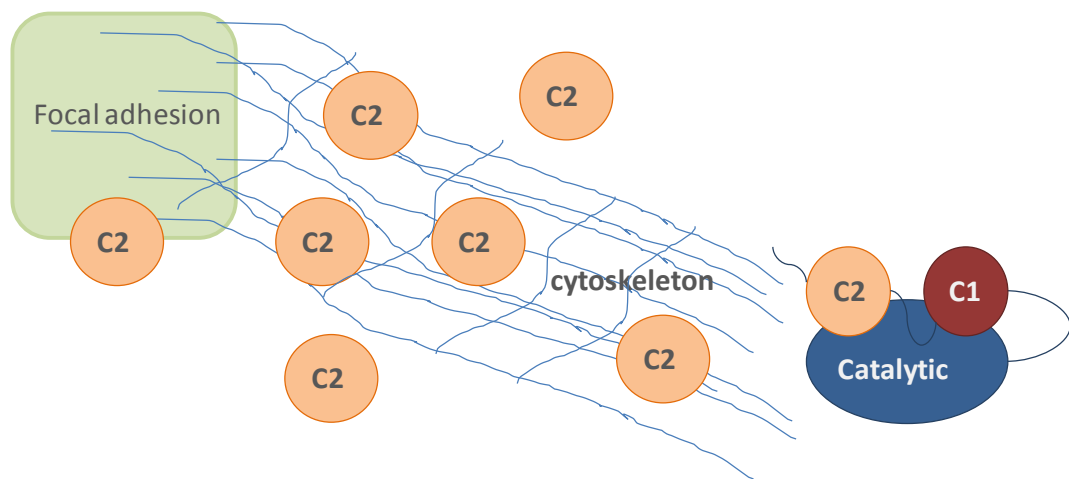


Figure 4.8: A suggested model for myc- δ C2 domain action with respect to cytoskeletal differences. The myc- δ C2 blocks the interaction of the endogenous PKC- δ to the cytoskeleton and focal adhesions, which would allow the cell to detach and become more motile.

A model can be established (Fig. 4.8) following the idea that the myc- δ C2 interferes with the PKC- δ interactions with the cytoskeleton. When these interactions are affected, the actin forms protrusions from the bulk of the cytoskeleton, thus allowing more extensive surface binding. However the localisation data shows that the positioning of PKC- δ is unaffected by myc- δ C2; therefore it may be that a variation on this premise occurs. As suggested above, the amount of myc- δ C2 in the cells may not be sufficient to interfere with the localisation of the PKC- δ . Instead, interactions could be made whereby binding of the C2 domain induces alterations in the binding partner.

Chapter 5: Investigation of the apparent growth advantage associated with myc- δ C2 expression

In Chapter 3 it was noted that there appeared to be a proliferation difference between the cell lines developed from MDA-MB-468 and MDA-MB-231 cells. However this did not appear to be the case for the MCF-7 transfected cell lines. This chapter further examines the transfected cell lines for proliferation differences by studying changes in cell number over time. In MDA-MB-468 and MDA-MB-231 cell lines, the presence of myc- δ C2 was associated with higher cell numbers. This was also true where myc-PKC- δ was expressed in MDA-MB-231 cells. There was no difference in MCF-7 cell lines where myc- δ C2 was expressed. However, myc-PKC- δ expression was associated with lower cell numbers. Apoptosis was examined in these cell lines to investigate whether this could

explain cell number differences. This was the case for the MDA-MB-468 cell lines,
but not for the MDA-MB-231 or MCF-7 cell lines.

5.1 Introduction

The un-transfected breast cancer cell lines exhibit several differences (see Chapter 1). For example, MCF-7 cells have higher endogenous levels of PKC- δ than MDA-MB-231 (Shanmugam et al., 2001). In Chapter 3, PKC- δ levels in MDA-MB-468 were found to be greater than those in MCF-7 cells. The order of the development of transfectants appeared similar in all three cell lines. The cells where myc- δ C2 was introduced appeared first, indicating there is a benefit to the cells when this domain is expressed. The transfectants of myc-PKC- δ appeared last, after the vector control cells, suggesting that PKC- δ over-expression may be detrimental. This response correlates with our hypothesis that the myc- δ C2 would competitively inhibit the endogenous PKC- δ , thus producing an effect in the cells which opposes the role of the endogenous PKC- δ .

By examining the three groups of cell lines, we aim to further characterise the effects of over-expressing PKC- δ and expression of the C2 domain on cell proliferation. This will allow a better understanding of the role of PKC- δ in these cells.

5.1.1 Analysing proliferation of a population by cell number

Proliferation of a cell population can be described as an increase in cell number. In order to study an increase in a cell population, cell numbers can be counted over a series of days, and the data charted in order to observe changes. By seeding the same amount of cells for each cell line considered, the proliferation rates can be compared. However, it is worth considering the balance of cell proliferation and apoptosis where a lesser increase in cell number does not necessarily identify lower proliferation, but may indicate a greater degree of apoptosis.

5.1.2 Flow cytometry

Flow cytometry can be used to examine phenotypic aspects of a cell population, including apoptosis. Flow cytometry is a process by which cells are passed through a 488nm laser beam in single file. Cell samples are mixed with sheath fluid which enables hydrodynamic focusing of the sample stream. This means the cells move through the laser beam one at a time along the same path and ensures sample analysis is undistorted. Cells can be studied based on the scattering of light to show their size and granularity. The forward scattering of light indicates a cell's size; this is measured at the opposite side of the flow cell to

the laser beam. Side scattering of light indicates a cells granularity, which is detected by the reflection of the 488nm laser beam on a filter at 90° (Fig. 5.1).

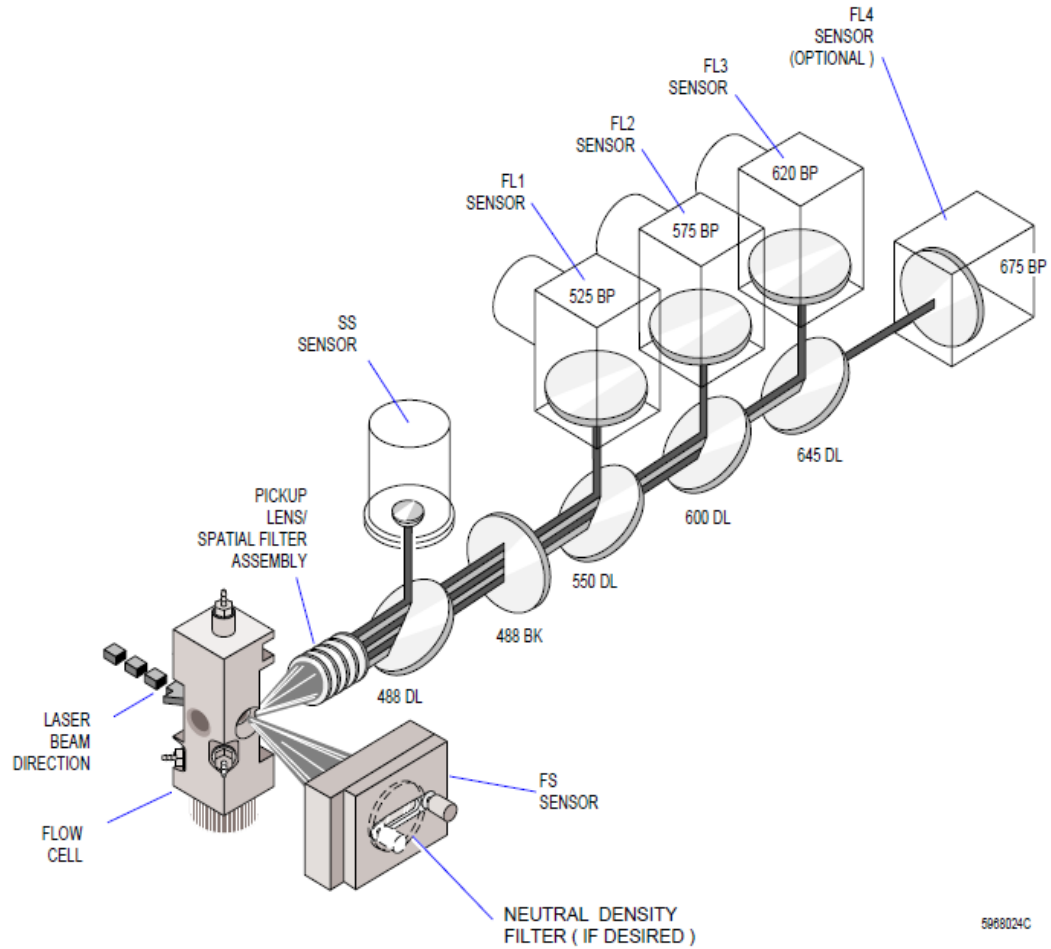


Figure 5.1: Configuration of the sensors and filters in the Coulter Epics XL Flow Cytometer.

Fluorescence occurs when light of one wavelength excites electrons from their ground energy state to an excited state. The electrons quickly relax to the lowest vibrational state of the excited energy level. Light is emitted at a longer

wavelength when the electrons return to the ground energy state. The 488nm laser can be used to excite fluorescent probes, for example FITC or propidium iodide (PI). Probes can be attached to antibodies. These can then be used to study numerous cell characteristics, such as the presence of a molecule on the cell surface. When these probes are excited and light is emitted at a longer wavelength, this light travels through a series of optical filters and can be detected, depending on its wavelength, at several detectors (Fig. 5.1). Prior to the fluorescent detectors is a 488nm blocking filter which blocks any remaining laser light so that only fluorescent light enters the remaining parts of the flow cytometer. The first sensor, FL1, detects light separated by the 550 DL filter and the 525 BP (band-pass) filter, of 505nm to 545nm wavelength. An example of a fluorophore detected at FL1 is FITC. The light transmitted through the 550 DL filter is further separated at the 600 DL filter. Reflected light hits the 575 BP filter to be detected at FL2 between 560nm and 590nm. An example of a fluorophore detected at FL2 is R-Phycoerythrin. The light transmitted through the 600 DL filter is then further separated at the 645 DL filter, and reflected light enters the FL3 sensor through the 620 BP filter at a wavelength of 605nm to 635nm. An example of a fluorophore detected at FL3 is PI. Any light remaining that has been transmitted through the 645 DL filter is finally filtered by a 675 BP filter which allows light of 660nm to 700nm through to the FL4 detector. An example of a fluorophore detected at FL4 is Cy5.

5.1.3 Analysing apoptosis

Apoptosis can be analysed using the AnnexinV – propidium iodide (AnnV - PI) flow cytometry assay (Vermes et al., 1995). The assay involves incubation with FITC tagged AnnexinV protein. AnnexinV is a Ca^{2+} dependent phospholipid-binding protein. It has a high affinity for phosphatidylserine (PS), a component of phospholipid bi-layer membranes. During the apoptotic process, PS is flipped from the inner membrane leaflet to the outer membrane leaflet (Vermes et al., 1995). Following this, FITC-AnnexinV can bind to the PS. Binding of FITC-AnnexinV to cells is thus a reflection of their apoptotic state (Schutte et al., 1998).

Another component of the assay is propidium iodide (PI). This is a ‘vital dye’, named as such as it is excluded from viable cells which have intact membranes, but not from dead and damaged cells, such as those in later stages of apoptosis. In early apoptosis cell membranes exclude PI, whereas in later apoptosis they cannot; thus the PI enters and intercalates with the DNA.

The flow cytometer detects the fluorescence of the FITC and PI and displays the cells according to their properties related to these two molecules. Quadrants are then drawn around the populations formed. If FITC-AnnexinV has not bound and PI has not intercalated, i.e. no fluorescent signal is detected, the cells are viable. If FITC-AnnexinV has not bound and PI has intercalated the cells are termed ‘leaky’; they are damaged but aren’t undergoing apoptosis. It may be that the processing of the cells for the assay has damaged them; generally this quadrant

only contains a very low percentage of the cell population. If FITC-AnnexinV has bound and PI has not intercalated, the cells are early apoptotic. These cells have initiated apoptosis but have not gone that far through the process to the point where the membrane is permeable and they break up. If FITC-AnnexinV has bound and PI has intercalated, these cells are late apoptotic or necrotic. The assay cannot distinguish between late apoptosis and necrosis here as the membranes are distorted and permeable. However, a sizable population in the early apoptotic quadrant indicates that the cells in the late apoptotic and necrotic quadrant are likely to have gone through initiation and progression of apoptosis (Fig 5.2).

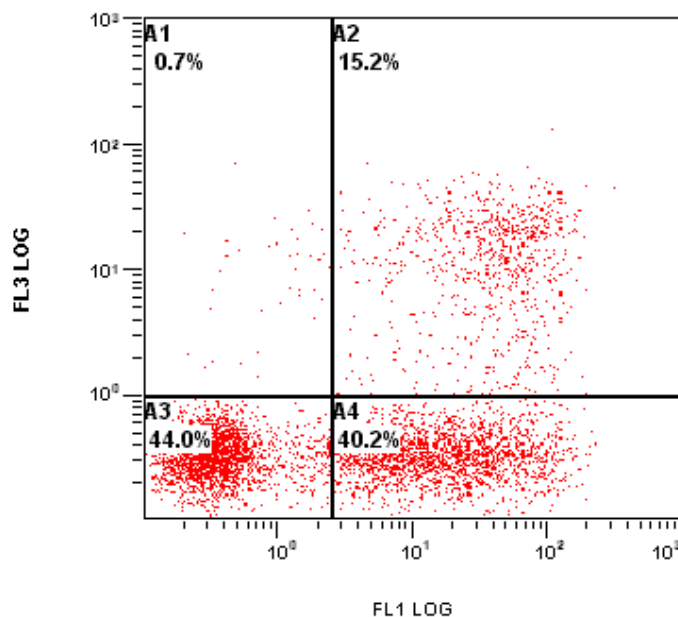


Figure 5.2: An example of the AnnexinV - PI apoptosis data showing the four quadrants which enable determination of the apoptotic status of

the population. Data shows apoptotic profile of MDA-MB-468 vector control cells treated with 500nM camptothecin. FL1 LOG shows the degree of FITC fluorescence displayed on a logarithmic scale. FL3 LOG shows the degree of PI fluorescence displayed on a logarithmic scale.

Apoptosis can be initiated through treatment with a trigger, for example, camptothecin. Camptothecin is an alkaloid which inhibits Topoisomerase I, thus blocking the elongation phase of DNA replication, thereby inducing apoptosis (Pommier, 2006). Analogues of camptothecin, irinotecan and topotecan, are used in the clinic (Pommier et al., 2010). Triggering apoptosis, in this case with camptothecin, may reveal differences in the apoptotic response of the cell lines.

5.2 Results

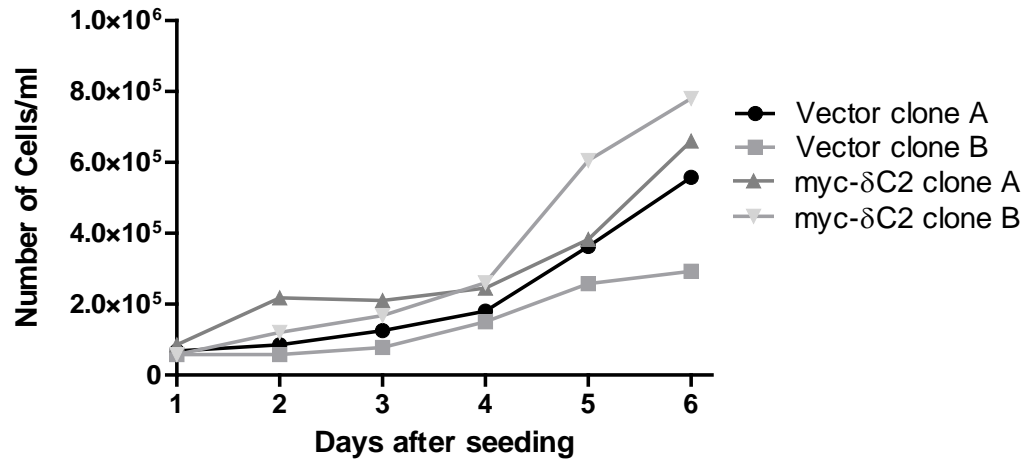
5.2.1 MDA-MB-468

5.2.1.1 *Cell numbers are higher in myc- δ C2 than vector cells*

During culturing of the MDA-MB-468 cells, the clones expressing myc- δ C2 appeared to be growing faster compared to the vector control clones. In order to quantify this effect a proliferation experiment was performed, whereby the cell numbers were tracked over several days.

Two clones expressing myc- δ C2 (A and B) and two vector control clones (A and B) were studied. Figure 5.3 shows that the myc- δ C2-expressing cells grow at a higher rate.

A



B

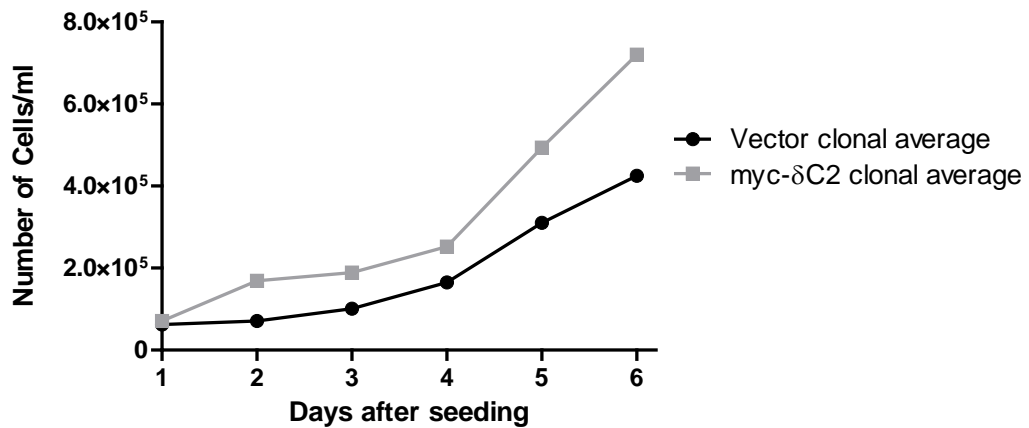


Figure 5.3: The effect of myc- δ C2 expression on proliferation rates of two clonal populations of MDA-MB-468 transfected cells when compared to two clonal populations of the vector control cells. A: shows the proliferation of two individual clones for each cell line type (n=2). B: shows the average growth of each clone type. myc- δ C2 clone average shows an increased proliferation rate by Day 6 over the vector clone average.

It may be argued that the differences could be due to clonal variation, as the clones examined had developed early in the process, rather than being associated with the transfected agent. Thus in order to verify that the observed effect was not an artefact of the selection process, the pooled populations of myc- δ C2 expressing cells and vector control cells were also studied (Fig. 5.4).

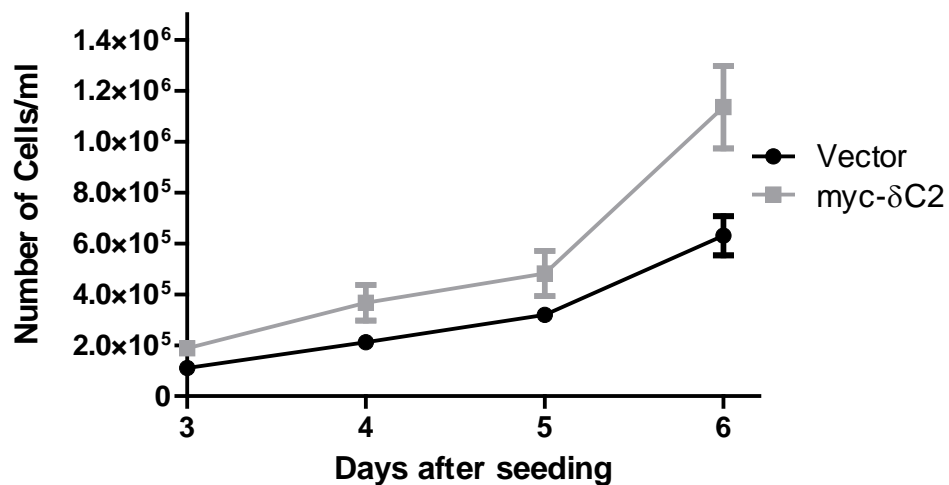


Figure 5.4: The effect of myc- δ C2 expression on proliferation rates of MDA-MB-468 transfected cells when compared to the vector control. Error bars are standard error of the mean (n=6). myc- δ C2 cells grow at an increased rate to vector cells by Day 6, ($p \leq 0.05$) in a paired t-test. The data was analysed in Excel using a paired t-test, in which one data

point from one repeat of the experiment for one cell line was paired with the equivalent data point from the other cell line.

By Day 6, increased cell numbers were associated with MDA-MB-468 pooled cells expressing myc- δ C2 (Fig 5.4). The cells increased in number by 1.8 times over the vector control. Thus for MDA-MB-468 cells, either clone or pool, the presence of myc- δ C2 is associated with higher proliferation rates. Perhaps the myc- δ C2 is blocking an interaction of the endogenous PKC- δ C2 domain with a binding partner that would induce apoptosis of the cells; thus allowing the cells to survive and the proliferation to continue at a greater rate than the vector cells (see Chapter 1).

5.2.1.2 Cells expressing myc- δ C2 have higher viability than vector cells

In order to examine the reasons for the proliferation differences identified above, the level of apoptosis within the pool populations were measured using the Annexin V-propidium iodide assay.

The presence of myc- δ C2 was associated with a greater percentage of 'alive' cells under normal cell culture conditions (Fig. 5.5). Also, there are significantly fewer cells in the early apoptotic fraction of myc- δ C2 cells than the vector control.

There is no significant difference between the two cell lines in the late apoptotic/necrotic fraction. This data suggests that the expression of the myc- δ C2 protein has a protective effect upon the MDA-MB-468 cells.

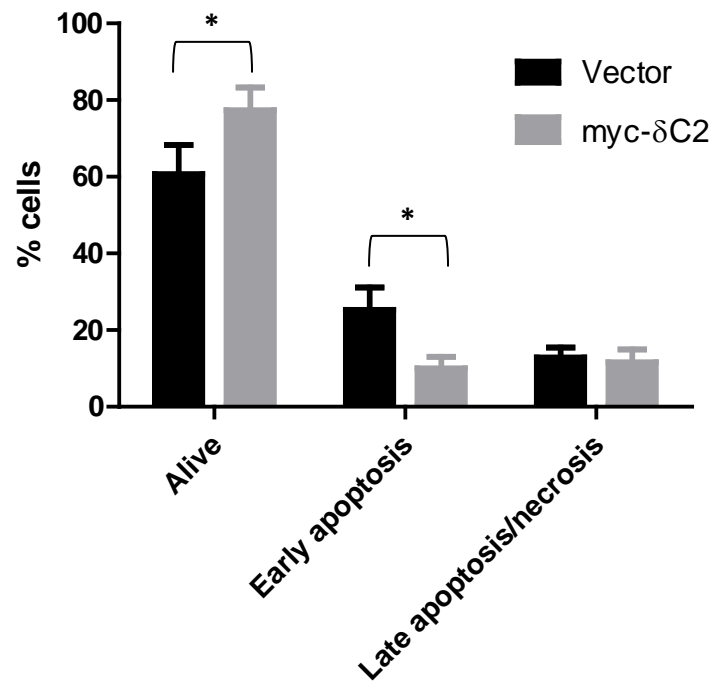


Figure 5.5: Analysis of apoptosis in the MDA-MB-468-myc- δ C2 and MDA-MB-468 vector control cell lines using the AnnexinV - propidium iodide assay illustrated the decrease in levels of apoptosis in cells. The differences indicated by * are significant in a paired Student's t-test ($p \leq 0.05$). Error bars are standard error of the mean (n=4).

The MDA-MB-468 cell lines were treated with 500nM camptothecin to induce apoptosis (Fig. 5.6). This concentration was chosen as it induced apoptosis, but did not kill all the cells within the 24 hours of treatment.

Apoptosis increases in both cell lines, but more so in the presence of myc- δ C2 where the decrease in viable cells is from 77.4% to 31.3% (46.1 percentage points). Whereas in vector cells viability is reduced by 36.4 percentage points from 60.7% to 24.3% (compare Figures 5.5 and 5.6). The previously significant differences between the cell lines were lost. The protective effect of myc- δ C2 seen in untreated cells does not continue when cells are camptothecin treated in order to induce apoptosis.

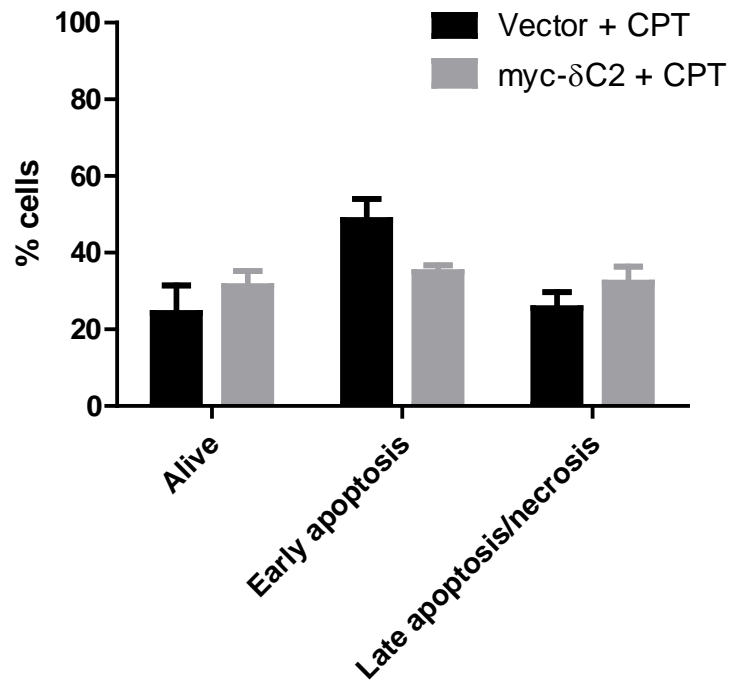


Figure 5.6: Analysis of apoptosis in the MDA-MB-468-myc-δC2 and MDA-MB-468 vector control cell lines when apoptosis is induced by camptothecin treatment using the AnnexinV - propidium iodide assay. Error bars are standard error of the mean (n=4).

In summary, in the MDA-MB-468 cell lines a clear difference is seen where the presence of myc-δC2 is associated with higher levels of 'alive' cells. Differences are also clear where the presence of myc-δC2 is associated with lower levels of early apoptosis. This data correlates with the proliferation data shown in Figure 5.3, where the myc-δC2 is associated with a greater number of cells following 6

days. This is due to a decreased level of apoptosis due to a protective effect of myc- δ C2. The myc- δ C2 may be interrupting the pro-apoptotic PKC- δ signal.

The treatment of these cell lines with camptothecin prevents the protective effect of the myc- δ C2. Camptothecin blocks Topoisomerase I. This means that DNA replication is halted. This DNA damage is an internal trigger to begin apoptosis. Under conditions where the drug is absent, and thus this does not occur, this DNA damage induced internal mechanism will not be activated. In untreated conditions, an alternate internal mechanism or an external trigger may be activated, where the C2 domain may play a role. It may be the case that the differing response of the cells, where myc- δ C2 provides a protective effect in one case but not the other, could be due to the pathways involved in apoptosis induction. For example, FADD is involved in extrinsically-stimulated apoptosis, but not where intrinsic signals stimulate apoptosis. The myc- δ C2 may only associate with a partner involved in a particular pathway. Alternatively, perhaps the concentration of camptothecin is too great and as such prevents observation of a protective effect. This could be tested by inducing apoptosis using lower concentrations of camptothecin.

5.2.2 MDA-MB-231

5.2.2.1 Cell numbers of myc- δ C2 expressing cells increase greater than vector cells.

Considering the effects of myc- δ C2 expression on the proliferation rates of the transfected MDA-MB-468 cell lines, the MDA-MB-231 transfected cell lines were also tested. Similar to the MDA-MB-468 cells, the pooled population of myc- δ C2 expressing cells also showed a significant increase in cell number over vector control cells (Fig. 5.7).

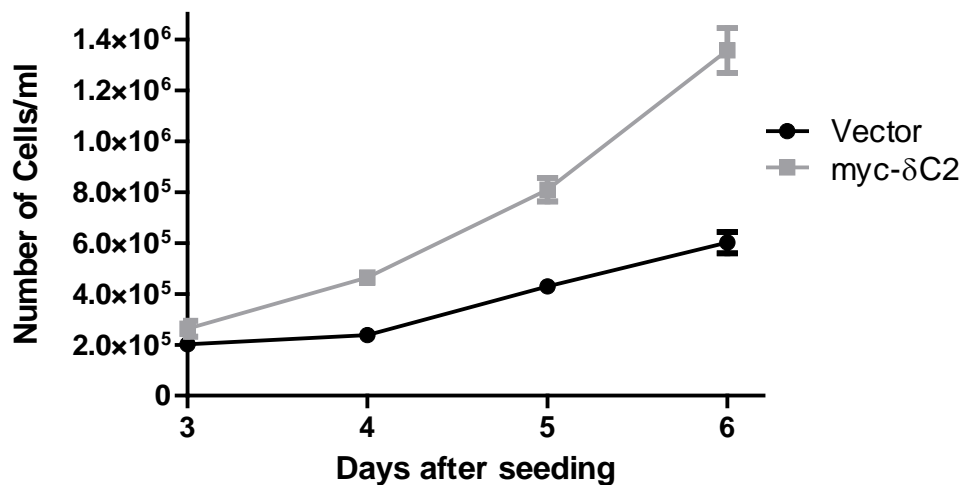


Figure 5.7: The effect of myc- δ C2 expression on proliferation rates of pool populations of MDA-MB-231 transfected cells when compared to the vector control pool cells. Error bars show standard error of the

mean (n=6). The myc- δ C2 pool cells showed a significantly increased proliferation rate by Day 6, $p \leq 0.002$ in a paired t-test.

The increase in proliferation in MDA-MB-231 cells is somewhat greater than that observed in the MDA-MB-468 cells. They have grown to 2.3 times the number of vector control cells by day 6 (1.8 times with MDA-MB-468).

5.2.2.2 The myc- δ C2 cells have lower viability than vector cells

In order to examine whether the differences in cell number would correlate with apoptosis, as they did in the MDA-MB-468 cells, apoptosis was examined in the MDA-MB-231 cell lines (Fig. 5.8). In this case the viability levels were significantly lower in myc- δ C2 cells. The late apoptosis/necrosis fraction of myc- δ C2 cells showed a significant increase over vector control cell levels.

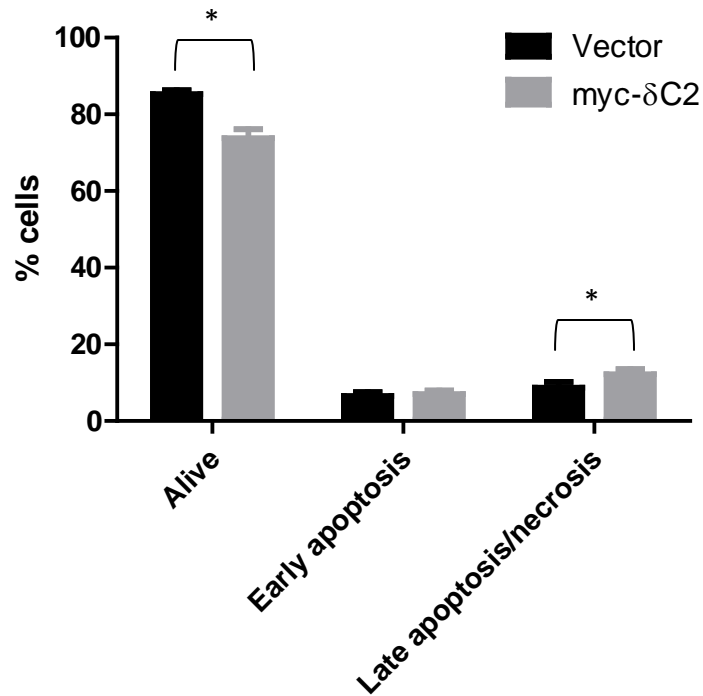


Figure 5.8: Analysis of apoptosis in the MDA-MB-231-myc- δ C2 and MDA-MB-231 vector control cell lines using the AnnexinV - propidium iodide assay. The differences indicated by * are significant according to unpaired Student's t-test where $p \leq 0.005$ for 'Alive' and $p \leq 0.02$ for 'Late apoptotic/necrotic'. Error bars are standard error of the mean (n=6).

Next, camptothecin was used to induce apoptosis. It transpired that in contrast to MDA-MB-468 cells, which required 500nM to become apoptotic, 2 μ M camptothecin was need to induce apoptosis in MDA-MB-231 cells. This illustrates a further difference between the two cell lines. The differences in apoptosis

between myc- δ C2 cells and vector cells were lost when they were treated with camptothecin (Fig. 5.9).

The camptothecin treatment induced significant changes in the 'alive' proportion of vector control cells, but not in the myc- δ C2 cell line. Significant changes were also observed in the early apoptotic fraction of myc- δ C2 cells following camptothecin treatment. However this was not seen in the vector cells.

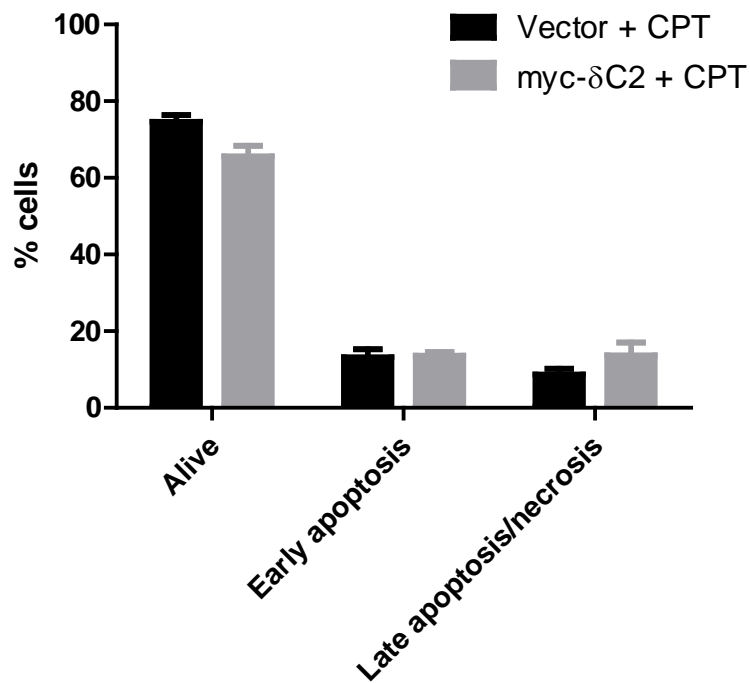


Figure 5.9: Analysis of apoptosis in the MDA-MB-231-myc- δ C2 and MDA-MB-231 vector control cell lines when apoptosis is induced by camptothecin treatment using the AnnexinV - propidium iodide assay. Error bars are standard error of the mean (n=6).

The myc- δ C2 expressing cells appear to be less affected by the camptothecin treatment (compare Fig. 5.8 and 5.9). In these cells the percentage of viable cells drops 4.93 percentage points, whereas the vector cells show a decrease of 12.5 percentage points, a 2.5 times greater decrease. When induced to apoptose, the myc- δ C2 appears to demonstrate a protective effect for the cells. Perhaps there are differences between the cell types, which mean that in this cell line, the function of PKC- δ and its C2 domain is required. The myc- δ C2 may block a required interaction of the endogenous PKC- δ C2 domain, thus limiting the levels of apoptosis.

The MDA-MB-231 cell lines show a different pattern to that exhibited by MDA-MB-468. Whereas in MDA-MB-468 cell lines the presence of myc- δ C2 reduced apoptosis; in MDA-MB-231 cells the presence of myc- δ C2 resulted in significantly less viable and more 'late apoptotic/necrotic' cells. This data does not complement the cell number data (Fig. 5.7) where myc- δ C2 cells proliferated at an increased rate over the vector control. Considering that the apoptosis data does not explain the differences in proliferation rate, it is likely that a proliferative pathway may be affected by PKC- δ , and that the C2 domain is important in facilitating this. The dominant negative effect of the myc- δ C2 on PKC- δ activity with respect to cell survival may suggest that the abundant myc- δ C2 protein is blocking an interaction of PKC- δ that is pro-survival. Indeed, the

literature supports the premise of PKC- δ demonstrating a pro-survival effect in this cell line (Lønne et al., 2009). Lønne et al illustrated the involvement of PKC- δ in suppressing the overactive ERK1/2 pathway in MDA-MB-231 cells. However, the literature did not examine the involvement of the C2 domain specifically. The lower viability of MDA-MB-231 myc- δ C2 expressing cells demonstrates that it is crucial in facilitating the action of PKC- δ in this pathway.

Upon camptothecin treatment of the MDA-MB-231 pool cell lines, the levels of viable cells decreased where myc- δ C2 was present and also in the vector control. However the myc- δ C2 cells show a lower decrease in viability than the vector control cells. This could suggest that the myc- δ C2 is providing a protective effect under treatment with camptothecin. The role of PKC- δ in apoptosis is considered to be complicated and varied. Perhaps in the MDA-MB-231 cell line the role of PKC- δ depends on the origin of the apoptotic signal. In normal conditions, where camptothecin does not induce DNA damage, PKC- δ is anti-apoptotic. However, where DNA damage is induced, e.g. by camptothecin, and detected through an internal mechanism to trigger apoptosis, the response and involvement of PKC- δ may differ and a pro-apoptotic role may transpire.

5.2.2.3 Expression of myc-PKC- δ is associated with increased cell numbers over vector control cells

The MDA-MB-468 cell line was not successfully transfected with myc-PKC- δ , perhaps due to a pro-apoptotic role of PKC- δ . However in the case of MDA-MB-231 cells, myc-PKC- δ expressing transfectants were successfully established.

Over-expression of PKC- δ in the MDA-MB-231 increased cell numbers by 1.7 times (at day 6 from the point of seeding) (Fig. 5.10). The increase is not as great as observed in cells expressing myc- δ C2 (which was 2.25 times over the vector control).

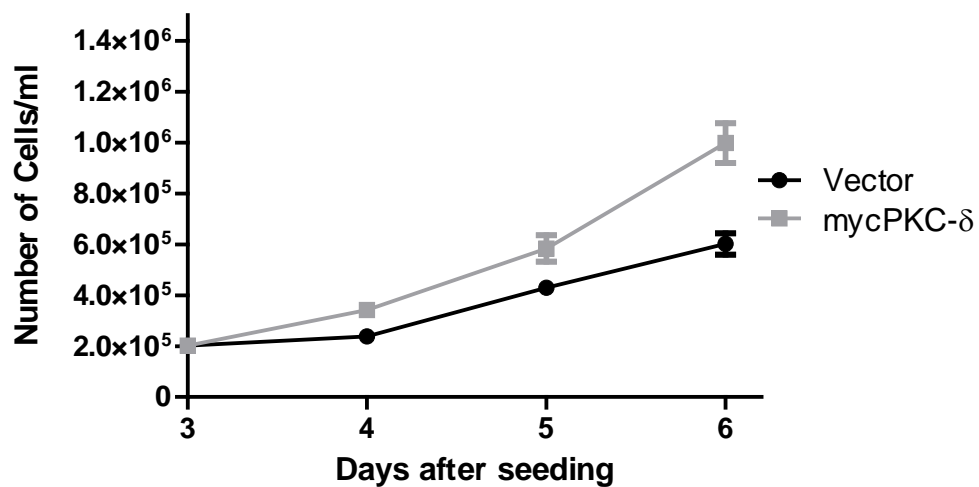


Figure 5.10: The effect of over-expression of myc-PKC- δ in MDA-MB-231 cells is to increase the rate of proliferation compared to the vector control cells. The increased proliferation rate is significant to $p \leq 0.004$

in a paired Student's t-test. Error bars show standard error of the mean (n=6).

The increase in proliferation caused by the presence of myc- δ C2 may indicate that the endogenous PKC- δ would normally have an inhibitory effect on cell growth. Thus when the PKC- δ protein is over-expressed it could be perceived that a decrease in proliferation over the vector would be identified. However, this is not seen. In fact, an increase in proliferation is seen, albeit lower than that with C2 domain. The increase is somewhat supported by the literature showing PKC- δ to be pro-survival in MDA-MB-231 cells (Lønne et al., 2009).

Perhaps when over-expressing the myc- δ C2 domain the myc- δ C2 prevents an endogenous PKC- δ activity to limit proliferation, thus allowing greater levels of proliferation. However endogenous PKC- δ may act in both an anti-proliferative activity and also a pro-proliferative activity, but perhaps the C2 domain is only involved in the former. Where PKC- δ is over-expressed it acts in both pathways, but perhaps more so in the latter, due to lower levels of a binding partner in the former pathway, thus overall increasing proliferation of the population.

5.2.2.4 *Apoptosis does not differ between vector cells and PKC- δ over-expressing cells*

As with myc- δ C2 expressing cells, apoptosis was examined in order to see if the effects of PKC- δ over-expression could explain the cell number differences (Fig. 5.11). This was assessed with and without camptothecin treatment at 2 μ M (Fig. 5.11 and 5.12). In neither case was a difference seen between the vector cells and myc-PKC- δ cells.

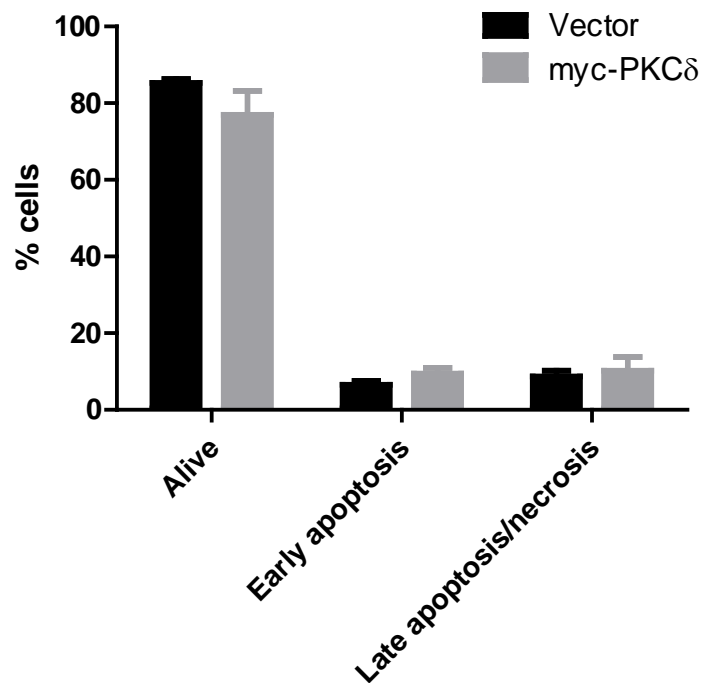


Figure 5.11: Analysis of apoptosis in the MDA-MB-231-myc-PKC- δ and MDA-MB-231 vector control cell lines using the AnnexinV - propidium iodide assay. Error bars are standard error of the mean (n=6).

Camptothecin treatment induced a difference ($p \leq 0.005$) in the percentage of alive vector cells. This was not seen with the myc-PKC- δ cells. MDA-MB-231 myc-PKC- δ cells appear to show an acquired resistance to camptothecin at $2\mu\text{M}$, through the over-expression of myc-PKC- δ . This could be an example of a protective effect of PKC- δ in these cells. It is surprising that the protective effect of PKC- δ is not more obvious considering the reported involvement of PKC- δ as a pro-survival factor (Lønne et al., 2009). However, as seen in the experiments with the myc- $\delta\text{C}2$ expressing cells, the pathway involved in camptothecin apoptotic induction may be complex.

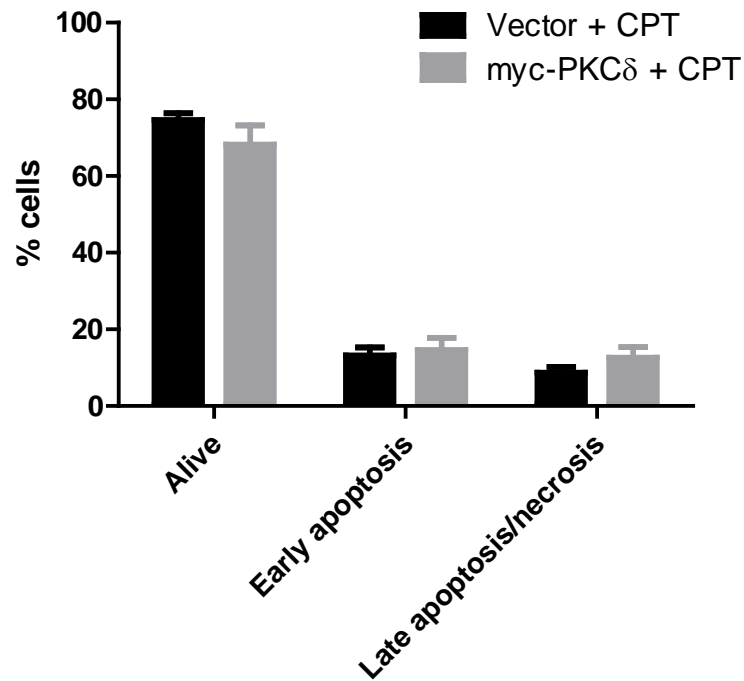


Figure 5.12: Analysis of apoptosis in the MDA-MB-231-myc-PKC- δ and MDA-MB-231 vector control cell lines when apoptosis is induced by camptothecin treatment using the AnnexinV - propidium iodide assay. Error bars are standard error of the mean (n=6).

Differences in apoptosis are not observed with PKC- δ over-expression in MDA-MB-231 cells. This is somewhat surprising given the effect on cell numbers, where PKC- δ over-expression induced a 1.66 times increase over vector control cells, and the reported pro-survival activity of PKC- δ (Lønne et al., 2009). However as the cell number is a balance of apoptosis and cell proliferation, it is perhaps the latter that is the predominant reason for the increase in numbers.

5.2.3 MCF-7

5.2.3.1 Cell numbers do not differ between vector and myc- δ C2 expressing cells

Expression of myc- δ C2 in MCF-7 cells did not significantly change the number of cells (Fig. 5.13) at any point along the time course.

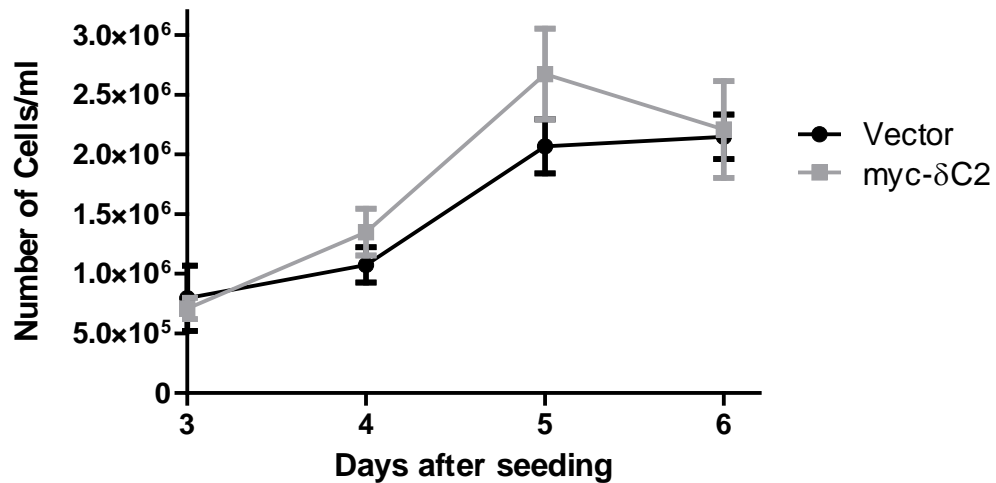


Figure 5.13: The effect of myc- δ C2 expression on proliferation rates of pool populations of MCF-7 transfected cells compared with the vector control pool cells. Error bars show standard error of the mean (n=6).

The MCF-7 cells may not respond to the presence of myc- δ C2 in the same way due to a part of the pathway differing in these cells; perhaps a key protein in the pathway is not expressed. For example, MCF-7 cells do not express caspase-3 (Janicke, 2009), which has been shown to participate in apoptosis involving PKC- δ (Reyland, 2007).

5.2.3.2 Apoptotic profiles do not differ between myc- δ C2 and vector cells

Analysis of the MCF-7 stable cell lines failed to show any differences between apoptotic profiles of the vector and myc- δ C2 containing cell lines (Fig. 5.14). The lack of difference between the cell line apoptotic profiles correlates well with the cell number data. In both cell lines a large proportion of the population is in the 'alive' category. The very low proportion of cells in the 'early apoptotic' division suggests they are not undergoing apoptosis.

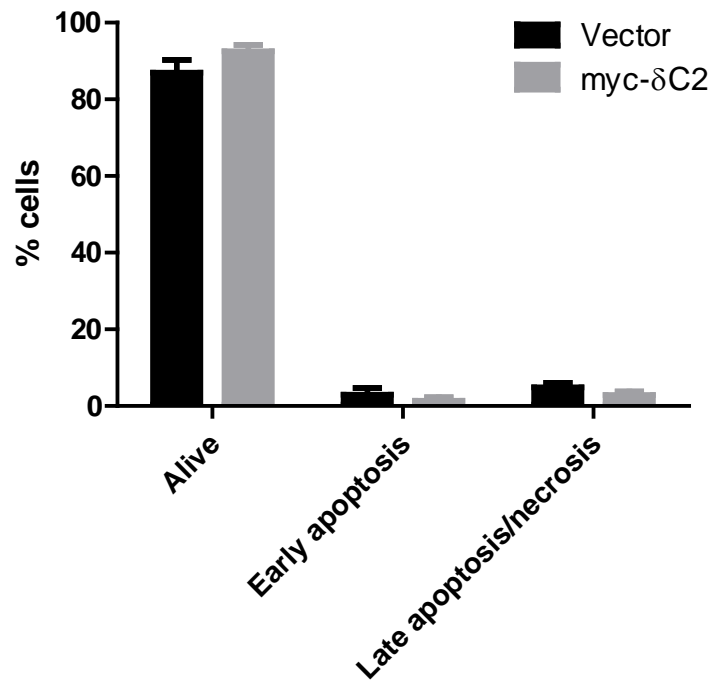


Figure 5.14: Analysis of apoptosis in the MCF-7 myc- δ C2 and MCF-7 vector control cell lines using the AnnexinV - propidium iodide assay. Error bars are standard error of the mean (n=6).

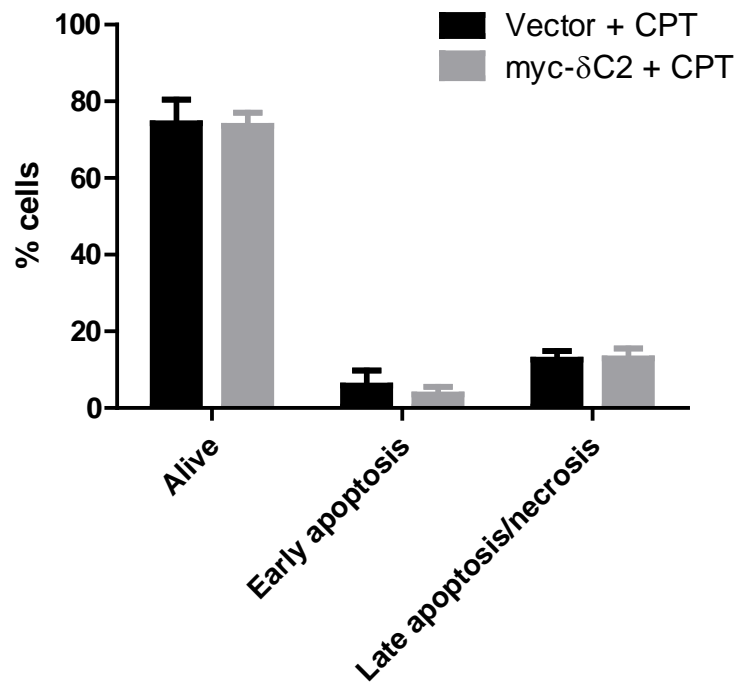


Figure 5.15: Analysis of apoptosis in the MCF-7-myc- δ C2 and MCF-7 vector control cell lines when apoptosis is induced by camptothecin treatment using the AnnexinV - propidium iodide assay. Error bars are standard error of the mean (n=6).

The treatment of camptothecin (Fig. 5.15) induces significant changes ($p \leq 0.03$) in the myc- δ C2 cell line in the 'Alive' division and in both the myc- δ C2 and vector cell lines in 'Late apoptotic/necrotic' division, but not in 'early apoptotic'. Comparison of the myc- δ C2 expressing and vector control cell lines, when treated with camptothecin, also fails to show any difference. As with the untreated samples (Fig. 5.14), the error bars reduce the 'early apoptotic' fraction

values down to approximately 0%. The increase in the 'Late apoptotic/necrotic' division suggests the camptothecin may induce necrosis of these cells.

MCF-7 cell lines do not show any differences in apoptotic profile. Although viability decreases with camptothecin treatment, the cell lines respond in the same manner and no differences are seen. This data correlates with the cell number data presented in Figure 5.13, where no differences can be observed between the myc- δ C2 containing and vector control cell lines.

5.2.3.3 PKC- δ over-expressing cells show decreased cell numbers from the vector control at day 5.

The MCF-7 cell line was successfully transfected with myc-PKC- δ and the proliferation was examined.

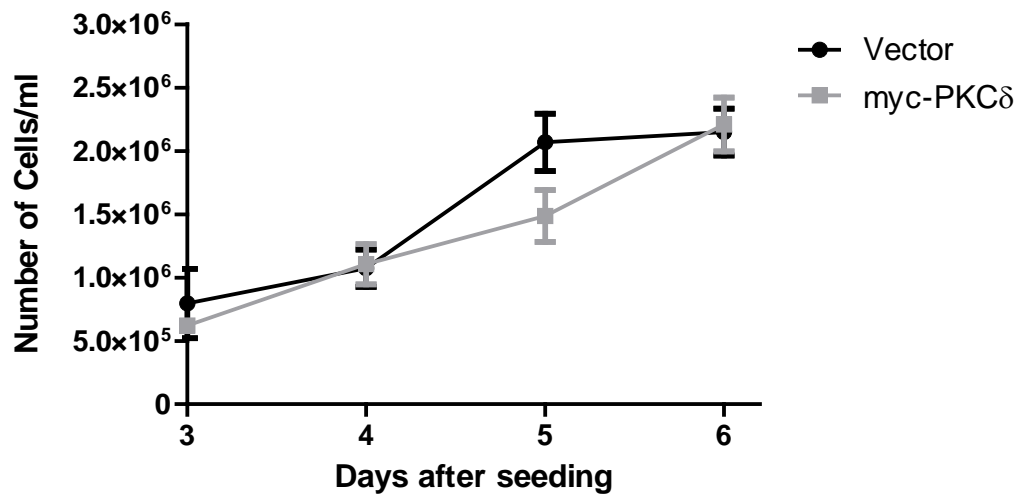


Figure 5.16: There is no effect on the proliferation rate where there is over-expression of PKC- δ in MCF-7 cells compared to the vector control cells. Day 5 decrease in growth in myc-PKC- δ cells is significant to $p \leq 0.05$ (in a paired Student's t-test). Error bars show standard error of the mean (n=6).

Over-expression of PKC- δ in the MCF-7 cells has a limited effect on the proliferation rate of cells, compared to the vector control transfected cells (Fig. 5.16). On day 6 there is no significant difference in cell number. However there is a significant difference in cell number on day 5, showing that the over-expression of PKC- δ is detrimental to the MCF-7 cells. In cell proliferation profiles, cells will normally expand exponentially and then reach a plateau where space and nutrients becoming limiting factors to cell proliferation. It appears that the vector control cells may reach this plateau at an earlier point than the myc-PKC- δ cells.

There was a decrease in proliferation rate of PKC- δ from the vector cells at day 5. Here the PKC- δ is producing an inhibitory effect on cell numbers. The inhibitory effect of PKC- δ over-expression is somewhat surprising given the absence of any effect of myc- δ C2 expression, and the clear involvement in the apoptotic programs of MDA-MB-468 and MDA-MB-231 cell lines. This would suggest that any effect of PKC- δ is not mediated by interactions of the C2 domain.

5.2.3.4 There are no differences in apoptosis between PKC- δ over-expressing and vector cells

The MCF-7 PKC- δ over-expressing cell were assessed for apoptosis and compared with vector cells (Fig. 5.17). In untreated cells there is no significant difference between the vector cells and the myc-PKC- δ cells. When the apoptosis profile was also assessed following camptothecin treatment at 2 μ M, there was no significant difference between the cell lines in any division (Fig. 5.18). The error bars suggest that there is no real proportion of 'Early apoptotic' cells, as the error reduces to 0%.

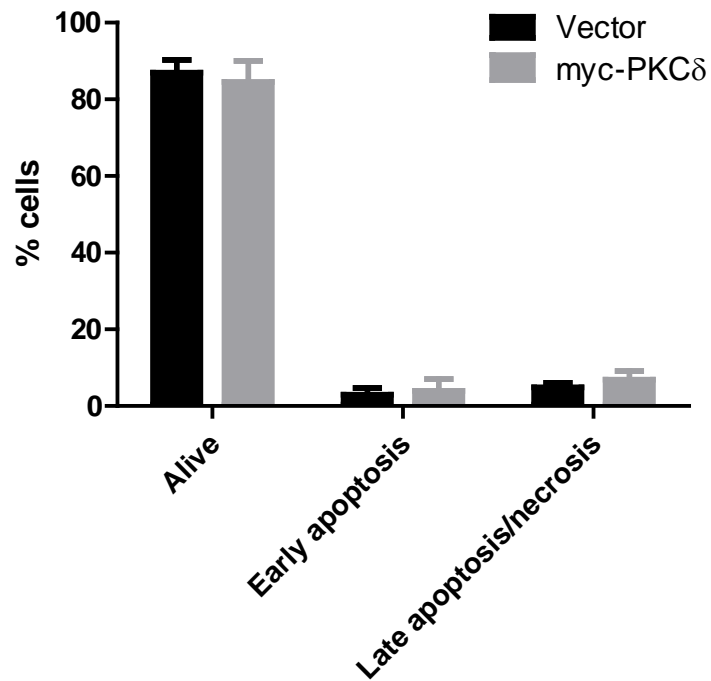


Figure 5.17: Analysis of apoptosis in the MCF-7-myc-PKC- δ and MCF-7 vector control cell lines using the AnnexinV - propidium iodide assay. Error bars are standard error of the mean (n=6).

It is worth noting that significant increases are induced by camptothecin treatment in the 'Late apoptotic/necrotic' division of the vector control cell line. This increase in the 'Late apoptotic/necrotic' quadrant following camptothecin treatment is not seen in the PKC- δ over-expressing cell line, suggesting a protective effect of the over-expression. As the differences are minimal between the 'Late apoptotic/necrotic' fractions of untreated and treated PKC- δ cells, the effect does not appear to carry pronounced influence on cell-survival.

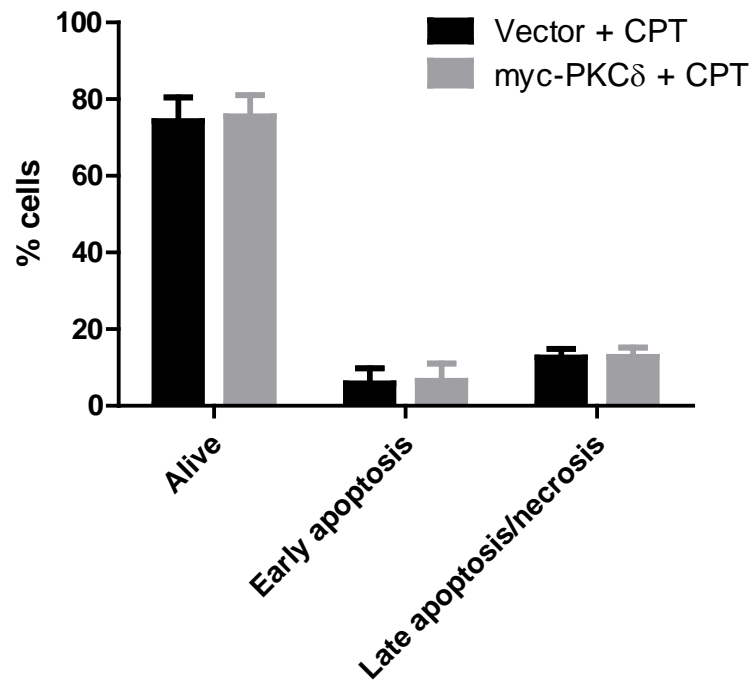


Figure 5.18: Analysis of apoptosis in the MCF-7-myc-PKC- δ and MCF-7 vector control cell lines when apoptosis is induced by camptothecin treatment using the AnnexinV - propidium iodide assay. Error bars are standard error of the mean (n=6).

5.3 Discussion

The 3 cell lines have been found to differ from each other, despite their similar origin (see Chapter 1). This is mirrored in their response to manipulation of PKC- δ . The MDA-MB-468 cell lines have demonstrated that endogenous PKC- δ holds a pro-apoptotic role. This is indicated by the anti-apoptotic effect of myc- δ C2 expression and also the inability to develop a PKC- δ over-expressing cell line. The literature describes a pro-apoptotic role for PKC- δ involving nuclear translocation and cleavage of the regulatory portion (Humphries et al., 2008). Tyrosine phosphorylation (of Y64 and Y155) has been shown to be vital for this effect. One of these residues is in the C2 domain of PKC- δ , thus indicating a role for the C2 domain in this apoptotic process. The data described in this chapter further supports the premise that the C2 domain is important in this process. Further research would be required to identify whether this role is more extensive than the previously identified phosphorylation aspect (perhaps demonstrating the effect illustrated in Fig. 5.19). As the C2 domain is a known protein binding domain (Dekker and Parker, 1997; Lopez-Lluch et al., 2001), it is possible that this role could be interlinked with the tyrosine phosphorylation, whereby it facilitates a key interaction in PKC- δ apoptotic activity.

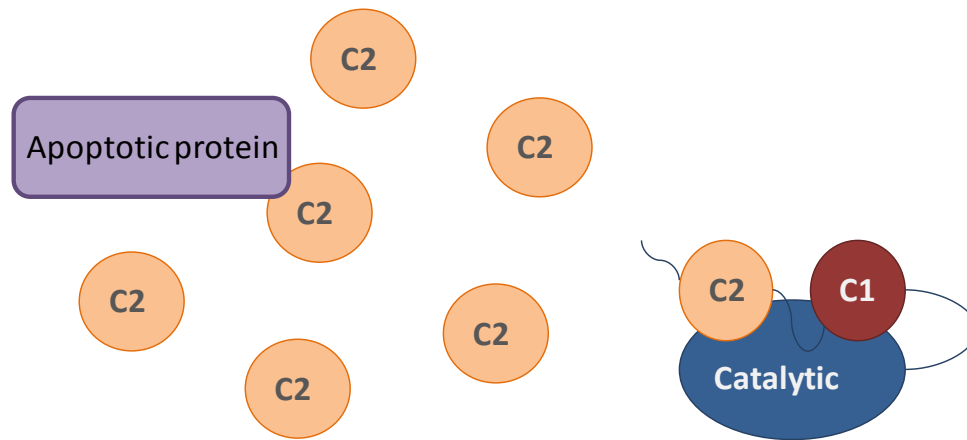


Figure 5.19: A suggested model for the response to myc- δ C2 expression in MDA-MB-468 cells. The myc- δ C2 interrupts the endogenous PKC- δ binding with the 'apoptotic protein' thus preventing apoptosis induction and allowing cell numbers to increase.

The MDA-MB-231 cell lines indicated an anti-apoptotic role for PKC- δ through the myc- δ C2 studies. The PKC- δ over-expressing cell data did not correlate with this. A straight-forward deduction would expect the over-expressing cells to have higher viability than the vector cells; however the PKC- δ over-expressing cells did not show a difference from the vector control. It may be that the myc- δ C2 is inhibiting an interaction of the PKC- δ in an anti-apoptotic role, but that the over-expression of PKC- δ cannot further stimulate this to induce greater survival. If the binding partner involved in transmitting this effect is not widely available in the cell, and there are already greater levels of endogenous PKC- δ relative to this binding partner, it is possible that the involved binding protein cannot 'work

harder'. The endogenous PKC- δ levels are lower in these cells than the other two cell lines examined in this study (Chapter 3). Perhaps the MDA-MB-231 cells are particularly sensitive to PKC- δ activity. It appears that the levels seen in the other cell lines are not required here in order to function normally.

The PKC- δ over-expressing MDA-MB-231 cells appear to illustrate a pro-proliferative role for PKC- δ . Cell numbers are higher in over-expressing cells, but apoptosis is unaffected. It may be that the C2 domain of PKC- δ is not involved in this pro-proliferative role; thus the role is only apparent under these PKC- δ over-expressing conditions.

In MDA-MB-231 cells, the differences observed under camptothecin treated conditions were suspected to be due to the involvement of PKC- δ and the C2 domain within different apoptotic induction mechanisms. Apoptosis can be induced through extrinsic or intrinsic pathways, where either cell-surface signalling or a DNA damage induced response initiates the pathway (Rossi and Gaidano, 2003). The two pathways are linked in certain areas (e.g. caspase-3) but are the result of separate initiation events. It could be that the presence of myc- δ C2 in the cells undergoing apoptosis induced from an extrinsic pathway led to greater levels of apoptosis due to prevention of the pro-survival PKC- δ role. However, where cells were camptothecin treated, and thus the intrinsic pathway was initiated, the PKC- δ may play an alternative role. Thus interference of myc- δ C2 with endogenous PKC- δ has alternative effects.

The literature describes cleavage of PKC- δ in the nucleus during apoptosis, between the regulatory and catalytic fragments by caspase-3 (DeVries-Seimon et al., 2007). The free catalytic domain further stimulates apoptosis. Caspases can have overlapping roles in cell signalling. In some cases other caspase family members can take over a role of a missing caspase. However, analysis of similar caspases 7 and 6, as well as caspases 1, 2 and 4 found they were incapable of performing the cleavage of PKC- δ (Ghayur et al., 1996). Thus without the caspase-3 this pro-apoptotic process cannot occur. MCF-7 cells do not express caspase-3 (Janicke, 2009); thus where absent, PKC- δ would not be cleaved and apoptosis may be averted. This may explain the lack of myc- δ C2 effect on the MCF-7 cells, as it cannot interfere with a process which is not occurring.

In the MCF-7 cells, the PKC- δ over-expressing cells show lower cell numbers. This is not related to higher apoptosis levels. Perhaps the cells cycle at a lower rate. This would allow lower numbers of cells, without affecting apoptotic mechanisms. This would indicate an anti-proliferative effect of PKC- δ , and that the C2 domain is not important in this action. However further investigation would be required to confirm this.

The MDA-MB-468 cell line data shown in this chapter indicates a pro-apoptotic role for PKC- δ , which is prevented through the action of the myc- δ C2. In Chapter 4 we observed that the myc- δ C2 had an effect on the cytoskeletal structure of

the cells (compared the vector control). If the more extensive structure is indeed aiding attachment of the cells to the surface, the levels of apoptosis in the population would be likely to decrease. This would be due to cells entering apoptosis when unattached, through the process of anoikis (Chiarugi and Giannoni, 2008). If this is the case the data from Chapter 4 and 5 indicate the C2 domain has an important role in preventing apoptosis of MDA-MB-468 cells by aiding attachment.

The effects in the three cell types are different. There does not appear to be a general PKC- δ role across all breast cancers. This mirrors the heterogeneity of tumours in the clinic and differential responses to treatments amongst patients. It seems clear that tumour profiling would be important in identifying treatment options with respect to any drugs developed as a result of this research.

Chapter 6: Investigations of the apoptotic pathway in MDA-MB-468 under starvation conditions

In Chapter 5 it was shown that in 10% serum, the expression of the myc- δ C2 domain provided a pro-survival signal to MDA-MB-468 cells. PKC- δ activity has been shown to be affected by tyrosine phosphorylation of specific residues (Blass et al., 2002; Humphries et al., 2008). Tyrosine phosphorylation has also demonstrated a role within regulation of apoptosis. The signal for tyrosine phosphorylation can be received from numerous stimuli (Brodie and Blumberg, 2003). By using serum starvation we aimed to prevent this process and study how the cells responded to the absence of this stimulation. Using this method, the apoptotic response of the transfected MDA-MB-468 cell lines was studied. When MDA-MB-468 cells were starved, expression of myc- δ C2 had a pro-apoptotic effect, which is opposite to the observation in 10% serum. This action

suggests an anti-apoptotic role for PKC- δ under starvation conditions. In parallel, the presence of the myc- δ C2 domain was associated with increased ERK1/2 phosphorylation, without affecting ERK1/2 levels. Furthermore, proteasome blockers prevented the pro-apoptotic effects associated with myc- δ C2 expression, demonstrating the importance of proteasome activity in facilitating the role of PKC- δ .

6.1 Introduction

The MDA-MB-468 cells transfected with myc- δ C2 showed an altered apoptotic response (See Chapter 5). In order to further examine the involvement of PKC- δ and its C2 domain within apoptosis in the MDA-MB-468 cell lines, the cells were scrutinized using several assays. Cells were serum-starved to examine whether the survival advantage provided by myc- δ C2 would be continued, and even enhanced, under stress conditions.

Tyrosine phosphorylation is involved in the regulation of PKC- δ activity in apoptosis (Brodie and Blumberg, 2003). Tyrosine residues are phosphorylated following stimulation of particular signalling pathways. Kajimoto et al revealed that the Src family of kinases were important in tyrosine phosphorylation related to nuclear activation and apoptosis (Kajimoto et al., 2010). The Src family can become activated following extracellular signalling events (Parsons and Parsons, 1997). Where serum is absent such signalling events would not be triggered. Serum starvation could thus be expected to silence tyrosine phosphorylation, altering the apoptotic response. By silencing the effect of tyrosine phosphorylation, it may be that the effects of the C2 domain on apoptosis would also be neutralised.

Further examination of pathways can be achieved through treatment with inhibitors. Commercially available PKC- δ inhibitors are not sufficiently specific.

However investigations can be performed on associated proteins in order to illustrate the role of PKC- δ . The role of tyrosine kinases in targeting and controlling PKC- δ activity appears to be extensive (Brodie and Blumberg, 2003). The Src family of kinases have demonstrated involvement in PKC- δ activity. Inhibition of Src may reveal further information about PKC- δ in apoptosis.

6.2 Results

6.2.1 When cells are serum-starved the apoptotic profile alters so that cells containing myc- δ C2 show more apoptosis

MDA-MB-468 transfected cells were starved for 72 hours and the apoptotic profile analysed in order to examine whether any differences between the response of myc- δ C2 and vector cells would be seen.

The profile illustrated a large difference between the myc- δ C2 and vector cells in 'alive', 'early apoptotic' and 'late apoptotic/necrotic' groups. This difference was such that the myc- δ C2 cells showed lower viability than the vector cells and higher levels of apoptosis in both early and late apoptotic/necrotic groups.

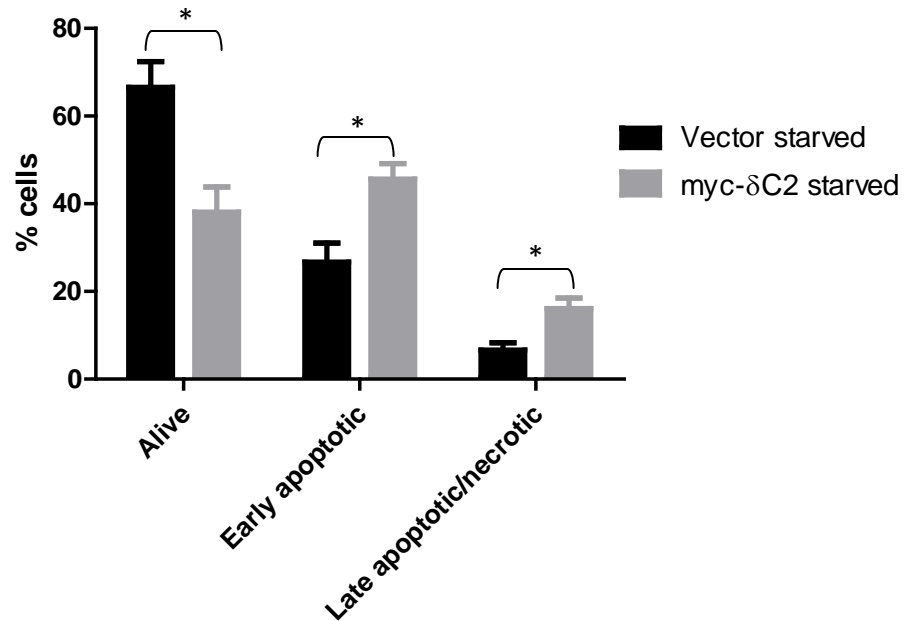


Figure 6.1: Apoptosis measured following 72 hours starvation showed myc- δ C2 cells have lower viability and more apoptosis than vector cells. Error bars are standard error of the mean (n=4). Differences (*) are significant in an unpaired t-test ($p \leq 0.03$).

The lower viability in the myc- δ C2 cells suggests the protein fragment is pro-apoptotic. As an inhibitor of the normal PKC- δ function, it can thus be deduced that the PKC- δ would exert an anti-apoptotic effect. This is in contrast with the role identified in Chapter 5 under 10% serum conditions.

6.2.2 Src does not appear to be involved in PKC- δ tyrosine phosphorylation. Overall tyrosine phosphorylation levels do not differ between the vector and myc- δ C2 cells.

6.2.2.1 Src inhibition using SU 6656.

Src has been implicated in tyrosine phosphorylation of PKC- δ (Kajimoto et al., 2010). Src activity would be stimulated by the effects of serum. Thus if Src tyrosine phosphorylation is involved in the targeting of PKC- δ to demonstrate the anti-apoptotic activity exemplified in Figure 6.1, then the inhibition of Src in the presence of serum should produce the equivalent result as when serum is omitted. Src inhibition would encourage PKC- δ to act in the anti-apoptotic role identified in serum-starved conditions. The myc- δ C2 would be expected to block the endogenous PKC- δ activity, as observed in starvation. Thus cells would show greater levels of apoptosis than the vector control cells.

The cells were grown in serum and treated with 100nM inhibitor for 24 hours prior to examination of apoptotic status. The concentration used was selected following testing to investigate a suitable concentration. Tests revealed that the inhibitor is toxic to the cells, but at this concentration the cells were able to survive for the required period. We used a treatment time of 24 hours, despite a

30 minute treatment window being utilised in the literature, to be sure that the signalling pathway would be appropriately affected by the treatment. Too short a period may not allow enough time for the serum stimulated effects to dissipate and the effect of the inhibitor to be seen.

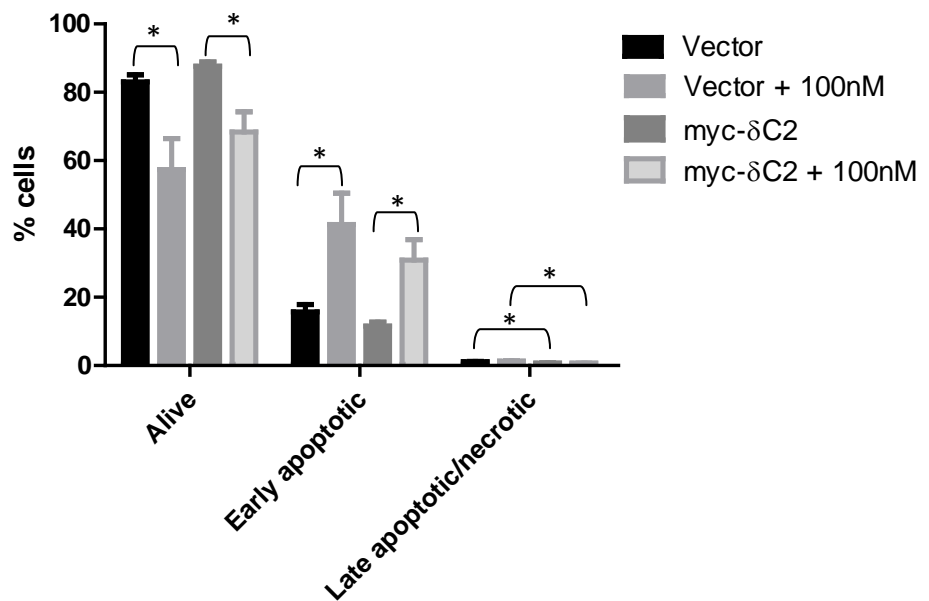


Figure 6.2: The effects of Src inhibitor SU6656 on MDA-MB-468 myc- δ C2 and vector cells following 24 hour treatment. Error bars are standard error of the mean (n=6). Differences (*) are significant in an unpaired t-test ($p \leq 0.04$).

Where the Src inhibitor is present there is greater apoptosis in both vector control and myc- δ C2 expressing cells (Fig. 6.2). However, the differences

observed under starvation between the vector control cells and the myc- δ C2 expressing cells did not persist under Src inhibition. Differences were identified in the 'Late apoptotic/necrotic' fraction between vector control cells and myc- δ C2 containing cells with and without treatment, where vector control cells show higher proportions of cells in this fraction. However the numbers within these portions are not high in either case; thus the differences, although significant, are minimal. The treatment induced changes in both the vector control cells and the myc- δ C2 cells, where the number of cells in the 'Alive' portion is decreased by treatment and the number in the 'Early apoptotic' section is increased.

It is worth noting that the data obtained in this experiment is not comparable to the data in Figure 5.5 due to differences in the methods used. These differing methods are possibly the reason for the variation observed between Figures 5.5 and 6.2 with respect to the proportion of viable vector control and myc- δ C2 expressing cells.

The lack of effect by the SU6656 inhibitor, to induce the differences seen between vector control cells and myc- δ C2 cells under starvation conditions, suggests that Src is not a key part of the process in this case.

6.2.2.2 Tyrosine phosphorylation

PKC- δ is subject to tyrosine phosphorylation by other kinases (Steinberg, 2008). This phosphorylation is involved in PKC- δ activation and targeting (Reyland, 2007). The tyrosine phosphorylation of particular residues, one in the C1 domain and one in the C2 domain, are key to the targeting of PKC- δ to the nucleus where it can be cleaved and becomes involved in apoptosis (Humphries et al., 2008; Kajimoto et al., 2010; Steinberg, 2008). Thus as tyrosine phosphorylation is of such importance to PKC- δ activity, we examined the tyrosine phosphorylation of both the PKC- δ , and in the myc- δ C2 cells, the myc- δ C2 domain.

As PKC- δ activation regularly involves tyrosine phosphorylation, cells were treated with a known activator of PKC- δ in order to test if tyrosine-phosphorylation status was altered. Phorbol 12-myristate 13-acetate (PMA), a phorbol ester compound, was thus used to treat a flask of each cell type prior to lysis.

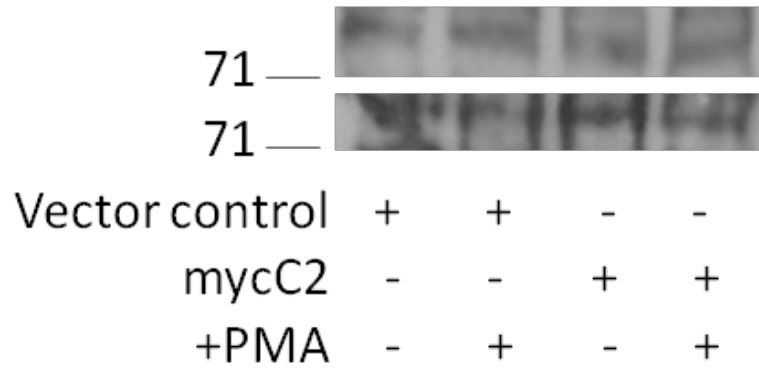


Figure 6.3: Two IP results where PKC- δ was used to immuno-precipitate and anti-p-tyrosine used to probe. Both experiments show a similar pattern, whereby no difference is seen between vector control and myc- δ C2 cells with or without PMA stimulatory treatment.

The band intensity did not vary between the vector control cells or myc- δ C2 cells, whether PMA treated or not (Fig. 6.3). Although a difference in activity was expected, as exemplified by tyrosine phosphorylation, the experiment indicates that the activity levels are comparable across all conditions. The PKC- δ in the cells may be equally tyrosine phosphorylated; however the tyrosine residues that are phosphorylated may differ. This is not taken into consideration when probing with phospho-tyrosine antibody. In order to do this, antibodies against phosphorylation of particular tyrosine residues would have to be used.

The PMA binds the C1 domain of the PKC- δ to activate the protein (Cho, 2001). However, PMA does not necessarily induce tyrosine phosphorylation. The

absence of a difference between the cell lines, whether PMA treated or not, does not indicate that the PMA treatment has not activated the protein, just that the overall tyrosine phosphorylation levels are unaffected in this case.

The presence of the myc- δ C2 domain alters the cell profile (as seen in Chapters 4 and 5). As tyrosine phosphorylation is used to control PKC- δ function, and the endogenous PKC- δ function appeared to be altered by the presence of myc- δ C2, it was possible that the tyrosine phosphorylation process may be interfered with. However, as the PKC- δ demonstrated similar levels of tyrosine phosphorylation under all the conditions examined, it does not seem to be the case that the myc- δ C2 interferes with the tyrosine phosphorylation status. This was somewhat confirmed by the examination of the myc- δ C2 IP with phospho-tyrosine probe (Fig. 6.4), where there was no identifiable signal for tyrosine phosphorylation of the C2 domain. It could be that the kinases responsible for the tyrosine phosphorylation identified in the literature can only interact with the whole protein, and not solely the C2 domain.

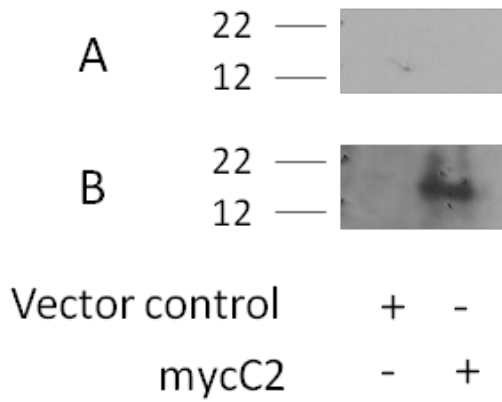


Figure 6.4: IP results of myc- δ C2 tyrosine phosphorylation study. Panel A shows tyrosine phosphorylation probe, panel B shows 9E10 myc-tag probe. No tyrosine phosphorylation of the myc- δ C2 domain is seen, the IP of the myc- δ C2 domain was confirmed by probing with 9E10 antibody.

6.2.3 Proteasome activity is vital for anti-apoptotic activity under starvation conditions.

The literature has previously described an anti-apoptotic role for PKC- δ in MDA-MB-231 cells (see Chapter 1). This pathway was active due to a *ras* mutation, and was found to be dependent on proteasome activity. Although a *ras* mutation in MDA-MB-468 cells has not been described in the literature, the effects of starvation on the cells advocated further examination of the pathway. This may provide evidence that the pathway is somehow implicated in the effects identified under starvation.

The cells were starved for 72 hours, and selected samples treated with MG132 for the final 5 hour period of this interval. The cells showed the same pattern with starvation as seen in Figure 6.1, where myc- δ C2 containing cells showed lower viability than the vector control cells. However with MG132 treatment the levels of viability in myc- δ C2 cells increased to a similar level as the vector control cells (Fig. 6.5). The increase in viability was significant, and when MG132 treated there was no longer a significant difference between the myc- δ C2 cells and vector control cells.

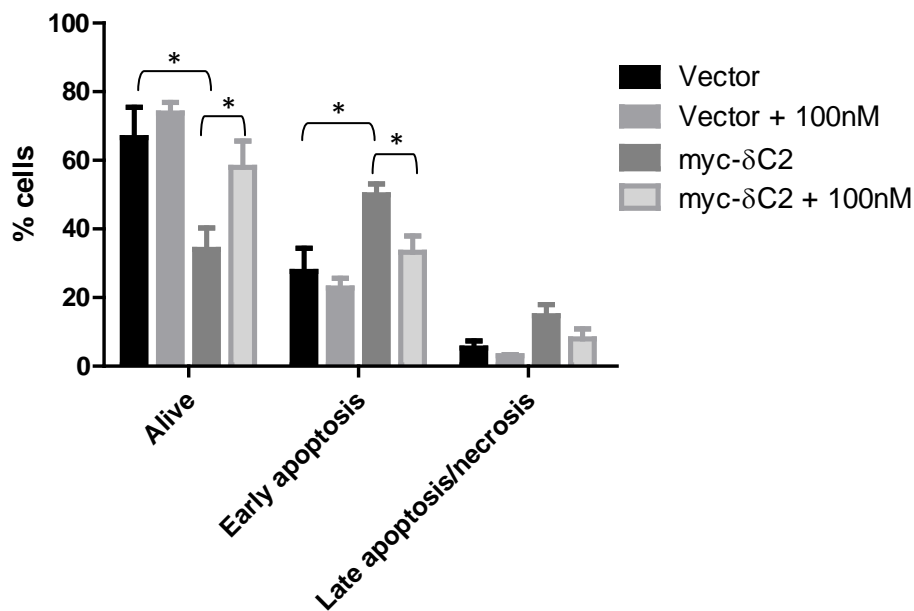


Figure 6.5: The effects of proteasome inhibitor MG132 and starvation on cells following 72 hours of starvation including the final 5 hours MG132 treatment. Error bars are standard error of the mean (n=6). Differences (*) are significant in an unpaired t-test ($p \leq 0.04$).

The cells were also tested for effects following 24 hours of starvation and MG132 treatment (Fig. 6.6). The results demonstrated that the cells did not appear to be fully starved, as the myc-δC2 had yet to produce the detrimental effects on the cell survival. However the treatment with MG132 did produce significant differences in viability of the myc-δC2 containing cells which was absent in the vector control cells. The myc-δC2 cells showed lower viability and higher proportions in both 'Early apoptotic' and 'Late apoptotic/necrotic' fractions. The

increase in 'Late apoptotic/necrotic' cells was minimal, with an increase from 1.1 to 2.8%. There is also a significant difference between vector control cells and the myc- δ C2 cells in the 'Late apoptotic/necrotic' fraction. However, once again the difference is minimal with vector control averaging 1.9 and myc- δ C2 1.1%.

Examination of this data is complicated due to the mixed status of these cells between 10% serum and 72 hour starvation conditions. The presence of a difference between the effects of the MG132 on the myc- δ C2 cells and the vector control cells suggests a possible further role for the C2 domain of PKC- δ . Further investigation would be required to elucidate this role.

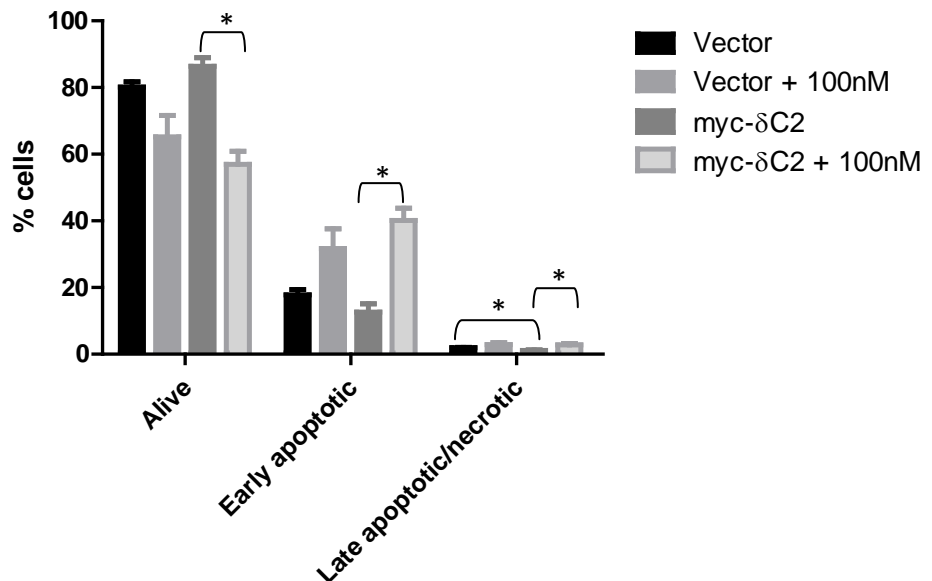


Figure 6.6: The effects of proteasome inhibitor MG132 and starvation on cells following 24 hours of treatment. Error bars are standard error of

the mean (n=5). Differences (*) are significant in an unpaired t-test (p≤0.01).

6.2.4 ERK phosphorylation status

The differences identified in apoptosis levels in the cells when starved (and where treated with proteasome inhibitor MG132), is possibly due to the action of a pathway involving ERK1/2 phosphorylation, since the level of ERK1/2 phosphorylation has been associated with apoptosis (Lønne et al., 2009; Lu and Xu, 2006; Subramaniam and Unsicker, 2010). PKC- δ is also known to be an upstream activator of ERK (Schonwasser et al., 1998).

Blots of MDA-MB-468 vector control and myc- δ C2 containing cell lines were examined to identify the levels of phosphorylated ERK1/2, but also the levels of total ERK1/2. This check ensured that the differences seen in the phosphorylation status were not due to increases and decreases in the levels of the ERK1/2 proteins themselves.

6.2.4.1 ERK1/2 phosphorylation in not-starved and starved conditions

The phosphorylation status of the ERK1/2 protein is an indication of the activity status of the protein. Western blots of MDA-MB-468 vector control and myc- δ C2 containing cell lines were probed with phosphorylated ERK1/2 antibody and

quantified, in order to examine the degree of ERK1/2 phosphorylation in the cells.

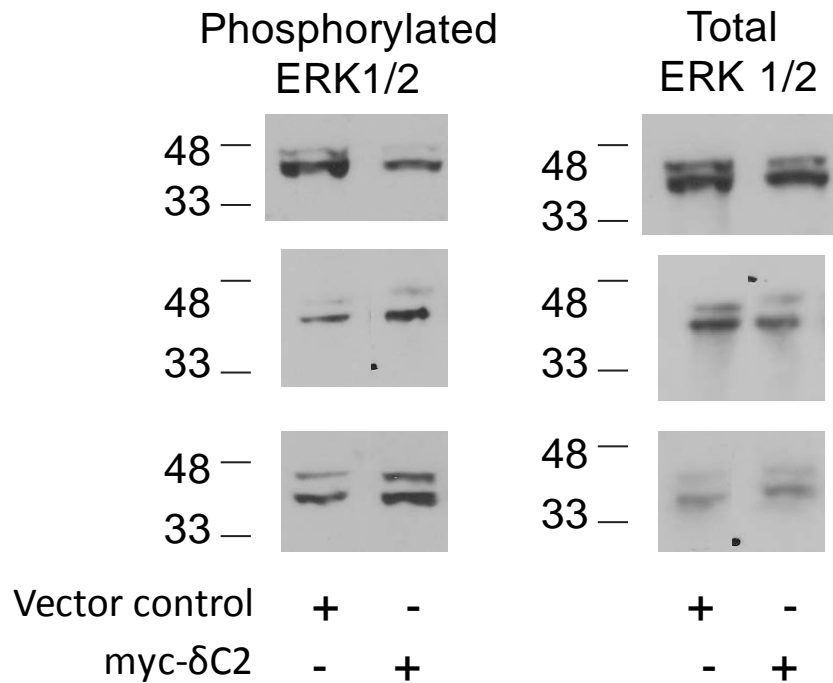


Figure 6.7: Phosphorylated and Total ERK1/2 levels in vector control and myc- δ C2 cells under 10% serum conditions.

Under not-starved conditions the levels of phosphorylated ERK1/2 do not vary greatly between the vector control and myc- δ C2 expressing cells (Figure 6.7). In two out of three cases the degree of phosphorylation increases slightly, as shown in Figure 6.8. The levels of total ERK1/2 do not vary between the vector control and myc- δ C2 cells, as also confirmed in Figure 6.8.

Phosphorylated and total ERK1/2 levels in vector control cells and myc- δ C2 cells under not-starved conditions were quantified (Fig 6.8).

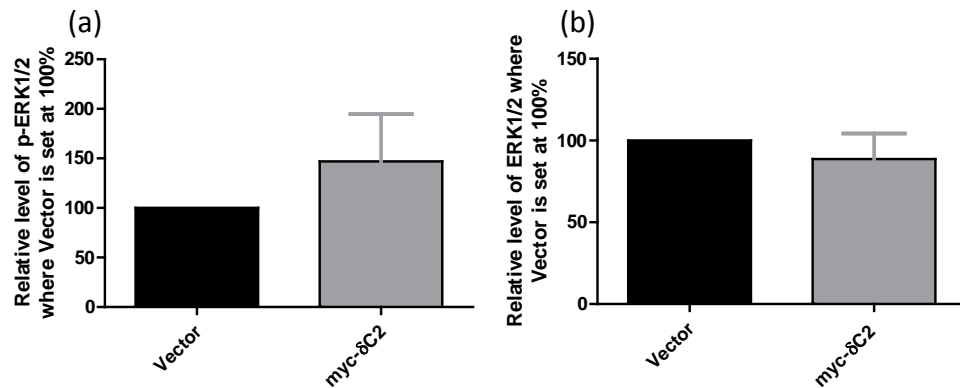


Figure 6.8: Comparison of phosphorylated (a) and total (b) ERK1/2 levels in not-starved myc- δ C2 cells where the not-starved vector is set at 100%. Error bars are standard error of the mean (n=3).

Little difference was seen between the levels of phosphorylated ERK1/2 under non-starved conditions (Fig. 6.8 (a)). The data was inconsistent. One data set showed a sharp decrease in phosphorylation, whilst the other two data sets showed an increase in phosphorylation in the myc- δ C2 cells. Whether the conflicting data set is included in the mean, or not, there is only a modest increase in phosphorylation.

Figure 6.8 (b) shows that total ERK1/2 levels are unaltered, thus the differences in phosphorylation of ERK1/2 are not due to variation in the general ERK1/2 level.

Starvation induced a difference in apoptotic response between the vector and myc- δ C2 expressing cells. As ERK1/2 phosphorylation can be associated with apoptosis, the differences were also examined between the vector control cells and the cells expressing myc- δ C2 under and starvation conditions (Fig. 6.9).

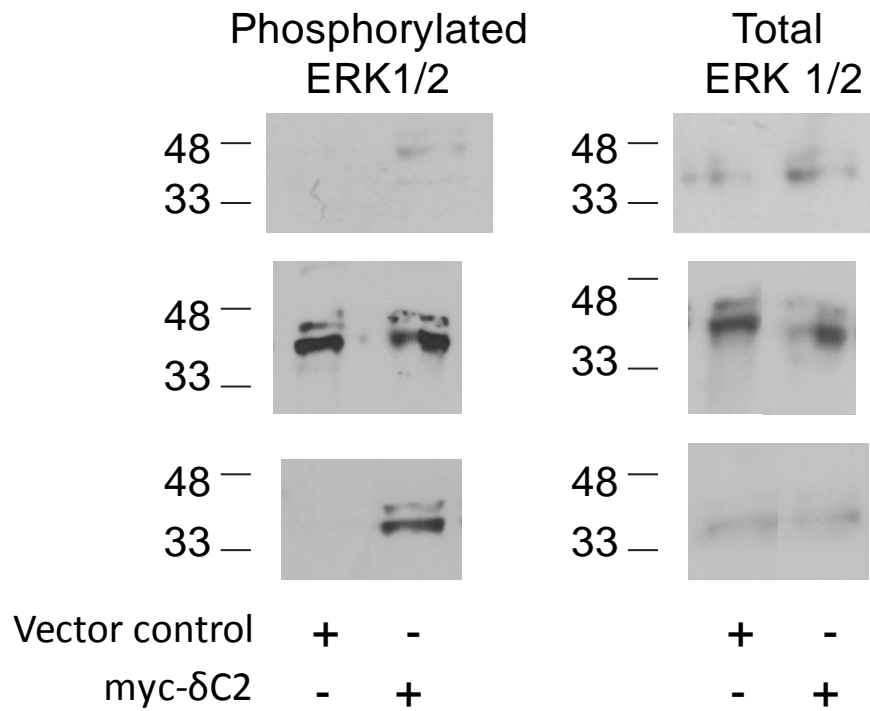


Figure 6.9: Phosphorylated and Total ERK1/2 levels in vector control and myc- δ C2 cells under starvation conditions (72 hours).

In starved conditions the phosphorylation status of ERK1/2 displays greater variation (Figure 6.9). In two out of three occasions, there is a clear increase in phosphorylated ERK1/2 levels from vector control to myc- δ C2 expressing cells, which is also indicated in Figure 6.10 (a). On the third occasion there was also an increase, but to a lesser degree. The levels of total ERK1/2 remain broadly unaffected (Figures 6.9 and 6.10).

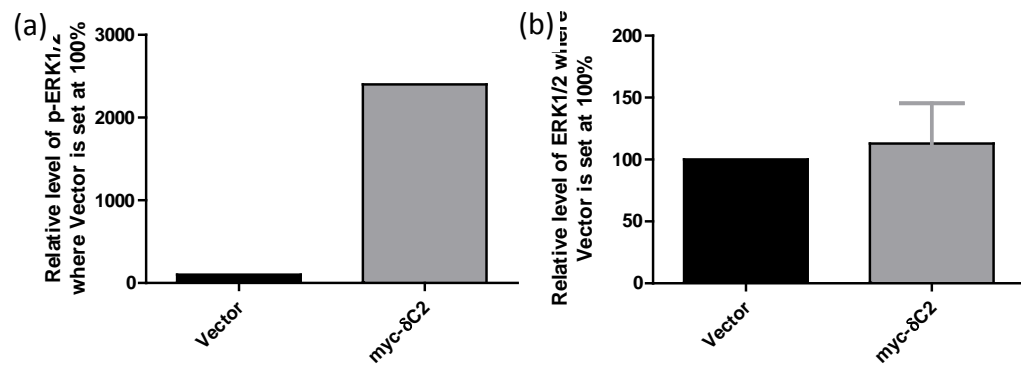


Figure 6.10: Comparison of phosphorylated (n=2*) and total (n=3) ERK1/2 levels in myc- δ C2 starved cells where starved vector cells are set at 100%. In (b) error bars are standard error of the mean. * The phosphorylation levels relative to vector control in starved cells could not be calculated for the third set of data as there was no phosphorylation of ERK in the vector cells under these conditions.

The phosphorylation levels relative to vector control in starved cells could not be calculated for the third set of data. However phosphorylation was seen in the myc- δ C2 cells, indicating an increase in ERK1/2 phosphorylation in corroboration with the data that could be analysed.

Figure 6.10 (b) shows that Total ERK1/2 levels remain unchanged, thus the differences in phosphorylation of ERK1/2 are not due to alterations in the overall level of ERK1/2.

6.2.4.2 ERK1/2 phosphorylation following MG132 treatment

Proteasome activity was shown to be important in the anti-apoptotic activity of PKC- δ in starved conditions. Thus ERK1/2 phosphorylation levels were examined following MG132 treatment (Figs. 6.11 and 6.12). Figure 6.11 is an example of a gel showing phosphorylated ERK1/2 amounts (and total ERK1/2 amounts) in starvation conditions, with and without MG132 treatment. The phosphorylated ERK1/2 levels are considerably lower in the vector control cells over the myc- δ C2 cells, whether MG132 is present or not. The levels of phosphorylated ERK1/2 in the myc- δ C2 cells is also seen to decrease, although not the vector control cell levels, with MG132 treatment. The total levels of ERK1/2 are quite similar (as seen when analysed in Figure 6.13) across the conditions.

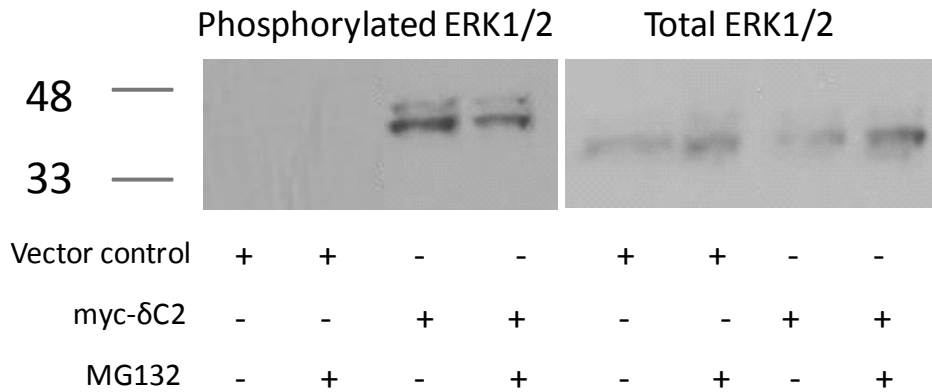


Figure 6.11: Phosphorylated ERK1/2 and total ERK1/2 showing differences with vector control and myc- δ C2 in starved conditions, with and without MG132 proteasome inhibitor present.

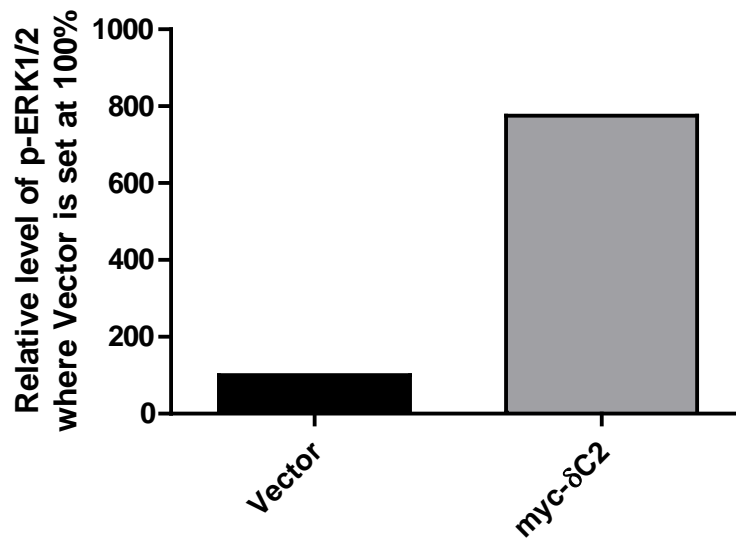


Figure 6.12: Comparison of phosphorylated ERK1/2 levels in starved myc- δ C2 cells with MG132 treatment where starved and MG132-treated vector cell are set at 100% (n=1).

The phosphorylation is greater in the myc- δ C2 cells than the vector control cells. However, overall the difference is lower in this case than in the untreated starved cells (see Fig. 6.10). This indicates a lower level of phosphorylation of ERK1/2 in myc- δ C2 cells where MG132 treatment was given. This decrease indicates that prevention of proteasome activity is correlated with ERK1/2 de-phosphorylation.

The phosphorylation levels relative to vector control in starved cells treated with MG132 could not be calculated for the second set of data, as there was no phosphorylation of ERK in the vector cells under these conditions. However there was phosphorylation in the myc- δ C2 cells. Thus the data supports the data set shown in Figure 6.12. The levels of ERK1/2 phosphorylation are very low, or non-existent in the vector cells. This limits the ability to analyse the data.

Figure 6.13 shows that total ERK1/2 levels vary little; thus the differences in phosphorylation of ERK1/2 are not due to differences in the total level of ERK1/2.

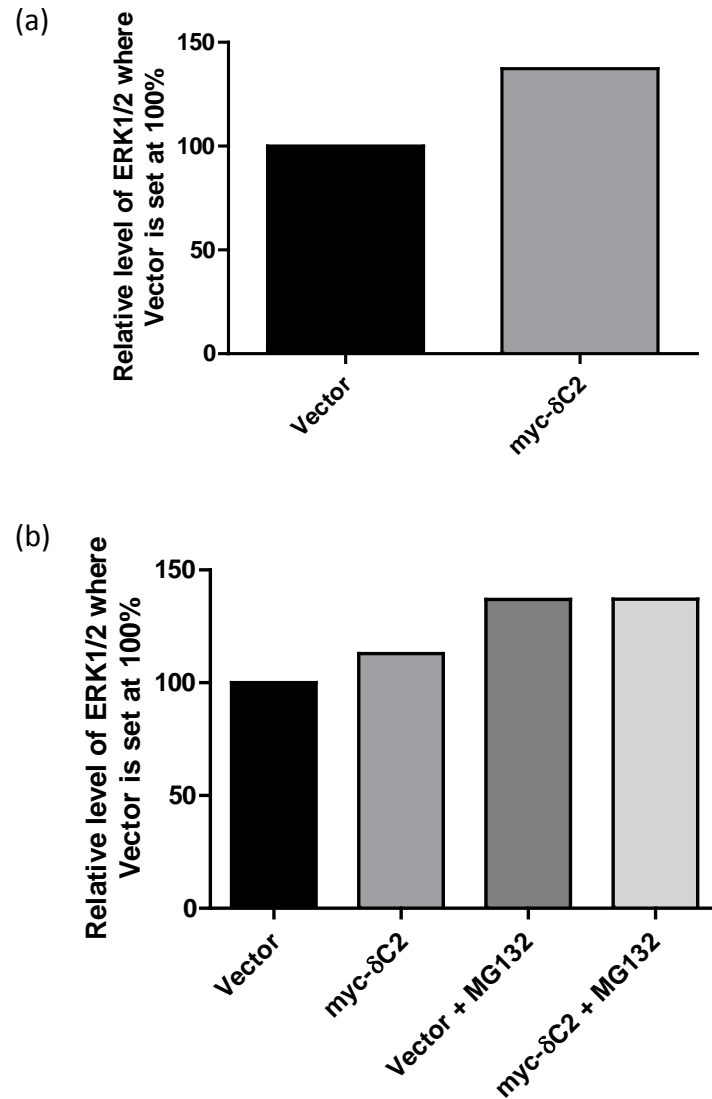


Figure 6.13: Total ERK1/2 levels in (a) starved and MG132 treated cells where vector is set at 100%; (b) shows starved untreated and treated cells where the untreated vector cells are set at 100% (n=2).

6.2.5 Sub-cellular fractionation demonstrates that although the cell lines do not demonstrate any significant differences between each other, starvation does induce differences in the profile of PKC- δ localisation

In starved cells (Table 6.1) the bound nuclear and cytoskeletal fractions are low. In the vector control cells the membrane fraction contains the highest level of PKC- δ , with the soluble nuclear and then cytosolic fractions containing progressively less. From the non-starved cells, the decrease in the amount in the cytosolic fraction is significant (paired Student's t-test, $p \leq 0.02$). This could be due to the PKC- δ becoming activated under cellular stress and localising to alternate cellular compartments. In myc- δ C2 expressing cells the highest amount of PKC- δ is seen in the membrane fraction, followed by the soluble nuclear and the cytosolic fractions. This is a similar pattern as seen with the vector control cells. Significant differences were also induced in the PKC- δ profile in the myc- δ C2 cells through starvation. A significant increase was seen in the membrane fraction ($p \leq 0.04$) and a significant decrease in the cytosolic fraction ($p \leq 0.01$). This suggests a shift of the PKC- δ from the cytosol to the membrane, presumably in response to activation through starvation allowing targeting to the compartments where it is required for action.

Table 6.1: Distribution of PKC- δ amongst the five sub-cellular extracts comparing not-starved cells and starved cells. Percentage distribution shown \pm standard deviation.

	Cytosol	Membrane	Soluble nuclear	Chromatin-bound nuclear	Cytoskeletal
Vector – 10% serum	32.78 \pm 18.1	41.68 \pm 14.0	22.70 \pm 13.4	2.00 \pm 2.1	3.90 \pm 6.2
Vector – starved	4.58 \pm 4.3	63.96 \pm 19.7	31.44 \pm 21.7	0.04 \pm 0.1	0.00 \pm 0.0
myc-δC2 – 10% serum	27.46 \pm 9.7	37.62 \pm 9.3	35.12 \pm 9.4	1.18 \pm 0.8	1.58 \pm 1.3
myc-δC2 – starved	9.50 \pm 7.9	53.38 \pm 11.2	37.12 \pm 12.6	0.00 \pm 0.0	0.00 \pm 0.0

6.3 Discussion

The response of MDA-MB-468 cell lines to starvation was surprising due to the opposite effect being identified in 10% serum conditions. However, the literature has previously described an anti-apoptotic role for PKC- δ , in MDA-MB-231 cells. The pathway described in MDA-MB-231 cells is reliant on the presence of a *ras* mutation which activates the ERK1/2 proteins to such a level that, without a suppressive action of PKC- δ , it would be lethal (Lønne et al., 2009). This pathway is described in Figure 6.14. This raises the question of what is happening in the MDA-MB-468 cells, where a *ras* mutation has not been identified. The ERK1/2 phosphorylation status of MDA-MB-468 cells was shown to be lower than in MDA-MB-231 cells, but still higher than another breast cancer cell line MCF-7 (Lønne et al., 2009). Thus perhaps these cells have an alternative mutation that is affecting and activating the pathway in some manner.

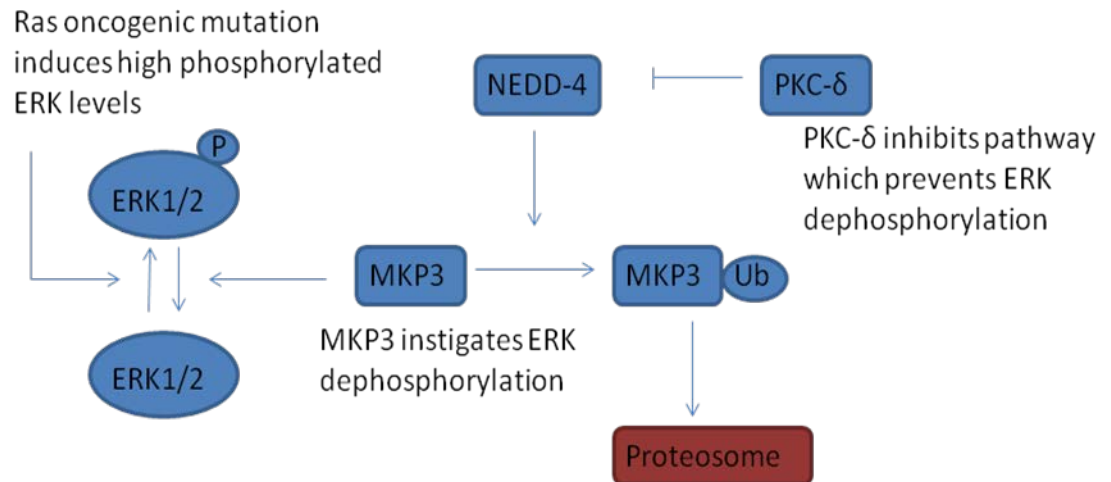


Figure 6.14: The anti-apoptotic pathway in which PKC- δ is involved (Lønne et al., 2009)

Studies have identified PKC- δ activity to be affected by phosphorylation. Src activity is a possible method of achieving this phosphorylation. A Src inhibitor was used to examine whether the cellular apoptotic profile would respond to show a similar effect to starvation conditions. This was not the case, and thus suggests that Src is not the key factor in facilitating the phosphorylation of PKC- δ in this situation. There are other tyrosine kinases that would need to be examined in order to identify the participating component. Alternatively, perhaps PKC- δ activation is achieved through action of DAG binding.

Tyrosine phosphorylation status of the protein in general was also examined to see whether this was altered by the presence of the myc- δ C2 in the system. This did not appear to differ between the two situations. However this is not a

conclusive examination of the tyrosine phosphorylation status of PKC- δ as this only examined overall tyrosine phosphorylation. Numerous papers have identified that the particular tyrosine residues phosphorylated in PKC- δ differs according to the stimulus (Blass et al., 2002; Hall et al., 2007; Konishi et al., 2001; Li et al., 1996). Thus examination of the particular residues would be required to create a more substantial profile of any tyrosine phosphorylation differences. However it may be that tyrosine phosphorylation is not involved in PKC- δ targeting and it is another factor. Perhaps DAG and PS binding is involved, or PKC- δ activation and targeting is more complex than initially thought.

We investigated further whether the cells responded in a similar manner to other aspects of the MDA-MB-231 study. The study identified proteasome activity as vital to the action of PKC- δ . As shown in Figure 6.14, MKP3 activity is important for cell survival as it de-phosphorylates the ERK1/2 to a level at which the cells are able to remain viable. MKP3 levels are regulated through ubiquitinylation and proteasome degradation. Thus the activity of the proteasome is key for breakdown of ubiquitinylated MKP3 and reduction of the protein levels. Without this breakdown the MKP3 may still instigate de-phosphorylation of ERK1/2, thus returning ERK1/2 phosphorylation to a level at which cells can survive. The literature has shown that where PKC- δ is active in this pathway, in this case under starvation conditions for 72 hours, the cells are able to survive. The literature also demonstrates that PKC- δ depletion leads to increased ERK1/2

phosphorylation and cell death. Where myc- δ C2 is present, and thus PKC- δ is unable to act, the cells would be expected to die, as seen in Figure 6.1.

The literature illustrates the combined effect of PKC- δ depletion and proteasome inhibition to be increased MKP3 levels, resulting in de-phosphorylation of ERK1/2 and thus cell survival. As the myc- δ C2 appears to act in a similar way to depletion of PKC- δ , the effects combined with the MG132 treatment would be expected to be the same, where the cell viability returns to the level seen with the vector control cells. Vector control cells treated with MG132 would be expected to show little difference to untreated cells, as the NEDD4 remains inhibited and the MKP3 remains free to de-phosphorylate ERK1/2. This shows that the part of the pathway requiring the proteasome identified in MDA-MB-231 cells is also vital in the MDA-MB-468 cells when starved, and suggests a similar pathway is in effect.

ERK1/2 phosphorylation has been demonstrated to be involved with cell survival and death (Lu and Xu, 2006; Subramaniam and Unsicker, 2010). The Lønne study (2009) showed that phosphorylation levels of ERK1/2 were important in whether the cells were viable or not, where extremely high levels induced apoptosis. The higher levels of apoptosis in starved MDA-MB-468 myc- δ C2 cells correlated with higher ERK1/2 phosphorylation than that seen in vector cells. This effect was not due to differing levels of the proteins themselves, but solely to phosphorylation levels.

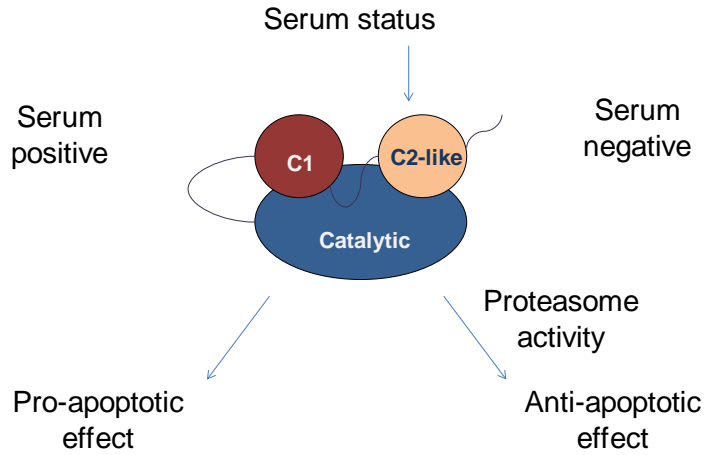


Figure 6.15: The C2 appears to be involved in ‘sensing’ the serum status and appropriately directing PKC- δ activity.

Altogether this evidence illustrates that it is likely that the pathway identified in the MDA-MB-231 cells is also active in the MDA-MB-468 cells when they are serum-starved. The difference in the cells where serum is present and where it is absent is an indication that the C2 domain may be involved in ‘sensing’ the serum status of the cells and appropriately directing the activity of the PKC- δ (Fig. 6.15). Thus far there has been no identification of a *ras* mutation in MDA-MB-468 cells. This is a hindrance to understanding the pathway involved. However the *ras* pathway is highly complex, involving numerous other proteins. It seems possible that mutations may be present, but have not yet been identified. The pathway only appears to be active under serum-starved conditions, where other pathways are not stimulated. This suggests a reason for why this effect has not been previously noted and examined. Further investigation into the pathway would be necessary to identify relevant mutations.

Chapter 7: Conclusions

The premise of the study was to examine more closely the role of the PKC- δ C2 domain within a breast cancer system, in order to further understand its roles in effecting the function of PKC- δ itself.

This study utilised three breast cancer cell lines; the MDA-MB-468, which the study focused on, as well as the MDA-MB-231 and MCF-7 cell lines. The MDA-MB-468 and MDA-MB-231 cell lines are triple negative cell lines. The triple negative status is relevant to tumours of a basal type and refers to the absence of oestrogen, HER2 and progesterone receptors. Identification of PKC- δ C2 domain as a drug target in these cells would be particularly advantageous as they are notoriously difficult to treat. The MCF-7 cell line is positive for the oestrogen receptor and was selected due to this difference. All three cell lines have been well studied in the literature; this will hopefully allow a more thorough interpretation of any results.

In order to examine the role of the PKC- δ C2 domain, a construct was created containing PKC- δ C2 sequence and transfected into cells. Expression of the myc- δ C2 domain protein in the cells was anticipated to act as a dominant negative for the endogenous PKC- δ . The C2 domain is a regulatory region of the PKC- δ protein, and has been shown to have

protein binding effects; thus expression was projected to interfere with protein binding functions of endogenous PKC- δ C2 domain through competitive inhibition. This would have a negative effect on the endogenous PKC- δ function. A further construct was also developed which contained the whole PKC- δ sequence with a myc-tag. Expression of this would enable visualisation of the effects of over-expression of PKC- δ on the cells.

7.1 Preparing the cell lines

The constructs were transfected into the three cell lines and stably transfected cells selected. Chapter 3 described the development of only vector control and myc- δ C2 transfectants in MDA-MB-468 cells. In addition to developing the vector control and myc- δ C2 stable transfectants, the MDA-MB-231 and MCF-7 cell lines also developed myc-PKC- δ transfectants. The fact that the MDA-MB-468 cells could not be transfected with myc-PKC- δ implies that the over-expression of PKC- δ in this cell line is highly detrimental to these cells. This could be the case if it had a pro-apoptotic role within these cells. The literature describes a pro-apoptotic role for PKC- δ where it translocates to the nucleus and is cleaved by caspase-3 into an active catalytic fragment (Reyland, 2007). With transfectants arising in the MDA-MB-231 and MCF-7 cells, the role of the PKC- δ does not appear to be comparative. There is evidence in the literature for PKC- δ employing an anti-apoptotic role in MDA-MB-231 cells (Lønne et al., 2009). Thus the beneficial effect of PKC- δ could explain the development of myc-PKC- δ expressing cells in relation to this cell line. The MCF-7 cells were also successfully transfected with myc-PKC- δ . There is no evidence in the literature for a similar effect of PKC- δ to that in MDA-MB-231 cells which have a *ras* mutation (Lønne et al., 2009). However, a mutation in the caspase-3 gene that renders this protein inexpressible can explain the development of these cells (Janicke, 2009). The pro-apoptotic role of PKC- δ relies on the activity of caspase-3. Therefore if this protein is not present this could not occur, and the detrimental effects seen in MDA-MB-468 cells, where the myc-PKC- δ cell line did not develop, would not occur. The development of stable cell lines containing myc- δ C2 indicates that the presence of this is not particularly detrimental to the cells. If the roles insinuated by the discussion above are true with respect to the pro-apoptotic role in

MDA-MB-468 cells, it may be that there is in fact an advantageous outcome to myc- δ C2 expression.

7.2 The cytoskeleton

The MDA-MB-468 cell lines were examined using immuno-fluorescence to identify the positioning of the myc- δ C2 domain within the cells. This showed the localisation of myc- δ C2 to the ends of actin protrusions from the bulk of the cytoskeleton, which did not appear to be a direct co-localisation event. Following the data obtained for the myc- δ C2 positioning study, the differences in the actin cytoskeleton were examined independently. The cells expressing the myc- δ C2 showed a more spread-out actin cytoskeleton with protrusions extending from the main bulk of the structure. This was absent in the vector cells where the cytoskeleton was more rounded and displayed fewer protrusions, which were generally less extensive. PKC- δ C2 domain has been identified as a binding partner of actin (Lopez-Lluch et al., 2001). Thus it could be hypothesized that the expression of myc- δ C2 may have an effect on the cytoskeletal structures.

The literature has identified numerous structures that actin may form under particular conditions. The 'spread-out' nature of the protrusions seen in Chapter 4 did not suggest directionality that would be identified if a cell was moving in a particular direction. Thus it seemed more probable that the protrusions were in fact associated with attachment of the cell to a surface.

The cytoskeleton is a complex of numerous proteins, some of which have a role in stabilisation of the structure, such as adducin. Protrusions from the main cell mass are likely to have a different complement of proteins, partially due to their positioning at the extremities, where there are fewer core cellular processes, i.e. key organelles such as the mitochondria and nucleus are in the core of the cell. Thus, overall these protrusions are

likely to have a certain complement of active proteins, which raises the question: which other proteins are localised to these protrusions that the C2 domain could be binding?

PKC- δ has activity at cell membranes throughout the cell, and in the nucleus for apoptosis, for example, but can also be associated with the cytoskeleton. However as the myc- δ C2 is not positioned throughout the cytoskeleton it may suggest that any interactions are related to the activity restricted to these protrusions. As the C2 should be inhibiting the action of the endogenous PKC- δ , it is interesting to consider the endogenous role. It could be considered that PKC- δ would normally prevent the attachment of protrusions to a surface, perhaps through inhibiting a link of the cytoskeleton to the focal adhesions. Where C2 is present it is inhibiting this inhibition, thus the cytoskeleton is firmly linked to the focal adhesions and the cell remains firmly attached to a surface.

The differences between the myc- δ C2 and vector control cell lines indicated PKC- δ may play a role in cell motility that over-expression of myc- δ C2 is preventing. There is evidence that PKC- δ has some involvement with the invasive and metastatic properties of cells. Kiley et al showed higher levels of PKC- δ were present in more invasive cell lines (Kiley et al., 1999). Where they increased the levels of the protein, the cells increasing grew independent of attachment, indicating a more invasive and metastatic profile. In addition to this they found regulatory domain expression prevented this effect, which could have been due to the action of the C2 domain, as a comparative effect can be identified in these studies.

7.3 Cell numbers

A difference was noted between the MDA-MB-468 myc- δ C2 and vector control cell lines in terms of how fast they appeared to be growing. Counts of the cells showed a consistently larger number of cells were found in the myc- δ C2 expressing cells over the vector control cells. This was also the case for the MDA-MB-231 cell lines, but not the MCF-7 cell lines. In the MDA-MB-231 cells there was also an increase in the myc-PKC- δ expressing cell lines, although to a lesser degree. The MCF-7 cell line expressing myc-PKC- δ appeared to show a decrease in cell number over the vector control.

Cell number can be considered as a balance between the cells proliferating and the cells apoptosing. Where proliferation is greater than apoptosis cell number increases, and where apoptosis is greater than proliferation cell number decreases. If, between two cell lines the proliferation is greater in one, and the degree of apoptosis similar, then cell number increases greater in that one more than the other. Equally, the effect on cell number will be the same if the level of proliferation is similar between the cell lines, but in one cell line apoptosis occurs to a greater degree, this one would display a lower cell number.

The effects on cell number of the MDA-MB-468 and MDA-MB-231 cells expressing myc- δ C2 could be due to the C2 inhibiting a pro-apoptotic action of PKC- δ , thus allowing the cells to survive, and the cell numbers to increase. However for the MDA-MB-231 cells this would not fit with the literature, or the ability to develop a myc-PKC- δ cell line. Alternatively it could be due to the C2 inhibiting an anti-proliferative action of PKC- δ , thus allowing proliferation to continue and cell numbers to increase. The absence of an effect in the MCF-7 cells could link the effect to apoptosis through the caspase-3

dependant pathway described previously. Where the caspase-3 is absent the pro-apoptotic pathway does not occur, thus the inhibition of this is extraneous. Therefore there would not be an effect to expressing myc- δ C2.

However, the expression of myc-PKC- δ in MDA-MB-231 cells had the effect of increasing cell numbers, although not to the same degree as with myc- δ C2 expression. At first glance this does not appear to fit with the idea that the myc- δ C2 is inhibiting the PKC- δ action. However, it could be that this is still happening, but that the over-expression of PKC- δ is to such a degree that it is 'flooding' the pathways, and a clear role for PKC- δ cannot be defined in this situation. The literature describes many roles for PKC- δ , some of which may have opposing effect. By allowing so many protein molecules to be expressed, without the control normally associated with cell metabolism, several of the pathways have become active and the result of multiple effects is being seen, illustrated by an increase in cell number. However if an anti-apoptotic effect is present in these cells, this could explain the benefit of PKC- δ over-expression, but it does not aid understanding of myc- δ C2 effects.

In the MCF-7 cells, the effects of expression of myc-PKC- δ did not have comparative effects to any of the other cell lines. In fact, the expression had the opposite effect and the cells had lower cell numbers than the vector control cells. The hypothesis for there being no effect of myc- δ C2 expression is that there is no pro-apoptotic effect to inhibit as the pathway cannot occur due to the lack of caspase-3. Thus if this pathway is not occurring, then over-expression of PKC- δ would not have an effect either. If the effects are not associated with apoptosis it would be likely that the effects could be in proliferation. If PKC- δ has an anti-proliferative action, the over-expression may

exacerbate this effect leading to lower cell numbers. It could be that no effect is seen with the myc- δ C2 cells as the C2 domain is not involved with this role. Perhaps the C1 domain is involved in regulation of this action.

Little could be clearly defined at this point of the study; however one thing that stood out was that the roles of PKC- δ are highly cell line dependent.

7.4 Apoptosis

The MDA-MB-468 cells have been the focus of this study, and the effects noted with the addition of the myc- δ C2 on cell number may be explained by differences in apoptosis; thus the apoptotic profiles of these cell lines were examined. The myc- δ C2 expressing cells demonstrated a higher level of viability than the vector control cells, in conjunction with a lower level of early apoptosis. This data indicates that through blocking the endogenous PKC- δ action, the myc- δ C2 is having a protective effect on the cells, thus reducing apoptosis, and resulting in the population showing an increased cell number. This is indicative of a pro-apoptotic effect of PKC- δ , as demonstrated in the literature. However, the involvement of the C2 domain in facilitating this process has not been previously noted. The pro-apoptotic pathway describes the tyrosine phosphorylation of a tyrosine residue in the C2 domain, as well as one in the C1 domain. This allows targeting of the PKC- δ to the nucleus through revealing a nuclear localisation sequence. It maybe that the PKC- δ C2 domain is vital for facilitating the interaction with the tyrosine kinase that is involved in this phosphorylation, and subsequent redirection of PKC- δ . Thus the fact that the C2 is widely present in the expressing cells would competitively inhibit the interaction of the tyrosine kinase with the C2 domain, thus preventing the pro-apoptotic role.

Bearing in mind the discoveries of an altered cytoskeleton in chapter 4, it is worth considering that the effects on apoptosis identified here could be attributed to the state of anoikis (Frisch and Screaton, 2001). Anoikis is a form of apoptosis related to a lack of anchorage to a surface. Where there is no anchorage a cell can be forced into an apoptotic program. This can be considered as a protective mechanism for preventing

invasive and metastatic phenotypes. Where the cells expressing myc- δ C2 have a more extensive actin cytoskeleton, they could be better attached and thus anoikis is prevented; this would allow for a higher level of viability within the population. PKC- δ endogenous activity has been shown to encourage anchorage-independent growth. This may induce a program of anoikis-related apoptosis. If this were the case, the C2 domain is of obvious importance in this activity. It could be blocking an interaction of the C2 domain on endogenous PKC- δ to allow cytoskeletal flexibility.

The effect was not seen in the MDA-MB-231 cells however. In fact the opposite effect was seen. The vector control cells demonstrated an increased level of viability over the myc- δ C2 cells; and although no difference was identified in the early apoptotic fraction (both populations were positive for early apoptotic cells), there was a lower level of late apoptotic/necrotic cells. This would suggest the myc- δ C2 domain is interfering with an anti-apoptotic effect of PKC- δ in this cell line. This anti-apoptotic effect of PKC- δ is supported in the literature, which also stated they did not see this effect in the MDA-MB-468 cell line. In Lønne et al (2009) they described a *ras* mutation that caused high phosphorylation levels of ERK1/2. The cells did not appear to be able to cope with this and would apoptose if it were not for the action of PKC- δ on NEDD4, and subsequently MKP3, to de-phosphorylate the ERK1/2 to a level at which apoptosis was not induced. Thus as a *ras* mutation is not present in the MDA-MB-468 cells, they would not demonstrate this apoptotic profile. However, this does not explain the beneficial effects of expressing myc- δ C2 on the cell numbers. Due to cell numbers being considered as a balance of apoptotic and proliferative abilities, it seems sensible to deduce that the effects seen in cell number are associated with a proliferative effect, whereby myc- δ C2 interferes with an anti-proliferative action.

In the PKC- δ over-expressing cell line, no differences could be identified in the apoptotic profile of the vector control cells and the over-expressing cells. From the myc- δ C2 cell data it may be expected that the identified anti-apoptotic effect of PKC- δ within this cell line would lead to an increased viability in the PKC- δ over-expressing cells; however this increase does not occur. Perhaps the absence of this viability increase is due to the fact that a binding partner of the PKC- δ is a limiting factor, i.e. there are only so many molecules of this binding partner, and the endogenous PKC- δ is already meeting the level which is necessary for the binding partner and the PKC- δ to bind and generate an effect.

The lack of an explanation for the increase in cell number of the myc-PKC- δ cells with the apoptosis data suggests that the answer may, as with the myc- δ C2 cells, lie with effects of PKC- δ in cell proliferation. Perhaps there may be several pathways involved here for both the PKC- δ over-expressing and myc- δ C2 expressing cell lines to demonstrate an increase in cell number, although to a differing degree, over the vector control cell line. This area would need further investigation within this cell line to identify any pathways and clarify the role of PKC- δ and the C2 domain within them. However, whatever network of interactions is involved, it is clear that the C2 domain can be considered vital to at least some of these, in order to allow the effects on cell numbers in myc- δ C2 expressing cells.

Despite the MCF-7 cells showing no difference in cell number with myc- δ C2 present, these cells were also examined for apoptosis. No differences were identified between the vector control and myc- δ C2 cells, supporting the cell number data described above. PKC- δ has been demonstrated to act through a pro-apoptotic mechanism involving

activation of the caspase cascade, a key component of which is caspase-3. However the MCF-7 cells do not express caspase-3. Thus this agrees with the data and the literature that, with the absence of caspase-3, the pro-apoptotic pathway cannot occur, and thus cell numbers are unaffected.

The PKC- δ over-expressing cell line was also studied and apoptosis data showed no differences between the vector control and over-expressing cell lines. The difference in cell number at day 5, where the PKC- δ over-expressing cell line was lower, does not appear to be due to the effects of apoptosis. It could be due to an anti-proliferative effect of PKC- δ activated through its over-expression; however further investigation would be required in order to clarify any mechanism by which this would take place. The lack of effect with the C2 domain on cell numbers is indicative of the C2 domain not being key in the interactions facilitating this role. The MDA-MB-231 data indicates that a proliferative effect could involve a network of pathways, and that the C2 is important for some, and not for others. Thus, perhaps the pathway where C2 is not important would be the active one in MCF-7 cells.

7.5 The effects of no serum

In order to further examine the apoptotic pathways involved in the MDA-MB-468 cells, the cells were serum-starved in order to induce stress, and cause apoptosis. The starvation of these cells produced an unexpected result, whereby the myc- δ C2 expressing cells displayed a significantly lower viability than the vector control cells. This was mirrored by an increase in the level of early apoptosis and late apoptosis/necrosis. Under starvation conditions, the cells expressing myc- δ C2 responded in an opposing manner to 10% serum. This blocked the endogenous PKC- δ role and induced apoptosis; thus illustrating an anti-apoptotic role for PKC- δ where serum is absent.

In MDA-MB-231 cells the PKC- δ also demonstrated an anti-apoptotic role in our apoptosis study, and also in the literature, but under full serum conditions. The pathway was active due to the effects of a *ras* mutation (Figure 6.2). There has, thus far, been no identification of a *ras* mutation in the MDA-MB-468 cell line. However the anti-apoptotic effects of PKC- δ in starved conditions, led us to examine aspects of the pathway, in order to study whether a similar situation was transpiring. Lønne et al (2009) used the proteasome inhibitor MG132 to identify whether preventing proteasomal degradation whilst using PKC- δ siRNA allowed MKP3 to continue its de-phosphorylating activity with regards to ERK1/2, which it did. We have used myc- δ C2 as an inhibitor of PKC- δ endogenous action, instead of siRNA. Thus by treating with MG132 as well, we could identify if a comparable effect occurred. The effect of myc- δ C2 in starved cells was reversed with the MG132 treatment, so that the viability was no longer significantly different from the vector control cells. This indicated that the pathway active in the

starved MDA-MB-468 cells also required the action of the proteasome, as in the MDA-MB-231 cells grown under normal conditions. The effect of myc- δ C2 expression indicates that the C2 domain of PKC- δ is important in the interactions essential for this pathway. The pathway described by Lønne et al (2009) described PKC- δ inhibiting NEDD4 action. It could be that the C2 domain is the region that binds this protein, perhaps near, or in, the active site, thus blocking its activity, or perhaps at an alternative location and inducing a conformational change preventing activity.

This pathway is important in the MDA-MB-231 cells as there is a *ras* mutation driving ERK1/2 phosphorylation excessively high. Therefore an important factor of this pathway is the phosphorylation status of ERK1/2. In MDA-MB-231 cells the ERK phosphorylation was lowered by PKC- δ activity; prevention of this activity increased phosphorylation and thus cell death. In the MDA-MB-468 cells we saw higher cell death in the starved cells, and thus examined whether an appropriate increase occurred in phosphorylation status, as this would indicate to what extent the pathway mirrored the situation in MDA-MB-231 cells. The ERK phosphorylation data identified a considerably higher level of ERK1/2 phosphorylation in the serum-starved myc- δ C2 cells, i.e. where endogenous PKC- δ activity is prevented.

The data obtained under serum starved conditions highlights a key role for the C2 domain in this pathway. It would be interesting to investigate whether this role is also present in the MDA-MB-231 cells, although the investigation into the similarities of the pathway between the two cell lines has shown strong correlation, thus it seems likely that the role of the C2 would remain conserved.

The differences identified in the myc- δ C2 expressing cell lines where serum is either present or absent is indicative of a 'sensing' role for the C2 domain. The variations of the method by which this could occur are extensive. However it could be that, due to the known action of tyrosine phosphorylation on PKC- δ targeting, tyrosine residues may become differentially phosphorylated. Perhaps binding of serum factors to receptors at the cell surface could lead to a cascade of reactions, some of which being to dephosphorylate certain residues, and phosphorylate others. The experiments performed in Chapter 6 began to examine this idea. They showed that there was no overall difference in the level of tyrosine phosphorylation of PKC- δ between the myc- δ C2 and vector control cell line. However more in-depth examination of specific residues may reveal differences. In addition, the experiments showed that the myc- δ C2 was not tyrosine phosphorylated. This may be due the kinase in question requiring the whole protein in order to act, or maybe that the phosphorylation would not involve the C2 domain directly. Perhaps the C2 domain would bind the kinase, but the phosphorylation would occur elsewhere in PKC- δ .

7.6 Key discoveries

- The C2 domain of PKC- δ is very important in mediating the roles of PKC- δ examined in this study.
- In MDA-MB-468 cells myc- δ C2 localises to the extremities of actin protrusions.
- In MDA-MB-468 cells inhibition of PKC- δ by myc- δ C2 allows cells to develop a more extensive cytoskeleton.
- In MDA-MB-468 cells myc- δ C2 prevents a pro-apoptotic role for PKC- δ .
- In MDA-MB-231 cells myc- δ C2 prevents an anti-apoptotic role for PKC- δ .
- In serum-starved MDA-MB-468 cells PKC- δ fulfils an anti-apoptotic role; the myc- δ C2 prevents this.
- Proteasome activity is vital to the PKC- δ anti-apoptotic role in starved MDA-MB-468 cells.
- ERK1/2 phosphorylation appears to be higher in starved MDA-MB-468 myc- δ C2 cells than vector control cells, correlating with an increase in apoptosis of myc- δ C2 cells.

The C2 was examined with the aim of investigating its role and discovering if it could be a suitable drug target. This research has indicated that it has an important role in directing PKC- δ activity. Depending on the conditions relevant to a tumour situation, it shows promise as a suitable drug target. However, there is a large amount of further work that remains to be undertaken to clarify roles in certain areas before a drug discovery program could be of value.

7.7 Further work

There are several aspects of this project that require further investigation as this project seems to have only scratched the surface of the complexity of the roles of PKC- δ within breast cancer. Expression of myc- δ C2 produced changes with respect to the cytoskeletal structure. Further investigation would be required to clarify the function of these changes. Although PKC- δ is already known to interact with the cytoskeleton, less is known regarding its effects. The C2 domain is obviously important in this interaction, but further research would be necessary to elucidate the role of this interaction. The data in this study have indicated that PKC- δ may have a destabilising action with respect to the cytoskeleton and the focal adhesions; further investigation would be required.

The apoptosis studies indicated differences where myc- δ C2 was interfering with the PKC- δ activity. It could be that this is linked to the cytoskeletal effects with reference to the phenomenon of anoikis; this should be investigated. However, the responses elicited through myc- δ C2 expression may be attributed to better understood apoptotic PKC- δ mechanisms; thus the binding partners involved in transmitting the effects of PKC- δ should be investigated.

The MDA-MB-231 apoptotic pathway, with relation to PKC- δ , has been examined in the literature. The anti-apoptotic effect of PKC- δ in these cells correlates with the effects of myc- δ C2 expression. However the lack of effect with PKC- δ over-expression should be further investigated. It seems likely that a binding partner could be a limiting factor in this pathway, but this should be confirmed.

The apoptotic pathway effects shown with myc- δ C2 expression can be explained by the literature. However, the differences in cell number with the MDA-MB-231 cell lines remains to be explained. There were also differences seen with MCF-7 cell line cell numbers. This did not relate to apoptotic differences. Thus this data suggests a key area of investigation should be PKC- δ effects in cell proliferation. It would appear, from the data obtained during this project, that the role of PKC- δ in proliferation may well be a cell dependant phenomenon, as MCF-7 and MDA-MB-231 cells appear to show PKC- δ having anti-proliferative and pro-proliferative effects, respectively.

Serum-starvation produced an interesting effect in MDA-MB-468 cells, whereby the apoptotic role of PKC- δ appeared reversed from 10% serum conditions. Investigation of this effect showed correlation with the study of an anti-apoptotic effect in MDA-MB-231 cells. However in MDA-MB-231 cells there is a *ras* mutation facilitating this process. The status of the RAS-RAF-MAPK-ERK pathway requires further investigation in the MDA-MB-468 cells. The entire pathway needs to be mapped out and examined in order to reveal a mutation which would allow the observed response to transpire. It could be that any stage of the pathway has been altered; it may be from the receptor level onwards through the pathway.

The differences between serum status responses would require investigation to examine a more relevant state of serum levels for a tumour situation. This would allow further study into the pathways that are active in this case. This would further allow consideration of whether the C2 would be a suitable drug target. The C2 does appear to be important in somehow 'sensing' the serum status; thus the methods by which this

occur should also be scrutinised in order to allow deliberation of the C2 domain suitability as a target for drugs.

Chapter 8: References

Abell, A.N., Granger, D.A., and Johnson, G.L. (2007). MEKK4 Stimulation of p38 and JNK Activity Is Negatively Regulated by GSK3 β . *Journal of Biological Chemistry* 282, 30476-30484.

Agrawal, B., Gendler, S., and Longenecker, B. (1998). The biological role of mucins in cellular interactions and immune regulation: prospects for cancer immunotherapy. *Mol Med Today* 4, 397 - 403.

Allen, W.E., Jones, G.E., Pollard, J.W., and Ridley, A.J. (1997). Rho, Rac and Cdc42 regulate actin organization and cell adhesion in macrophages. *Journal of Cell Science* 110, 707-720.

Arnold, H.K., Zhang, X., Daniel, C.J., Tibbitts, D., Escamilla-Powers, J., Farrell, A., Tokarz, S., Morgan, C., and Sears, R.C. (2009). The Axin1 scaffold protein promotes formation of a degradation complex for c-Myc. *EMBO J* 28, 500-512.

Assender, J.W., Gee, J.M.W., Lewis, I., Ellis, I.O., Robertson, J.F.R., and Nicholson, R.I. (2007). Protein kinase C isoform expression as a predictor of disease outcome on endocrine therapy in breast cancer. *Journal of Clinical Pathology* 60, 1216-1221.

Baines, A.J. (2009). Evolution of spectrin function in cytoskeletal and membrane networks. *Biochemical Society Transactions* 37, 796-803.

Barry, S.T., and Critchley, D.R. (1994). The RhoA-dependant assembly of focal adhesions in Swiss 3T3 cells is associated with increased tyrosine phosphorylation and the recruitment of both pp125FAK and protein kinase C-delta to focal adhesions. *Journal of Cell Science* 107, 2033-2045.

Benes, C.H., Wu, N., Elia, A.E.H., Dharia, T., Cantley, L.C., and Soltoff, S.P. (2005). The C2 domain of PKC delta is a phosphotyrosine binding domain. *Cell* 121, 271-280.

Berghs, S., Aggujaro, D., Dirx, R., Maksimova, E., Stabach, P., Hermel, J.-M., Zhang, J.-P., Philbrick, W., Slepnev, V., Ort, T., et al. (2000). β IV Spectrin, a New Spectrin Localized at Axon Initial Segments and Nodes of Ranvier in the Central and Peripheral Nervous System. *The Journal of Cell Biology* 151, 985-1002.

Berghs, S., Ferracci, F., Maksimova, E., Gleason, S., Leszczynski, N., Butler, M., De Camilli, P., and Solimena, M. (2001). Autoimmunity to β IV spectrin in paraneoplastic lower motor neuron syndrome. *Proceedings of the National Academy of Sciences of the United*

States of America 98, 6945-6950.

Blass, M., Kronfeld, I., Kazimirsky, G., Blumberg, P.M., and Brodie, C. (2002). Tyrosine Phosphorylation of Protein Kinase C δ Is Essential for Its Apoptotic Effect in Response to Etoposide. *Mol Cell Biol* 22, 182-195.

Bonadonna, G., Hortobagyi, G.N., and Gianni, A.M., eds. (2001). *Textbook of Breast Cancer: A Clinical Guide to Therapy*, second edn (London, Martin Dunitz).

Brito, G.C., Fachel, Â.A., Vettore, A.L., Vignal, G.M., Gimba, E.R.P., Campos, F.S., Barcinski, M.A., Verjovski-Almeida, S., and Reis, E.M. (2008). Identification of protein-coding and intronic noncoding RNAs down-regulated in clear cell renal carcinoma. *Molecular Carcinogenesis* 47, 757-767.

Brodie, C., and Blumberg, P.M. (2003). Regulation of cell apoptosis by protein kinase c δ . *Apoptosis* 8, 19-27.

Buschman, M.D., Bromann, P.A., Cejudo-Martin, P., Wen, F., Pass, I., and Courtneidge, S.A. (2009). The Novel Adaptor Protein Tks4 (SH3PXD2B) Is Required for Functional Podosome Formation. *Mol Biol Cell* 20, 1302-1311.

Cailleau, R., Olive, M., and Cruciger, Q.V.J. (1978). Long-Term Human Breast Carcinoma Cell Lines Of Metastatic Origin: Preliminary Characterization. *In Vitro* 14, 911-915.

Cailleau, R., Young, R., Olive, M., and Reeves, W.J. (1974). Breast Tumor Cell Lines From Pleural Effusions. *Journal of the National Cancer Institute* 53, 661-674.

Chen, C.-J., Nguyen, T., and Shively, J.E. (2010). Role of calpain-9 and PKC- δ in the apoptotic mechanism of lumen formation in CEACAM1 transfected breast epithelial cells. *Experimental Cell Research* 316, 638-648.

Chen, C.L., Hsieh, Y.T., and Chen, H.C. (2007). Phosphorylation of adducin by protein kinase C delta promotes cell motility. *Journal of Cell Science* 120, 1157-1167.

Chen, J.-L., Lin, H.H., Kim, K.-J., Lin, A., Ou, J.-H.J., and Ann, D.K. (2009). PKC delta signalling: a dual role in regulating hypoxic stress-induced autophagy and apoptosis. *Autophagy* 5, 244-246.

Chiarugi, P., and Giannoni, E. (2008). Anoikis: A necessary death program for anchorage-dependent cells. *Biochemical Pharmacology* 76, 1352-1364.

Cho, W. (2001). Membrane targeting by C1 and C2 domains. *The Journal of Biological Chemistry* 276, 32407-32410.

Chou, W.-H., Choi, D.-S., Zhang, H., Mu, D., McMahon, T., Kharazia, V.N., Lowell, C.A., Ferriero, D.M., and Messing, R.O. (2004). Neutrophil protein kinase C δ as a mediator of stroke-reperfusion injury. *The Journal of Clinical Investigation* 114, 49-56.

Cooper, J.A. (1987). Effects of Cytochalasin and Phalloidin on Actin. *The Journal of Cell Biology* 105, 1473-1478.

Courbard, J.-R., Fiore, F., Adelaide, J., Borg, J.-P., Birnbaum, D., and Ollendorf, V. (2002). Interaction between two ubiquitin-protein isopeptide ligases of different classes, CBL and AIP4/ITCH. *The Journal of Biological Chemistry* 277, 45267-45275.

Dampier, K., Hudson, E.A., Howells, L.M., Manson, M.M., Walker, R.A., and Gescher, A. (2001). Differences between human breast cell lines in susceptibility towards growth inhibition by genistein. *Br J Cancer* 85, 618-624.

Decker, M., Arand, M., and Cronin, A. (2009). Mammalian epoxide hydrolases in xenobiotic metabolism and signalling. *Archives of Toxicology* 83, 297-318.

Dekker, L.V., and Parker, P.J. (1997). Regulated binding of the protein kinase C substrate GAP-43 to the VO/C2 region of protein kinase C-delta. *Journal of Biological Chemistry* 272, 12747-12753.

DeVries-Seimon, T.A., Ohm, A.M., Humphries, M.J., and Reyland, M.E. (2007). Induction of Apoptosis Is Driven by Nuclear Retention of Protein Kinase C δ . *Journal of Biological Chemistry* 282, 22307-22314.

Diacumakos, E.G. (1973). Methods for micromanipulation of human somatic cells in culture. *Methods in Cell Biology* 7, 287-311.

Dorn, D.C., Kou, C.A., Png, K.J., and Moore, M.A.S. (2009). The effect of cantharidins on leukemic stem cells. *International Journal of Cancer* 124, 2186-2199.

Dorner, A.J., Semler, B.L., Jackson, R.J., Hanecak, R., Duprey, E., and Wimmer, E. (1984). In Vitro Translation of Poliovirus RNA: Utilization of Internal Initiation Sites in Reticulocyte Lysate. *Journal of Virology* 60, 507-514.

Early Breast Cancer Trialists' Collaborative Group (1998). Tamoxifen for early breast cancer: an overview of the randomised trials. *Lancet* 351, 1451-1467.

Essen, L.O., Perisic, O., Lynch, D.E., Katan, M., and Williams, R.L. (1997). A ternary metal binding site in the C2 domain of phosphoinositide-specific phospholipase C-delta1. *Biochemistry* 36, 2753-2762.

Ferlay, J., Shin, H.R., Bray, F., Forman, D., Mathers, C., and Parkin, D.M. (2010). GLOBOCAN 2008 v1.2, Cancer incidence and Mortality Worldwide: IARC CancerBase No. 10 (Lyon, France, International Agency for Research on Cancer).

Foecking, M.K., and Hofstetter, H. (1986). Powerful and versatile enhancer-promoter unit for mammalian expression vectors. *Gene* 45, 101-105.

Forrest, A.P. (1974). Hormones and neoplasia. *Journal of Clinical Pathology Supplement (Royal College of Pathologists)* 7, 65-71.

Fraley, R., Subramani, S., Berg, P., and Papahadjopoulos, D. (1980). Introduction of Liposome-encapsulated SV40 DNA into Cells. *The Journal of Biological Chemistry* 255, 10431-10435.

Frisch, S.M., and Screaton, R.A. (2001). Anoikis mechanisms. *Current Opinion in Cell*

Biology 13, 555-562.

Furuhashi, M., Yagi, K., Yamamoto, H., Furukawa, Y., Shimada, S., Nakamura, Y., Kikuchi, A., Miyazono, K., and Kato, M. (2001). Axin Facilitates Smad3 Activation in the Transforming Growth Factor {beta} Signaling Pathway. *Mol Cell Biol* 21, 5132-5141.

Garg, M., Kanojia, D., Khosla, A., Dudha, N., Sati, S., Chaurasiya, D., Jagadish, N., Seth, A., Kumar, R., Gupta, S., et al. (2008). Sperm-Associated Antigen 9 Is Associated With Tumor Growth, Migration, and Invasion in Renal Cell Carcinoma. *Cancer Res* 68, 8240-8248.

Gascoyne, D.M., Long, E., Veiga-Fernandes, H., de Boer, J., Williams, O., Seddon, B., Coles, M., Kioussis, D., and Brady, H.J.M. (2009). The basic leucine zipper transcription factor E4BP4 is essential for natural killer cell development. *Nat Immunol* 10, 1118-1124.

Ghayur, T., Hugunin, M., Talanian, R.V., Ratnofsky, S., Quinlan, C., Emoto, Y., Pandey, P., Datta, R., Huang, Y., Kharabanda, S., et al. (1996). Proteolytic Activation of Protein Kinase C delta by an ICE/CED 3-Like Protease Induces Characteristics of Apoptosis. *Journal of Experimental Medicine* 184, 2399-2404.

Giorgione, J.R., Lin, J.H., McCammon, J.A., and Newton, A.C. (2006). Increased membrane affinity of the C1 domain of protein kinase C delta compensates for the lack of involvement of its C2 domain in membrane recruitment. *Journal of Biological Chemistry* 281, 1660-1669.

Glinsky, G.V. (2006). Genomic Models of Metastatic Cancer: Functional Analysis of Death-From-Cancer Signature Genes reveals Aneuploid, Anoikis-Resistant, Metastasis-Enabling Phenotype with Altered Cell Cycle Control and Activated Polycomb Group (PcG) Protein Chromatin Silencing Pathway. *Cell Cycle* 5, 1208-1216.

Goodwin, E.C., and Rottman, F.M. (1992). The 3'-flanking sequence of the bovine growth hormone gene contains novel elements required for efficient and accurate polyadenylation. *J Biol Chem* 267, 16330-16334.

Gordge, P., Hulme, M., Clegg, R.A., and Miller, W.R. (1996). Elevation of protein kinase A and protein kinase C activities in malignant as compared with normal human breast tissue. *European journal of cancer* 32A, 2120-2126.

Graham, F.L., Veldhuisen, G., and Wilkie, N.M. (1973). Infectious Herpesvirus DNA. *Nature New Biology* 245, 265-266.

Grandinetti, K.B., and David, G. (2008). Sin3B: An essential regulator of chromatin modifications at E2F target promoters during cell cycle withdrawal. *Cell Cycle* 7, 1550-1554.

Griner, E.M., and Kazanietz, M.G. (2007). Protein kinase C and other diacylglycerol effectors in cancer. *Nat Rev Cancer* 7, 281-294.

Grossoni, V.C., Falbo, K.B., Kazanietz, M.G., Joffé, E.D.B.d.K., and Urtreger, A.J. (2007). Protein kinase C delta enhances proliferation and survival of murine mammary cells. *Molecular Carcinogenesis* 46, 381-390.

- Hall, A. (1994). Small GTP-binding proteins and the regulation of the actin cytoskeleton. *Annu Rev Cell Biol* 10, 31-54.
- Hall, K.J., Jones, M.L., and Poole, A.W. (2007). Coincident regulation of PKC δ in human platelets by phosphorylation of Tyr311 and Tyr565 and phospholipase C signalling. *The Biochemical Journal* 406, 501-509.
- Hamer, D.H., and Leder, P. (1979). Splicing and the Formation of Stable RNA. *Cell* 18, 1299-1302.
- Hanahan, D., and Weinberg, R.A. (2000). The Hallmarks of Cancer. *Cell* 100, 57-70.
- Hanahan, D., and Weinberg, Robert A. (2011). Hallmarks of Cancer: The Next Generation. *Cell* 144, 646-674.
- Hanks, S., and Hunter, T. (1995). Protein kinases 6. The eukaryotic protein kinase superfamily: kinase (catalytic) domain structure and classification. *The FASEB Journal* 9, 576-596.
- Hibi, K., Nakayama, H., Kodera, Y., Ito, K., Akiyama, S., and Nakao, A. (2004). CDH13 promoter region is specifically methylated in poorly differentiated colorectal cancer. *Br J Cancer* 90, 1030-1033.
- Hiratsuka, S., Watanabe, A., Aburatani, H., and Maru, Y. (2006). Tumour-mediated upregulation of chemoattractants and recruitment of myeloid cells predetermines lung metastasis. *Nature Cell Biology* 8, 1369-75
- Hu, Z., Fan, C., Oh, D., Marron, J., He, X., Qaqish, B., Livasy, C., Carey, L., Reynolds, E., Dressler, L., *et al.* (2006). The molecular portraits of breast tumors are conserved across microarray platforms. *BMC Genomics* 7, 96.
- Huang, M.T.F., and Gorman, C.M. (1990). Intervening sequences increase efficiency of RNA 3' processing and accumulation of cytoplasmic RNA. *Nucleic Acids Research* 18, 937-947.
- Humphries, M.J., Limesand, K.H., Schneider, J.C., Nakayama, K.I., Anderson, S.M., and Reyland, M.E. (2006). Suppression of Apoptosis in the Protein Kinase C δ Null Mouse in Vivo. *Journal of Biological Chemistry* 281, 9728-9737.
- Humphries, M.J., Ohm, A.M., Schaack, J., Adwan, T.S., and Reyland, M.E. (2008). Tyrosine phosphorylation regulates nuclear translocation of PKC δ . *Oncogene* 27, 3045-3053.
- Hurley, J.H., Newton, A.C., Parker, P.J., Blumberg, P.M., and Nishizuka, Y. (1997). Taxonomy and function of C1 protein kinase C homology domains. *Protein Science* 6, 477-480.
- Inoue, K., Wen, R., Rehg, J.E., Adachi, M., Cleveland, J.L., Rousset, M.F., and Sherr, C.J. (2000). Disruption of the ARF transcriptional activator DMP1 facilitates cell immortalization, Ras transformation, and tumorigenesis. *Genes & Development* 14, 1797-1809.

- Jackson, A.L., Bartz, S.R., Schelter, J., Kobayashi, S.V., Burchard, J., Mao, M., Li, B., Cavet, G., and Linsley, P.S. (2003). Expression profiling reveals off-target gene regulation by RNAi. *Nature Biotechnology* 21.
- Jackson, D.N., and Foster, D.A. (2004). The enigmatic protein kinase Cd: complex roles in cell proliferation and survival. *FASEB* 18, 627-636.
- Jang, S.K., Krausslich, H.G., Nicklin, M.J., Duke, G.M., Palmenberg, A.C., and Wimmer, E. (1988). A segment of the 5' nontranslated region of encephalomyocarditis virus RNA directs internal entry of ribosomes during in vitro translation. *J Virol* 62, 2636-2643.
- Janicke, R.U. (2009). MCF-7 breast carcinoma cells do not express caspase-3. *Breast Cancer Research and Treatment* 117, 219-221.
- Johnson, D.A., Akamine, P., Radzio-Andzelm, E., Madhusudan, M., and Taylor, S.S. (2001). Dynamics of cAMP-dependant protein kinase. *Chemical Reviews* 101, 2243-2270.
- Kajimoto, T., Sawamura, S., Tohyama, Y., Mori, Y., and Newton, A.C. (2010). Protein Kinase C δ -specific Activity Reporter Reveals Agonist-evoked Nuclear Activity Controlled by Src Family of Kinases. *The Journal of Biological Chemistry* 285, 41896-41910.
- Kazanietz, M.G., Wang, S., Milne, G.W.A., Lewin, N.E., Liu, H.L., and Blumberg, P.M. (1995). Residues in the Second Cysteine-rich Region of Protein Kinase C δ Relevant to Phorbol Ester Binding as Revealed by Site-directed Mutagenesis. *Journal of Biological Chemistry* 270, 21852-21859.
- Kemmner, W., Wan, K., Ruttinger, S., Ebert, B., Macdonald, R., Klamm, U., and Moesta, K.T. (2008). Silencing of human ferrochelatase causes abundant protoporphyrin-IX accumulation in colon cancer. *FASEB J* 22, 500-509.
- Keshamouni, V.G., Mattingly, R.R., and Reddy, K.B. (2002). Mechanism of 17- β -Estradiol-induced Erk1/2 Activation in Breast Cancer Cells. *Journal of Biological Chemistry* 277, 22558-22565.
- Kharait, S., Dhir, R., Lauffenburger, D., and Wells, A. (2006). Protein kinase C delta signaling downstream of the EGF receptor mediates migration and invasiveness of prostate cancer cells. *Biochemical and Biophysical Research Communications* 343, 848-856.
- Khawaja, A., and Tatton, L. (1999). Caspase-Mediated Proteolysis and Activation of Protein Kinase Cdelta Plays a Central Role in Neutrophil Apoptosis. *Blood* 94, 291-301.
- Kiley, S.C., Clark, K.J., Duddy, S.K., Welch, D.R., and Jaken, S. (1999a). Increased protein kinase C delta in mammary tumor cells: relationship to transformation and metastatic progression. *Oncogene* 18, 6748-6757.
- Kiley, S.C., Clark, K.J., Goodnough, M., Welch, D.R., and Jaken, S. (1999b). Protein kinase C delta involvement in mammary tumor cell metastasis. *Cancer Research* 59, 3230-3238.
- King, R.J., and Robins, M.W. (2006). *Cancer Biology*, Third edn (London, Pearson

Education Limited).

Konishi, H., Yamauchi, E., Taniguchi, H., Yamamoto, T., Matsuzaki, H., Takemura, Y., Ohmae, K., Kikkawa, U., and Nishizuka, Y. (2001). Phosphorylation sites of protein kinase C δ in H₂O₂-treated cells and its activation by tyrosine kinase in vitro. *Proceedings of the National Academy of Sciences* *98*, 6587-6592.

Koriyama, H., Kouchi, Z., Umeda, T., Saido, T.C., Momoi, T., Ishiura, S., and Suzuki, K. (1999). Proteolytic Activation of Protein Kinase C [δ] and [ϵ] by Caspase-3 in U937 Cells During Chemotherapeutic Agent-Induced Apoptosis. *Cellular Signalling* *11*, 831-838.

Lee, M.H., and Bell, R.M. (1986). The lipid binding, regulatory domain of protein kinase C. A 32-kDa fragment contains the calcium- and phosphatidylserine-dependent phorbol diester binding activity. *Journal of Biological Chemistry* *261*, 14867-14870.

Legendre, J.-Y., and Szoka, F.C. (1993). Cyclic amphipathic peptide-DNA complexes mediate high-efficiency transfection of adherent mammalian cells. *Proceedings of the National Academy of Sciences of the United States of America* *90*, 893-897.

Lei, Y., Moore, C.B., Liesman, R.M., O'Connor, B.P., Bergstralh, D.T., Chen, Z.J., Pickles, R.J., and Ting, J.P.Y. (2009). MAVS-Mediated Apoptosis and Its Inhibition by Viral Proteins. *PLoS ONE* *4*, e5466.

Leitges, M., Mayr, M., Braun, U., Mayr, U., Li, C., Pfister, G., Ghaffari-Tabrizi, N., Baier, G., Hu, Y., and Xu, Q. (2001). Exacerbated vein graft arteriosclerosis in protein kinase C δ -null mice. *The Journal of Clinical Investigation* *108*, 1505-1512.

Levine, D.M., and Stephan, D.F. (2011). *Even You Can Learn Statistics: A Guide for Everyone Who Has Ever Been Afraid of Statistics*, 2 edn (Upper Saddle River, New Jersey, FT Press).

Li, W., Li, W., Chen, X.-H., Kelley, C.A., Alimandi, M., Zhang, J., Chen, Q., Bottaro, D.P., and Pierce, J.H. (1996). Identification of Tyrosine 187 as a Protein Kinase C- δ Phosphorylation Site. *Journal of Biological Chemistry* *271*, 26404-26409.

Liu, Y., Graham, C., Li, A., Fisher, R.J., and Shaw, S. (2002). Phosphorylation of the protein kinase C- θ activation loop and hydrophobic motif regulates its kinase activity, but only activation loop phosphorylation is critical to in vivo nuclear factor- κ B induction. *Biochem J* *361*, 255-265.

Lønne, G.K., Masoumi, K.C., Lennartsson, J., and Larsson, C. (2009). Protein Kinase C δ Supports Survival of MDA-MB-231 Breast Cancer Cells by Suppressing the ERK1/2 Pathway. *Journal of Biological Chemistry* *284*, 33456-33465.

Lopez-Lluch, G., Bird, W.M., Canas, B., Godovac-Zimmerman, J., Ridley, A., Segal, A.W., and Dekker, L.V. (2001). Protein kinase C- δ C2-like domain is a binding site for actin and enables actin redistribution in neutrophils. *Biochemical Journal* *357*, 39-47.

Lu, Z., and Xu, S. (2006). ERK1/2 MAP Kinases in Cell Survival and Apoptosis. *IUBMB Life*

58, 621-631.

Mallakin, A., Sugiyama, T., Taneja, P., Matisse, L.A., Frazier, D.P., Choudhary, M., Hawkins, G.A., D'Agostino Jr, R.B., Willingham, M.C., and Inoue, K. (2007). Mutually Exclusive Inactivation of DMP1 and ARF/p53 in Lung Cancer. *Cancer Cell* 12, 381-394.

Mans, D.A., Voest, E.E., and Giles, R.H. (2008). All along the watchtower: Is the cilium a tumor suppressor organelle. *Biochimica et Biophysica Acta* 1786, 114-125.

Marrs, W., and Stella, N. (2007). 2-AG + 2 New Players = Forecast for Therapeutic Advances. *Chemistry & Biology* 14, 1309-1311.

Martinez-Salas, E. (1999). Internal ribosomal entry site biology and its use in expression vectors. *Current Opinion in Biotechnology* 10, 458-464.

Mathers, C., Boerma, T., and Fat, D.M. (2008). The global burden of disease: 2004 update (Geneva, World Health Organisation).

Matsumura, T., Kawamura-Tsuzuku, J., Yamamoto, T., Semba, K., and Inoue, J.-i. (2009). TRAF-Interacting Protein with a Forkhead-Associated Domain B (TIFAB) Is a Negative Regulator of the TRAF6-Induced Cellular Functions. *J Biochem* 146, 375-381.

McCracken, M.A., Miraglia, L.J., McKay, R.A., and Strobl, J.S. (2003). Protein Kinase C delta Is a Prosurvival Factor in Human Breast Tumor Cell Lines1. *Molecular Cancer Therapeutics* 2, 273-281.

McKiernan, E., O'Brien, K., Grebenchtchikov, N., Geurts-Moespot, A., Sieuwerts, A.M., Martens, J.W.M., Magdolen, V., Evoy, D., McDermott, E., Crown, J., et al. (2008). Protein kinase C[delta] expression in breast cancer as measured by real-time PCR, western blotting and ELISA. *Br J Cancer* 99, 1644-1650.

Mellor, H., and Parker, P.J. (1998). The extended protein kinase C superfamily. *Biochem J* 332, 281-292.

Menard, S., Pupa, S.M., Campiglio, M., and Tagliabue, E. (2003). Biologic and therapeutic role of HER2 in cancer. *Oncogene* 22, 6570-6578.

Metz, J., and Hampshire, M., eds. (2007). *Oncolink Patient Guide: Breast Cancer* (Philadelphia, Elsevier Saunders).

Miyake, M., Ishii, M., Kawashima, K., Kodama, T., Sugano, K., Fujimoto, K., and Hirao, Y. (2009). siRNA-mediated Knockdown of the Heme Synthesis and Degradation Pathways: Modulation of Treatment Effect of 5-Aminolevulinic Acid-based Photodynamic Therapy in Urothelial Cancer Cell Lines. *Photochemistry and Photobiology* 85, 1020-1027.

Miyamoto, A., Nakayama, K., Imaki, H., Hirose, S., Jiang, Y., Abe, M., Tsukiyama, T., Nagahama, H., Ohno, S., Hatakeyama, S., et al. (2002). Increased proliferation of B cells and auto-immunity in mice lacking protein kinase C[delta]. *Nature* 416, 865-869.

Morita, M., Matsuzaki, H., Yamamoto, T., Fukami, Y., and Kikkawa, U. (2008). Epidermal Growth Factor Receptor Phosphorylates Protein Kinase C δ at Tyr332 to form a Trimeric

Complex with p66Shc in the H₂O₂-stimulated Cells. *Journal of Biochemistry* 143, 31-38.

Mukherjee, P., Tinder, T.L., Basu, G.D., and Gendler, S.J. (2005). MUC1 (CD227) interacts with Ick tyrosine kinase in Jurkat lymphoma cells and normal T cells. *Journal of Leukocyte Biology* 77, 90-99.

Mulligan, R.C., Howard, B.H., and Berg, P. (1979). Synthesis of rabbit beta-globin in cultured monkey kidney cells following infection with a SV40 beta-globin recombinant genome. *Nature* 277, 108-114.

Munirah, M.A., Siti-Aishah, M.A., Reena, M.Z., Rohaizak, M., Norlia, A., Rafie, M.K., Asmiati, A., Hisham, A., Fuad, I., Shahrun, N.S., et al. (2011). Identification of different subtypes of breast cancer using tissue microarray. *Romanian Journal of Morphology and Embryology* 52, 669-677.

Nabha, S.M., Glaros, S., Hong, M., Lykkesfeldt, A.E., Schiff, R., Osborne, K., and Reddy, K.B. (2005). Upregulation of PKC- δ contributes to antiestrogen resistance in mammary tumor cells. *Oncogene* 24, 3166-3176.

Nakashima, H., Frank, G.D., Shirai, H., Hinoki, A., Higuchi, S., Ohtsu, H., Eguchi, K., Sanjay, A., Reyland, M.E., Dempsey, P.J., et al. (2008). Novel Role of Protein Kinase C- δ Tyr311 Phosphorylation in Vascular Smooth Muscle Cell Hypertrophy by Angiotensin II. *Hypertension* 51, 232-238.

Neo, S.Y., Zhang, Y., Yaw, L.P., Li, P., and Lin, S.-C. (2000). Axin-Induced Apoptosis Depends on the Extent of Its JNK Activation and Its Ability to Down-Regulate [beta]-Catenin Levels. *Biochemical and Biophysical Research Communications* 272, 144-150.

Neumann, E., Schaefer-Ridder, M., Wang, Y., and Hofscheider, P.H. (1982). Gene transfer into mouse lymphoma cells by electroporation in high electric fields. *The EMBO Journal* 1, 841-845.

Nielsen, T.O., Hsu, F.D., Jensen, K., Cheang, M., Karaca, G., Hu, Z., Hernandez-Boussard, T., Livasy, C., Cowan, D., Dressler, L., et al. (2004). Immunohistochemical and clinical characterization of the basal-like subtype of invasive breast carcinoma. *Clinical Cancer Research* 10, 5367-5374.

Nobes, C.D., and Hall, A. (1995). Rho, Rac and Cdc42 GTPases Regulate the Assembly of Multimolecular Focal Complexes Associated with Actin Stress Fibres, Lamellipodia, and Filopodia. *Cell* 81, 53-62.

O'Brian, C.A., Vogel, V.G., Eva Singletary, S., and Ward, N.E. (1989). Elevated Protein Kinase C Expression in Human Breast Tumor Biopsies Relative to Normal Breast Tissue. *Cancer Res* 49, 3215-3217.

Ono, Y., Fujii, T., Igarashi, K., Kuno, T., Tanaka, C., Kikkawa, U., and Nishizuka, Y. (1989). Phorbol ester binding to protein kinase C requires a cysteine-rich zinc-finger-like sequence. *Proceedings of the National Academy of Sciences* 86, 4868-4871.

Pannall, P., and Kotasek, D. (1997). *Cancer and Clinical Biochemistry* (London, ACB

Venture Publications).

Pappa, H., Murray-Rust, J., Dekker, L.V., Parker, P.J., and McDonald, N.Q. (1998). Crystal structure of the C2 domain from protein kinase C-delta. *Structure* 6, 885-894.

Parsons, J.T., and Parsons, S.J. (1997). Src family protein tyrosine kinases: Cooperating with growth factor and adhesion signalling pathways. *Current Opinion in Cell Biology* 9, 187-192.

Pasleau, F., Tocci, M.J., Leung, F., and Kopchick, J.J. (1985). Growth hormone gene expression in eukaryotic cells directed by the Rous sarcome virus long terminal repeat or cytomegalovirus immediate-early promoter. *Gene* 38, 227-232.

Perou, C.M., Sorlie, T., Eisen, M.B., van de Rijn, M., Jeffrey, S.S., Rees, C.A., Pollack, J.R., Ross, D.T., Johnsen, H., Akslen, L.A., *et al.* (2000). Molecular portraits of human breast tumours. *Nature* 406, 747-752.

Polyak, K. (2007). Breast cancer: origins and evolution. *The Journal of Clinical Investigation* 117, 3155-3163.

Pommier, Y. (2006). Topoisomerase I inhibitors: camptothecins and beyond. *Nature Reviews Cancer* 6, 789-802.

Pommier, Y., Leo, E., Zhang, H., and Marchand, C. (2010). DNA Topoisomerases and Their Poisoning by Anticancer and Antibacterial Drugs. *Chemistry & Biology* 17, 421-433.

Ponting, C.P., and Parker, P.J. (1996). Extending the C2 domain family: C2s in PKCs δ , ϵ , η , θ , phospholipases, GAPs, and perforin. *Protein Science* 5, 162-166.

Quin, R., and McGuckin, M. (2000). Phosphorylation of the cytoplasmic domain of the MUC1 mucin correlates with changes in cell-cell adhesion. *Int J Cancer* 87, 499 - 506.

Reese, R.J. (2004). *Analysis of Genes and Genomes* (Chichester, John Wiley & Sons Ltd).

Ren, J., Li, Y.Q., and Kufe, D. (2002). Protein kinase C delta regulates function of the DF3/MUC1 carcinoma antigen in beta-catenin signaling. *Journal of Biological Chemistry* 277, 17616-17622.

Reyland, M.E. (2007). Protein kinase C δ and apoptosis. *Biochemical Society Transactions* 35, 1001-1004.

Reyland, M.E., Anderson, S.M., Matassa, A.A., Barzen, K.A., and Quissell, D.O. (1999). Protein Kinase C δ Is Essential for Etoposide-induced Apoptosis in Salivary Gland Acinar Cells. *Journal of Biological Chemistry* 274, 19115-19123.

Richfield, D., and Haggstrom, M. (2009). *Enzymes, their cellular location, substrates and products in human steroidogenesis* (Wikimedia Foundation, Inc.).

Rincon, S.V.d., Guo, Q., Morelli, C., Shiu, H.-Y., Surmacz, E., and Miller, W.H., Jr. (2004). Retinoic acid mediates degradation of IRS-1 by the ubiquitin-proteasome pathway, via a PKC-dependant mechanism. *Oncogene* 23, 9269-9279.

Roodink, I., Raats, J., van der Zwaag, B., Verrijp, K., Kusters, B., van Bokhoven, H., Linkels, M., de Waal, R.M.W., and Leenders, W.P.J. (2005). Plexin D1 Expression Is Induced on Tumor Vasculature and Tumor Cells: A Novel Target for Diagnosis and Therapy? *Cancer Res* 65, 8317-8323.

Roodink, I., Verrijp, K., Raats, J., and Leenders, W. (2009). Plexin D1 is ubiquitously expressed on tumor vessels and tumor cells in solid malignancies. *BMC Cancer* 9, 297.

Roses, D.F. (1999). *Breast Cancer* (Philadelphia, Churchill Livingstone).

Rossi, D., and Gaidano, G. (2003). Messengers of death: apoptotic signalling in health and disease. *Haematologica* 88, 212-218.

Rossi, M., De Laurenzi, V., Munarriz, E., Green, D.R., Liu, Y.-C., Vousden, K.H., Cesareni, G., and Melino, G. (2005). The ubiquitin-protein ligase Itch regulates p73 stability. *EMBO J* 24, 836-848.

Rowntree, D. (2000). *Statistics Without Tears: An Introduction for Non-Mathematicians* (London, Penguin).

Rumsey, D. (2010). *Statistics Essentials for Dummies* (Hoboken, New Jersey, Wiley).

Sakaino, M., Ishigaki, M., Ohgari, Y., Kitajima, S., Masaki, R., Yamamoto, A., and Taketani, S. (2009). Dual mitochondrial localization and different roles of the reversible reaction of mammalian ferrochelatase. *FEBS Journal* 276, 5559-5570.

Salahshor, S., and Woodgett, J.R. (2005). The links between axin and carcinogenesis. *Journal of Clinical Pathology* 58, 225-236.

Savinainen, J.R., Saario, S.M., and Laitinen, J.T. (2011). The serine hydrolases MAGL, ABHD6 and ABHD12 as guardians of 2-arachidonoylglycerol signalling through cannabinoid receptors. *Acta Physiologica* 202, 267-76.

Saviozzi, S., Ceppi, P., Novello, S., Ghio, P., Lo Iacono, M., Borasio, P., Cambieri, A., Volante, M., Papotti, M., Calogero, R.A., et al. (2009). Non-Small Cell Lung Cancer Exhibits Transcript Overexpression of Genes Associated with Homologous Recombination and DNA Replication Pathways. *Cancer Res* 69, 3390-3396.

Schaefer-Ridder, M., Wang, Y., and Hofschneider, P.H. (1982). Liposomes as Gene Carriers: Efficient Transformation of Mouse L Cells by Thymidine Kinase Gene. *Science* 215, 166-168.

Schonwasser, D.C., Marais, R.M., Marshall, C.J., and Parker, P.J. (1998). Activation of the mitogen-activated protein kinase/extracellular signal-regulated kinase pathway by conventional, novel and atypical protein kinase C isotypes. *Mol Cell Biol* 18, 790-798.

Schroeder, J.A., Adriance, M.C., Thompson, M.C., Camenisch, T.D., and Gendler, S.J. (2003). MUC1 alters beta-catenin-dependent tumor formation and promotes cellular invasion. *Oncogene* 22, 1324-1332.

Schutte, B., Nuydens, R., Geerts, H., and Ramaekers, F. (1998). Annexin V binding assay

as a tool to measure apoptosis in differentiated neuronal cells. *Journal of Neuroscience Methods* 86, 63-69.

Shanmugam, M., Krett, N.L., Maizels, E.T., Cutler Jr, R.E., Peters, C.A., Smith, L.M., O'Brien, M.L., Park-Sarge, O.-K., Rosen, S.T., and Hunzicker-Dunn, M. (1999). Regulation of protein kinase C [delta] by estrogen in the MCF-7 human breast cancer cell line. *Molecular and Cellular Endocrinology* 148, 109-118.

Shanmugam, M., Krett, N.L., Maizels, E.T., Murad, F.M., Rosen, S.T., and Hunzicker-Dunn, M. (2001). A role for protein kinase C [delta] in the differential sensitivity of MCF-7 and MDA-MB 231 human breast cancer cells to phorbol ester-induced growth arrest and p21WAF1/CIP1 induction. *Cancer Letters* 172, 43-53.

Shanmugam, M., Krett, N.L., Maizels, E.T., Murad, F.M., Rosen, S.T., and Hunzicker-Dunn, M. (2001). A role for protein kinase C [delta] in the differential sensitivity of MCF-7 and MDA-MB 231 human breast cancer cells to phorbol ester-induced growth arrest and p21WAF1/CIP1 induction. *Cancer Letters* 172, 43-53.

Singh, R., Lei, P., and Andreadis, S.T. (2009). PKC- δ binds to E-cadherin and mediates EGF-induced cell scattering. *Experimental Cell Research* 315, 2899-2913.

Sleeman, J.P., and Cremers, N. (2007). New concepts in breast cancer metastasis: tumor initiating cells and the microenvironment. *Clin Exp Metastasis* 24, 707-715.

Solodukhin, A.S., Caldwell, H.L., Sando, J.J., and Kretsinger, R.H. (2002). Two-Dimensional Crystal Structures of Protein Kinase C-[delta], Its Regulatory Domain, and the Enzyme Complexed with Myelin Basic Protein. *Biophysical Journal* 82, 2700-2708.

Soltoff, S.P. (2007). Rotterlin: an inappropriate and ineffective inhibitor of PKC-delta. *TRENDS in Pharmacological Sciences* 28, 453-458.

Sørli, T., Wang, Y., Xiao, C., Johnsen, H., Naume, B., Samaha, R., and Børresen-Dale, A. (2006). Distinct molecular mechanisms underlying clinically relevant subtypes of breast cancer: gene expression analyses across three different platforms. *BMC Genomics* 7, 127.

Soule, H.D., Vasquez, J., Long, A., Albert, S., and Brennan, M. (1973). A Human Cell Line From a Pleural Effusion Derived From a Breast Carcinoma. *Journal of the National Cancer Institute* 51, 1409-1416.

Stahelin, R.V., Digman, M.A., Medkova, M., Ananthanarayanan, B., Rafter, J.D., Melowic, H.R., and Cho, W.H. (2004). Mechanism of diacylglycerol-induced membrane targeting and activation of protein kinase C delta. *Journal of Biological Chemistry* 279, 29501-29512.

Statistics', O.f.N. (2010). Cancer statistics registration: Registrations of cancer diagnosed in 2008, England (London, Office for National Statistics).

Steinberg, S.F. (2004). Distinctive activation mechanisms and functions for protein kinase Cdelta. *Biochem J* 384, 449-459.

Steinberg, S.F. (2008). Structural Basis of Protein Kinase C Isoform Function. *Physiol Rev* 88, 1341-1378.

Steinberg, S.F. (2008). Structural Basis of Protein Kinase C Isoform Function. *Physiol Rev* 88, 1341-1378.

Subramaniam, S., and Unsicker, K. (2010). ERK and cell death: ERK1/2 in neuronal cell death. *FEBS Journal* 277, 22-29.

Szallasi, Z., Denning, M.F., Chang, E.Y., Rivera, J., Yuspa, S.H., Lehel, C., Olah, Z., Anderson, W.B., and Blumberg, P.M. (1995). Development of a Rapid Approach to Identification of Tyrosine Phosphorylation Sites: Application to PKC δ Phosphorylated upon Activation of the High Affinity Receptor for IgE in Rat Basophilic Leukemia Cells. *Biochemical and Biophysical Research Communications* 214, 888-894.

Takino, T., Nakada, M., Miyamori, H., Watanabe, Y., Sato, T., Gantulga, D., Yoshioka, K., Yamada, K.M., and Sato, H. (2005). JSAP1/JIP3 Cooperates with Focal Adhesion Kinase to Regulate c-Jun N-terminal Kinase and Cell Migration. *Journal of Biological Chemistry* 280, 37772-37781.

Takino, T., Yoshioka, K., Miyamori, H., Yamada, K.M., and Sato, H. (2002). A scaffold protein in the c-Jun N-terminal kinase signalling pathway is associated with focal adhesion kinase and tyrosine-phosphorylated. *Oncogene* 21, 6488-6497.

Tessema, M., Willink, R., Do, K., Yu, Y.Y., Yu, W., Machida, E.O., Brock, M., Van Neste, L., Stidley, C.A., Baylin, S.B., et al. (2008). Promoter Methylation of Genes in and around the Candidate Lung Cancer Susceptibility Locus 6q23-25. *Cancer Res* 68, 1707-1714.

Thangaraju, M., Kaufmann, S.H., and Couch, F.J. (2000). BRCA1 Facilitates Stress-induced Apoptosis in Breast and Ovarian Cancer Cell Lines. *Journal of Biological Chemistry* 275, 33487-33496.

Thompson, A., Brennan, K., Cox, A., Gee, J., Harcourt, D., Harris, A., Harvie, M., Holen, I., Howell, A., Nicholson, R., et al. (2008). Evaluation of the current knowledge limitations in breast cancer research: a gap analysis. *Breast Cancer Research* 10.

Thomsen, D.R., Stenberg, R.M., Goins, W.F., and Stinski, M.F. (1984). Promoter-regulatory region of the major immediate early gene of human cytomegalovirus. *Proceedings of the National Academy of Sciences of the United States of America* 81, 659-663.

Tillman, D., Izeradjene, K., Szucs, K.S., Douglas, L., and Houghton, J.A. (2003). Rotterlin sensitizes colon carcinoma cells to tumour necrosis factor-related apoptosis-inducing ligand-induced apoptosis via uncoupling of the mitochondria independent of protein kinase C. *Cancer Res* 63, 5118-5125.

Tseng, P.-H., Wang, Y.-C., Weng, S.-C., Weng, J.-R., Chen, C.-S., Brueggemeier, R.W., Shapiro, C.L., Chen, C.-Y., Dunn, S.E., Pollak, M., et al. (2006). Overcoming Trastuzumab Resistance in HER2-Overexpressing Breast Cancer Cells by Using a Novel Celecoxib-Derived Phosphoinositide-Dependent Kinase-1 Inhibitor. *Molecular Pharmacology* 70,

1534-1541.

Vermes, I., Haanen, C., Steffens-Nakken, H., and Reutelingsperger, C. (1995). A novel assay for apoptosis Flow cytometric detection of phosphatidylserine expression on early apoptotic cells using fluorescein labelled Annexin V. *Journal of Immunological Methods* 184, 39-51.

Vucenik, I., Ramakrishna, G., Tantivejkul, K., Anderson, L., and Ramljak, D. (2005). Inositol hexaphosphate (IP6) blocks proliferation of human breast cancer cells through a PKC δ -dependent increase in p27Kip1 and decrease in retinoblastoma protein (pRb) phosphorylation. *Breast Cancer Research and Treatment* 91, 35-45.

Wagstaff, M.J.D., Lilley, C.E., Smith, J., Robinson, M.J., Coffin, R.S., and Latchman, D.S. (1998). Gene transfer using a disabled herpes virus vector containing the EMCV IRES allows multiple gene expression in vitro and in vivo. *Gene Therapy* 5, 1566-1570.

Wang, Z., Shen, D., Parsons, D.W., Bardelli, A., Sager, J., Szabo, S., Ptak, J., Silliman, N., Peters, B.A., van der Heijden, M.S., *et al.* (2004). Mutational Analysis of the Tyrosine Phosphatome in Colorectal Cancers. *Science* 304, 1164-1166.

Webster, M.-T., Rozycka, M., Sara, E., Davis, E., Smalley, M., Young, N., Dale, T.C., and Wooster, R. (2000). Sequence variants of the axin gene in breast, colon, and other cancers: An analysis of mutations that interfere with GSK3 binding. *Genes, Chromosomes and Cancer* 28, 443-453.

Weinberg, R.A. (2007). *The Biology of Cancer* (New York, Garland Science).

Wu, C.H., Wilson, J.M., and Wu, G.Y. (1989). Targeting Genes: Delivery and Persistent Expression of a Foreign Gene Driven by Mammalian Regulatory Elements *in Vivo*. *The Journal of Biological Chemistry* 264, 16985-16987.

Wu, G., and Wu, C. (1988). Receptor-mediated Gene Delivery and Expression *in Vivo*. *The Journal of Biological Chemistry* 263, 14621-14624.

Xu, Z.-B., Chaudhary, D., Olland, S., Wolfrom, S., Czerwinski, R., Malakian, K., Lin, L., Stahl, M.L., Joseph-McCarthy, D., Benander, C., *et al.* (2004). Catalytic Domain Crystal Structure of Protein Kinase C- θ (PKC θ). *Journal of Biological Chemistry* 279, 50401-50409.

Xue, Z.-H., Zhao, C.-Q., Chua, G.-L., Tan, S.-W., Tang, X.-Y., Wong, S.-C., and Tan, S.-M. (2010). Integrin α M β 2 Clustering Triggers Phosphorylation and Activation of Protein Kinase C δ that Regulates Transcription Factor Foxp1 Expression in Monocytes. *The Journal of Immunology* 184, 3697-3709.

Xu-Yu, Y., Cai-Ping, R., Lei, W., Hui, L., Chun-Jie, J., Hong-Bo, Z., Ming, Z., and Kai-Tai, Y. (2005). Identification of differentially expressed genes in metastatic and non-metastatic nasopharyngeal carcinoma cells by suppression subtractive hybridization. *Cellular Oncology* 27, 215-223.

Yamaguchi, Y., Hironaka, K., Okawaki, M., Okita, R., Matsuura, K., Ohshita, A., and Toge, T. (2005). HER2-specific Cytotoxic Activity of Lymphokine-activated Killer Cells in the Presence of Trastuzumab. *Anticancer Research* 25, 827-832.

Yaspan, B.L., Breyer, J.P., Cai, Q., Dai, Q., Elmore, J.B., Amundson, I., Bradley, K.M., Shu, X.-O., Gao, Y.-T., Dupont, W.D., et al. (2007). Haplotype Analysis of CYP11A1 Identifies Promoter Variants Associated with Breast Cancer Risk. *Cancer Res* 67, 5673-5682.

Yoshida, T., Kobayashi, T., Itoda, M., Muto, T., Miyaguchi, K., Mogushi, K., Shoji, S., Shimokawa, K., Iida, S., Uetake, H., et al. (2010). Clinical Omics Analysis of Colorectal Cancer Incorporating Copy Number Aberrations and Gene Expression Data. *Cancer Informatics* 9, 147-61.

Zhang, G.G., Kazanietz, M.G., Blumberg, P.M., and Hurley, J.H. (1995). Crystal-structure of the cys2 activator-binding domain of Protein-kinase C-delta in complex with phorbol ester. *Cell* 81, 917-924.

Zhang, X.-y., Pfeiffer, H.K., Thorne, A.W., and McMahon, S.B. (2008a). USP22, an hSAGA subunit and potential cancer stem cell marker, reverses the polycomb-catalyzed ubiquitylation of histone H2A. *Cell Cycle* 7, 1522-1524.

Zhang, X.-Y., Varthi, M., Sykes, S.M., Phillips, C., Warzecha, C., Zhu, W., Wyce, A., Thorne, A.W., Berger, S.L., and McMahon, S.B. (2008b). The Putative Cancer Stem Cell Marker USP22 Is a Subunit of the Human SAGA Complex Required for Activated Transcription and Cell-Cycle Progression. *Molecular Cell* 29, 102-111.

Zhang, Z., Sun, P., Liu, J., Fu, L., Yan, J., Liu, Y., Yu, L., Wang, X., and Yan, Q. (2008c). Suppression of FUT1/FUT4 expression by siRNA inhibits tumor growth. *Biochimica et Biophysica Acta (BBA) - Molecular Cell Research* 1783, 287-296.

Zhu, Z.H., Yu, Y.P., Shi, Y.K., Nelson, J.B., and Luo, J.H. (2008). CSR1 induces cell death through inactivation of CPSF3. *Oncogene* 28, 41-51.